学位論文

Study of microbial metabolism based on efficient utilization of non-food competing algal biomass

（食糧と非競合な藻類バイオマスの微生物による効率的代謝に関する研究）

平成 28 年 12 月博士（理学）申請

東京大学大学院理学系研究科

生物科学専攻

土井　秀高

ACKNOWLEDGMENTS

I thank Prof. Hiroo Fukuda at the University of Tokyo for his kind and patient academic guidance. I thank Prof. Masahiko Ikeuchi at the University of Tokyo for important academic discussions about this work. I thank Dr. Hisayoshi Nozaki at the University of Tokyo for taxonomic advice. I thank Prof. Ichiro Terashima at the University of Tokyo for important academic advice about this work. I thank Dr. Kyoko Ohashi-Ito at the University of Tokyo for her academic advice about this work. I thank Prof. Hiroyuki Kojima at Ajinomoto Co., Inc. and Tokyo Institute of Technology for his generous and very encouraging support for this study. I thank Dr. Yoshihiro Usuda at Ajinomoto Co., Inc. for his guidance and discussions about scientific metabolic engineering technologies. I thank Mr. Yoshihiko Hara at Ajinomoto Co., Inc. for his leading and support for this study. I thank Mr. Kazuo Nakanishi at Ajinomoto Co., Inc. for his very kind support for my phD course entrance. I thank Dr. Yuri Nagai at Ajinomoto Co., Inc. for her very kind advice about the planning of macroalgal biomass research. I thank Dr. Akito Chinen at Ajinomoto Co., Inc. for his appropriate and keen discussions about this study and revision. I thank Dr. Yoko Asakura for her discussions and supporting macroalgal biomass research. I thank Mr. Yuji Joe at Ajinomoto Co, Inc. for his guidance about microbial strain engineering. I thank Mr. Takuji

Ueda at Ajinomoto Co, Inc. for his guidance about Jar fermentation technologies. I thank Dr. Hisao Ito at Ajinomoto Co, Inc. for his discussion about my microbial research. I thank Dr. Osamu Kurahashi at Ajinomoto Co, Inc. for his discussions and general support for this work. I thank Dr. Yasuo Yoshikuni at Joint Genome Institute for important discussions regarding microbial alginate metabolism. I thank Prof. Tomoo Sawabe at Hokkaido University for his important discussions about the ecology of the genus *Vibrio*. I thank Prof. Fukuda's laboratory members for their friendship, I thank all of the members of BFPD-1 at Ajinomoto Co., Inc. for their friendship.

List of Abbreviations

ROS: Reactive Oxygen Species

LB : Luria-Bertani

CT : Cultivation Time

ANI : Average Nucleotide Identity

GGDC : Genome-To-Genome Distance Calculator.

DDH : DNA-DNA Hybridization

Aly : Alginate Lyase

Abstract

The demand of food is growing year by year along with the global population increase. Food materials are also used as biomass for microbial fermentation bioindustry. Because the mass production of algal biomass does not compete against a conventional crop production in most cases, the bioindustry has paid attention to algal biomass production on a large scale and its bioconversion technologies.

The major compounds of algal biomass are fatty acids in microalgae and alginate in macroalgae. Fatty acids are a promising raw material for substance production because of their highly reduced and anhydrous nature, which can provide higher fermentation yields than sugars. However, they are insoluble in water and are poorly utilized by microbes in industrial fermentation production. Then I tried to use fatty acids as raw materials for L-lysine fermentation by emulsification, and to improve the limited fatty acid-utilization ability of *Escherichia coli*. I succeeded in obtaining a fatty acid-utilizing mutant strain with a laboratory evolution method. The mutant possessed *rpsA*^{D210Y} mutation. The novel mutation *rpsA*^{D210Y} promoted cell growth, fatty-acid utilization and L-lysine production from fatty acid, suggesting that this mutation is useful for efficient fermentation of fatty-acid. The *rpsA*^{D210Y} mutant expressed lower oxidative-stress than wild-type and introduction of this *rpsA*^{D210Y} mutation into a wild-type strain resulted in lower H_2O_2 concentrations. The overexpression of superoxide dismutase (*sodA*) increased intracellular H_2O_2 concentrations

and inhibited *E. coli* fatty-acid utilization, whereas overexpression of an oxidative-stress regulator (*oxyS*) decreased intracellular H_2O_2 concentrations and promoted *E. coli* fatty-acid utilization and L-lysine production. Addition of the reactive oxygen species (ROS) scavenger thiourea promoted L-lysine production from fatty acids, and decreased intracellular H_2O_2 concentrations. Among the ROS generated by fatty-acid β-oxidation, H_2O_2 critically affected *E. coli* growth and L-lysine production. These results indicate that the regression of ROS stress, which is produced in the process of fatty-acid β-oxidation, is crucial for efficient fatty-acid utilization.

The major compound of macroalgal biomass is alginate. Alginate is a marine non-food-competing polysaccharide that also has potential applications in biorefinery. Owing to its large size (molecular weight > 300,000 Da) and its viscosity, most microorganism species cannot degrade and utilize alginate. Therefore, a fermentation system of alginate with microorganism has not been established yet. Then, at first, I tried to screen an alginate assimilating bacterium from the environment that possesses plenty of alginate. As a result I isolated an agarose and alginate assimilating, Gram-negative, non-motile, rod-shaped bacterium, designated strain SA2^T from the gut of a turban shell sea snail (*Turbo cornutus*) collected near Noto Peninsula, Ishikawa Prefecture, Japan. The 16S rRNA sequence of strain SA2^T was 99.59 % identical to that of *Vibrio rumoiensis* DSM 19141^T, 98.19 % identical to that of *Vibrio litoralis* DSM 17657^T. This suggested that strain SA2^T could be a subspecies of *V. rumoiensis* or *V. litoralis*. However, DNA-DNA hybridization results showed only 37.5 % relatedness to DSM 19141^T and 44.7 % relatedness to DSM 17657^T. Strain SA2^T could assimilate agarose as a sole carbon source, whereas strains DSM 19141^T and DSM 17657^T

could not assimilate it at all. Furthermore their enzymatic and physiological phenotypes were also different. These results suggested that strain SA2^T represented a novel species within the genus *Vibrio*. The major isoprenoid quinone in SA2^T was Q-8 and its major polar lipids were phosphatidylethanolamine and phosphatidylglycerol. The major fatty acids were summed feature 3 , (comprising $C_{16:1\omega6c}$ and/or $C_{16:1\omega7c}$), $C_{16:0}$, and summed feature 8 (comprising $C_{18:1\omega6c}$ and/or $C_{18:1\omega7c}$). The DNA G + C content of SA2^T was 40.7 mol%. Based on these results, the name was proposed for this novel *Vibrio* species as *Vibrio algivorus* sp. nov., with the type strain designated:SA2^T (= DSM 29824^T = NBRC 111146^T).

Alginate cannot pass through the bacterial cell membrane owing to its large size (molecular weight > 300,000 Da). Therefore, bacteria that utilize alginate are presumed to have an enzyme that degrades extracellular alginate. Therefore, *Vibrio algivorus* SA2^T should have an extracellular alginate degrading enzyme. To address this issue, I screened the *V. algivorus* genomic DNA library for a gene(s) encoding a polysaccharide-decomposing enzyme(s) using a novel double-layer plate screening method, and identified *alyB* as a candidate. AlyB of *V. algivorus* heterologously expressed in *Escherichia coli* depolymerized extracellular alginate without requiring concentration or purification. I found seven homologs in the *V. algivorus* genome (*alyB, alyD, oalA, oalB, oalC, dehR,* and *toaA*) that are thought to encode enzymes responsible for alginate transport and metabolism. Introducing these genes into *E. coli* enabled the cells to assimilate soluble alginate depolymerized by *V. algivorus* AlyB as the sole carbon source. The alginate was bioconverted into L-lysine (43.3 mg/l) in *E. coli* strain AJIK01. These findings provide a simple alginate biocatalyst and fermentation system with potential applications in industrial biorefinery.

In this study, I found a novel suppression mechanism in fatty acids bioconversion into L-lysine and its overcoming method. I also demonstrated that alginate can be bioconverted into L-lysine with a synthetic biological technology including the use of a new enzyme that I found

in this study. These results will contribute to not only the understanding of bioconversion of algal biomass but also the application of non-food-competing biomass utilization.

Chapter 1 Preface

According to the report of the statistical analysis of Food and Agriculture Organization (FAO), the natural resources per person of the growing population (e.g. land or water resources per person) will certainly continue to decline and the yield growth potential is more limited than in the past (http:/www.fao.org/docrep/004/y3557e/y3557e03.htm). It causes the slowing down of the growth of crop production. Global aggregate crop production is projected to grow over the period to 2030 at 1.4 percent per year, down from the annual growth of 2.1 percent of the past 30 years (Bruinsma 2003). On the other hand, crop is utilized as biomaterials in bioindustry. Because of the shortage of crop, people should seek a new biomass that does not compete against a conventional crop production. Algal biomass is a powerful candidate of such a biomass and therefore people has paid attention to production of algal biomass on a large scale and its bioconversion to useful materials.

The major compounds of algal biomass in microalgae are fatty acids. Fatty acids are stored as triglycerides within organisms, and are an important source of energy as they are both highly reduced and anhydrous. Indeed, the energy yield from 1 g fatty acid is more than twice of that from carbohydrate. However, industrial production by fermentation mainly uses sugars such as glucose and sucrose as raw materials, because fatty acids are insoluble in water and are poorly utilized by producer strains. Recently, biodiesel production from microalgae as a renewable energy source has received considerable attention (Chisti 2007).

Commercial microalgae cultures for fatty acid production and the bioconversion of fatty acids to fuels and chemicals by microorganisms are attractive alternative carbon resources for substance production (Chen et al. 2011; Dellomonaco et al. 2010; Hu et al. 2008; Rosenberg et al. 2008; Service 2009). In Chapter 2, I tried the promotion of the fatty acid bioconversion into a commodity chemical using *E. coli*, which is used to produce several industrial primary metabolites, amino acids, and organic acids (Leuchtenberger et al. 2005; Wendisch et al. 2006). Among them, L-lysine is used in food and feed additives, and is produced worldwide at quantities of over 1,500,000 metric tons per year. The use of this bacterium has economic advantages because of its fast growth and substrate consumption rates. In addition, more biochemical, molecular biological, and post-genomic data are available for this model organism than for others. High-yield aerobic fermentation by *E coli* from fatty acids to renewable fuels and chemicals such as ethanol, acetate, acetone, butanol, and propionate has previously been proposed (Dellomonaco et al. 2010), suggesting that fatty acids could become an effective carbon source for industrial production.

Alginate, which is an abundant sugar in marine brown macroalgae (Chapman, 1970) is also considered as an efficient and non-food-competing candidate raw material for biorefinery. Sugars from cane or corn starch are currently the major raw materials of biorefinery; however, an ethical challenge associated with their production is that it competes with food production. In contrast, the cultivation of marine brown macroalgae does not

require arable land, fresh water, pesticide, or fertilizer (John et al., 2011), and has the advantage of rapid growth (Stephens et al., 2013).

Alginate consists of a long-chain polymer of α-L-guluronic acid and β-D-mannuronic acid that form a high-molecular weight macromolecule (> 300,000 Da) that is poorly soluble in water (Gacesa, 1988). Raw alginate is too large to import through the cell membrane. As such, most microorganisms cannot degrade or utilize alginate. However, novel alginate-utilizing microbial species have recently been discovered (Kita et al., 2015; Doi et al., 2016), while various fermentation processes using alginate as raw material have been proposed. For example, ethanol for biofuel production has been derived from alginate by fermentation using metabolically engineered *Sphingomonas* sp. A1 strain (Takeda et al., 2011), *Escherichia coli* (Wargacki et al., 2012), and *Saccharomyces cerevisiae* (Enquist-Newman et al., 2014), while pyruvate has been produced by *Sphingomonas* sp. A1 (Kawai et al., 2014). These studies exploit specific alginate-assimilating species and/or their enzymes. However, there are certain challenges for the industrialization of alginate fermentation, including the need to pretreat alginate for degradation and ensuring efficient bioconversion of alginate into products. These can potentially be circumvented by identifying a novel alginate-utilizable bacterium and its novel alginate-degrading and -utilizing enzymes, which could be used for the production of commodity chemicals. In Chapter 3, I tried to discover an alginate-utilizing bacterial strain and succeeded in isolation of a novel *Vibrio* species, *Vibrio algivorus* sp. SA2^{T}.

In Chapter 4, I try to identify a gene for an alginate-degrading enzyme from *Vibrio algivorus* sp. SA2^{T}, and identified *alyB*. Introduction of seven genes in the *V. algivorus* genome that are thought to encode enzymes responsible for alginate transport and metabolism into *E. coli* assimilated soluble alginate depolymerized by *V. algivorus* AlyB into L-lysine.

In Chapter 5, based on these results, I discussed the possible use of the algal biomass by bioconversion of metabolism.

Chapter 2 Reduction of hydrogen-peroxide stress derived from fatty-acid beta-oxidation improves fatty-acid utilization in *Escherichia coli*

Abstract

Fatty acids are a promising raw material for substance production because of their highly reduced and anhydrous nature, which can provide higher fermentation yields than sugars. However, they are insoluble in water and are poorly utilized by microbes in industrial fermentation production. I used fatty acids as raw materials for L-lysine fermentation by emulsification, and improved the limited fatty acid-utilization ability of *Escherichia coli*. I obtained a fatty acid-utilizing mutant strain by laboratory evolution, and demonstrated that it expressed lower levels of an oxidative-stress marker than wild-type. The intracellular hydrogen peroxide (H_2O_2) concentration of a fatty acid-utilizing wild-type *E. coli* strain was higher than that of a glucose-utilizing wild-type *E. coli* strain. The novel mutation *rpsA*^{D210Y} identified in my fatty acid-utilizing mutant strain enabled me to promote cell growth, fatty-acid utilization and L-lysine production from fatty acid. Introduction of this *rpsA*^{D210Y} mutation into a wild-type strain resulted in lower H_2O_2 concentrations. The overexpression of superoxide dismutase (*sodA*) increased intracellular H_2O_2 concentrations and inhibited *E. coli* fatty-acid utilization, whereas overexpression of an oxidative-stress regulator (*oxyS*) decreased intracellular H_2O_2 concentrations and promoted *E. coli* fatty-acid utilization and L-

lysine production. Addition of the reactive oxygen species (ROS) scavenger thiourea promoted L-lysine production from fatty acids, and decreased intracellular H_2O_2 concentrations. Among the ROS generated by fatty-acid β-oxidation, H_2O_2 critically affected *E. coli* growth and L-lysine production. This indicates that the regression of ROS stress promotes fatty-acid utilization, which is beneficial for fatty acids used as raw materials in industrial production.

Introduction

Fatty acids are stored as triglycerides within organisms, and are an important source of energy as they are both highly reduced and anhydrous. Indeed, the energy yield from 1 g fatty acid is more than twice that from carbohydrate. However, industrial production by fermentation mainly uses sugars such as glucose and sucrose as raw materials, as fatty acids are insoluble in water and are poorly utilized by producer strains. Recently, biodiesel production from microalgae as a renewable energy source has received considerable attention (Chisti 2007). Commercial microalgae cultures for fatty acid production and the bioconversion of fatty acids to fuels and chemicals by microorganisms are attractive alternative carbon resources for substance production (Chen et al. 2011; Dellomonaco et al. 2010; Hu et al. 2008; Rosenberg et al. 2008; Service 2009). High-yield aerobic fermentation by *Escherichia coli* from fatty acids to renewable fuels and chemicals such as ethanol, acetate, acetone, butanol, and propionate has previously been proposed (Dellomonaco et al. 2010), suggesting that fatty acids could become an effective carbon source for industrial production.

E. coli is used to produce several industrial primary metabolites, amino acids, and organic acids (Leuchtenberger et al. 2005; Wendisch et al. 2006). Among these, L-lysine is used in food and feed additives, and is produced worldwide at quantities of over 1,500,000 metric tons per year. The use of this bacterium has economic advantages because of its fast

growth and substrate consumption rates. In addition, more biochemical, molecular biological, and post-genomic data are available for this model organism than for most others.

Fatty acids are assimilated and degraded to acetyl-CoA in *E. coli* by the β-oxidation-pathway proteins FadL, FadD, FadE, FadB, and FadA under both aerobic and anaerobic conditions (Cronan and Subrahmanyam 1998). All of the *E. coli* fatty-acid β-oxidation pathway genes (*fadL, fadD, fadE, fadB, fadA, fadI*, and *fadJ*) and short-chain fatty acid utilizing genes (*atoD, atoA*, and *atoB*) have been identified (Jenkins and Nunn 1987), and most β-oxidation pathway genes are regulated by FadR (Cronan and Subrahmanyam 1998). FadR also upregulates *fabA, fabB*, and *iclR* genes, and downregulates *fad* genes (*fadL, fadD, fadE, fadB, fadA, fadI*, and *fadJ*) and the *uspA* gene. *fabA* and *fabB* are involved in fatty acid synthesis (Magnuson et al. 1993), whereas IclR regulates acetyl-CoA metabolism through *aceBA*, which encodes glyoxylate shunt-pathway enzymes (Resnik et al. 1996). The *uspA* gene is induced by various stresses, including heat and oxidative (Nachin et al. 2005), and *fabA* overexpression decreases the monounsaturated fatty acid content of *E. coli* cell membranes, leading to increased cell resistance to oxidative stress or stress caused by reactive oxygen species (ROS)-generating compounds (Pradenas et al. 2012).

Here, I examined the mechanism of fatty acid degradation by *E. coli* to promote fatty acid utilization. The *E. coli* genome evolves and adapts to laboratory cultivation conditions (Fong et al. 2005; Herring et al. 2006). I therefore initiated wild-type *E. coli*

cultivation for fatty acid utilization on minimal medium supplied with sodium oleate as the sole carbon source. Oleate was used because it is common in vegetable oils and is relatively easy to handle experimentally. I analyzed the physiological phenotype of the *E. coli* mutant obtained that could utilize oleate efficiently and investigated the effects of oxidative stress, especially those caused by ROS-generating compounds, on cell growth and lysine production.

Materials and methods

Bacterial strains and plasmids. All strains, plasmids, and primers used are listed in Table 2-1. The *oxyS* gene encoding an oxidative-stress regulator and its promoter region was amplified by the polymerase chain reaction (PCR) using the *E. coli* MG1655 genome and the primer set oxyS1 (5′-TACCCGGGGATCCTCTAGAGTTCCGCGAGGCGCACCATATTGTTGGTGAA-3′) and oxyS2 (5′-TTGCATGCCTGCAGGTCGACAGAAACGGAGCGGCACCTCTTTTAACCCT-3′).

The PCR product was purified with the Wizard SV gel and PCR clean-up system (Promega, Madison, WI), digested by *Sal* I, and cloned into pTWV229 digested by *Sal* I using the In-Fusion PCR cloning system (Clontech, Mountain View, CA). The resultant plasmid was designated pTWV228-oxyS.

The *sodA* gene encoding the superoxide dismutase overexpressing plasmid pTWV229-sodA was constructed as follows. The *sodA* open reading frame (ORF) region was amplified using sodA1 (5′-TGATTACGCCAAGCTTAGGAGGTTAAATGAGCTATACCCTGCCATCCCTGCCGTA-3′) and sodA2 (5′-ATCCTCTAGAGTCGACGCGGCCGCTACTTATTTTTTCGCCGCAAAACGTGCCGCTGC-3′) primers. The PCR product was purified, digested by *Hin*d III and *Sal* I, and cloned

into pTWV229 digested with the same restriction enzymes.

Adaptive evolution and analysis of an effective mutation. Minimal medium M9 (Miller 1992) supplemented with 1 mM $MgSO_4$, 0.1 mM $CaCl_2$, 0.001% thiamine, 0.5% Tween80 (polyoxyethylene sorbitan monooleate, CAS:9005-65-6), and 2 g/L sodium oleate was used in adaptive evolution experiments. One loop of *E. coli* MG1655 was inoculated onto an M9 plate and incubated for 20 h at 37 °C. Cells were cultured in L-shaped test tubes using a TN-2612 rocking incubator (Advantec, Tokyo, Japan) at 37 °C with constant shaking at 70 rpm. The optical density at 600 nm of the culture was measured continuously, and test-tube cultivation started at approximately OD_{600} 0.006 and finished at OD_{600} 0.3. The culture broth was transferred into fresh minimal medium, and the test-tube cultivation was repeated 22 times for a total cultivation time of 445 h. A single colony was then isolated from the resultant broth spread onto an M9 plate and designated FitnessOle.

The addition of Tween80 as an emulsifying agent of sodium oleate clarified the medium and allowed us to accurately measure the OD_{600} in fatty acid supplied medium (Suzuki et al., unpublished data). I ascertained that *E. coli* MG1655 and FitnessOle could not grow and utilize Tween80 as a sole carbon source in test-tube and flask cultivation using M9 medium (data not shown).

The FitnessOle genome was analyzed by whole genome sequencing with an Illumina Genome Analyzer II (GAII; Illumina Inc, San Diego, CA). In order to introduce the *rpsA*^{D210Y}

mutation into the genomes of other strains, a FitnessOle *ycaI* deletion mutant was constructed by PCR and the λ red deletion method using ycaI1 primer (5′-agacaaccgctcaacaaagttgcacactttccataaacagggaggggtgcTCTAGACGCTCAAGTTAGTATA-3′) and ycaI2 primer (5′-gttgtttgtagtgacgccagatactgtgcacgcaggctacaattcggttcAGATCTTGAAGCCTGCTTT -3′) as *ycaI* is located close to *rpsA* in the genome. Because *ycaI* gene is located about 1.7 kbps of $rpsA^{D210Y}$ mutation in the *E. coli* genome and no significant phenotypes in this study were observed by *ycaI* gene deletion (data not shown), I introduced the $rpsA^{D210Y}$ mutation with *ycaI* gene deletion by using the phage P1 without phenotypic influence. MG1655 containing the $rpsA^{D210Y}$ mutation and WC196LC containing the $rpsA^{D210Y}$ mutation were constructed by phage P1 transduction using the phage P1 obtained from the FitnessOle *ycaI* deletion strain.

Statistical testing and estimation of *p*-values. The standard error of the mean calculation and a two-tailed unpaired Student's *t*-test were performed using Excel software (Microsoft Corporation, Redmond, WA) from more than three independent samples.

Culture conditions. For test-tube cultivation, *E. coli* MG1655 and its derivative strains were grown overnight at 37 °C on M9 plates supplemented with 1 mM $MgSO_4$, 0.1 mM $CaCl_2$, 0.001% thiamine, and 2 g/L glucose. One loop of the grown cells was inoculated into 10 mL minimal medium M9 supplemented with 1 mM $MgSO_4$, 0.1 mM $CaCl_2$, 0.001%

thiamine, 0.5% Tween80, and 1 g/L carbon source (sodium oleate or glucose) in L-shaped test tubes, and cultivated at 37 °C with constant shaking at 70 rpm using a TN-2612 rocking incubator.

For flask cultivation, *E. coli* MG1655 and its derivative cells were grown overnight at 37 °C on M9 plates supplemented with 1 mM $MgSO_4$, 0.1 mM $CaCl_2$, 0.001% thiamine, and 2 g/L glucose were inoculated into 20 mL of M9 medium supplemented with 1 mM $MgSO_4$, 0.1 mM $CaCl_2$, 0.001% thiamine, 0.5% Tween80, and 10 g/L carbon source (oleic acid, elaidic acid, acetate, maltose, glycerol, or glucose) in a Sakaguchi flask (500 mL) at an initial OD_{600} of 0.2 and cultivated at 37 °C with reciprocal shaking at 120 rpm. The pH of each component was adjusted to 7.0 before sterilization.

For L-lysine fermentation from fatty acids in flasks, *E. coli* strains derived from WC196LC (Leuchtenberger et al. 2005) were cultivated overnight at 37 °C on LB plates composed of 1.0% Bacto tryptone, 0.5% Bacto yeast extract, 1% NaCl, and 1.5% agar. Cells were then inoculated into 40 mL flask-fermentation medium comprising 2 g/L yeast extract, 1 g/L $MgSO_4 \cdot 7H_2O$, 24 g/L $(NH_4)_2SO_4$, 1 g/L KH_2PO_4, 0.01 g/L $FeSO_4 \cdot 7H_2O$, 0.082 g/L $MnSO_4 \cdot 7H_2O$, 20 g/L PIPES, and 10g /L sodium oleate in Erlenmeyer flasks (500 mL) at an initial OD_{600} of 0.25. The pH of the medium was adjusted to 7.0 before sterilization. Fermentation was performed at 37 °C with rotary shaking at 200 rpm.

For L-lysine fermentation from fatty acids in a jar fermenter, *E. coli* WC196LC and its

derivative strains grown overnight at 37 °C on LB plates were transferred to 300 mL jar-fermentation medium comprising 2 g/L yeast extract, 1 g/L $MgSO_4 \cdot 7H_2O$, 24 g/L $(NH_4)_2SO_4$, 1 g/L KH_2PO_4, 0.01 g/L $FeSO_4 \cdot 7H_2O$, 0.082 g/L $MnSO_4 \cdot 7H_2O$, and 10 g/L carbon source (sodium oleate or glucose) in 1-L glass vessels (Able Corporation, Tokyo, Japan) at an initial OD_{600} of 0.04 and subjected to batch cultivation in jar fermenters DPC-2A (Able Corporation, Tokyo, Japan) at 37 °C. The pH of the culture was maintained at 6.7 by adding ammonia gas.

Analytical methods. Aggregation indexes of *E. coli* MG1655 and the FitnessOle strain were measured as previously described (Malik et al. 2003). Cell growth was analyzed by measuring the OD_{600} with a spectrophotometer U-2900 (Hitachi, Tokyo, Japan), and by counting the number of living cells. Tween80 solution (10%) was used for dilution to eliminate the influence of fatty acids on OD_{600nm}. Living cell counting in the fermentation broth was carried out by diluting the broth with saline and counting the number of colonies on LB plates after cultivation for 24 h at 37 °C. The maximum specific growth rate (μ_{max}) and maximum specific substrate-consumption rate (ν_{max}) were calculated by nine-dimension polynomial approximations using the numerical computation software package MATLAB (MathWorks, Natick, MA). R-squared values of the approximations were greater than 0.995.

Carbonylated protein concentrations were measured using a protein carbonyl colorimetric assay kit (Cayman Chemical Company, Ann Arbor, MI). To measure cells in the

same growth phase, I sampled the cells from the flask-fermentation broth when the residual carbon source concentration reached 1 g/L for the carbonylated protein assay, and measured the OD_{600} to confirm that sampled cells were divided a similar number of times. Glucose and L-lysine were assayed by a biotech analyzer AS310 (Sakura Si Co., Ltd., Tokyo, Japan). Glycerol was assayed by an electrochemical biosensor BF-5 (Oji Scientific Instruments, Hyogo, Japan), maltose by an ion chromatography system ICS-3000 (Dionex, Sunnyvale, CA), acetate by a liquid chromatograph LC-10AD (Shimadzu, Kyoto, Japan), and oleic acid and elaidic acid by a gas chromatograph GC-2014 (Shimadzu).

Intracellular hydrogen peroxide (H_2O_2) was measured as previously described (González-Flecha and Demple 2003; Maisonneuve et al. 2008). Briefly, bacterial cells were collected from culture broths by centrifugation (13,800 × *g*) for 2 min at 4 °C, and resupended in phosphate buffer (pH 7.3) at an approximate density of 10^6 cells/mL. After 10 min diffusion of intracellular H_2O_2 into the buffer through cellular membranes, the cells were removed by centrifugation at 13,800 × *g* for 2 min at 4 °C. Then, 10 µL supernatant was suspended separately in Solution A (2 µM horseradish peroxidase and 10 µM HPF (Maisonneuve et al. 2008) in 100 mM phosphate buffer (pH 7.3)) and Solution B (2 µM catalase and 10 µM HPF (Maisonneuve et al. 2008) in 100 mM phosphate buffer solution (pH 7.3)).

The resusupended samples were incubated at 37 °C for 75 min in the dark, and the

emitted fluorescence at 515 nm was measured using excitation at 490 nm. The intracellular H_2O_2 concentration was calculated by subtracting the fluorescence of Solution B from that of Solution A.

Results

Acquisition of fatty acid-utilizing *E. coli* mutant strain by laboratory evolution and analysis of physiological phenotypes. To improve fatty acid utilization by *E. coli*, I attempted to obtain a mutant with enhanced function. I cultivated the wild-type *E. coli* strain MG1655 in minimal media supplemented with sodium oleate as a sole carbon source for 445 h. I then isolated a mutant with improved utilization of fatty acid and designated it FitnessOle. Figure 2-1 shows the growth (Fig. 2-1A) and oleate concentration (Fig. 2-1B) profiles of the wild-type and FitnessOle strains in flask culture. The FitnessOle strain showed significantly enhanced growth in oleate culture with enhanced consumption of oleate. I ascertained that four other independent colonies isolated from the same broth after 445 h cultivation showed the same enhanced growth phenotype as the FitnessOle strain in oleate culture. The FitnessOle strain also showed higher μ_{max} and ν_{max} values when grown on fatty acids (oleic or elaidic acids), glycerol, or acetate as the sole carbon source compared with the wild-type strain (Table 2-2). The FitnessOle strain also showed increased cell biomass accumulation when grown on oleic acid as the sole carbon source under aerobic conditions compared with the wild-type strain. But the FitnessOle strain showed the same cell biomass accumulation as the wild-type strain when grown on oleic acid under anaerobic conditions. Cell aggregation of the FitnessOle strain appeared to be facilitated compared with the wild-type strain. I also measured the aggregation index (Malik et al. 2003) and found the

aggregation tendency of the FitnessOle strain to be significantly increased (Fig. 2-2C).

The *uspA* gene, encoding a universal stress protein with unknown functions, has been reported to be a target of FadR that is upregulated when *E. coli* is exposed to oxidative stress (Nachin et al. 2005). FadR functions as switch between fatty acid β-oxidation and fatty acid biosynthesis (Xu et al. 2001) Based on these facts, I investigated the relationship between fatty acid utilization and oxidative stress. I measured the carbonylated protein concentration, a major oxidative-stress marker, of *E. coli* cells utilizing glucose or oleate as the sole carbon source (Maisonneuve et al. 2008), and found it to be decreased in the FitnessOle strain compared with wild-type after a similar number of cell divisions (Fig. 2-1C), indicating decreased oxidative stress in this strain. I next measured the concentration of intracellular H_2O_2, a major ROS, and also found it to be decreased in the FitnessOle strain compared with wild-type when the cells utilized oleate as the sole carbon source (Fig. 2-1D).

To identify an effective mutation for fatty acid utilization in the genome of the fatty acid-utilizing *E. coli* mutant strain, I carried out whole genome sequencing and discovered the $rpsA^{D210Y}$ mutation (Fig. 2-2A). The $rpsA^{D210Y}$ mutation was present in the genomes of four other independent colonies isolated from the broth after 445 h minimal media cultivation. Introduction of this mutation into the MG1655 genome resulted in enhanced cell growth when oleate was used as the sole carbon source (Fig. 2-2B) and higher μ_{max} and ν_{max} values than those of the wild-type MG1655. Furthermore, introduction of the $rpsA^{D210Y}$

mutation caused a decrease in the concentration of intracellular H_2O_2 when the strain utilized oleate as a sole carbon source (Fig. 2-2D) in despite no significant change in aggregation index (Fig. 2-2C). Introduction of the *rpsA*^{D210Y} mutation into the genome of the *E. coli* L-lysine producer strain WC196LC/pCABD2 (Kikuchi et al. 1997) resulted in increased cell growth and L-lysine accumulation when the *E. coli* L-lysine producer strain utilized oleate (Table 2-3). There were, however, no apparent differences in L-lysine production, cell growth, or glucose consumption following introduction of the *rpsA*^{D210Y} mutation when the *E. coli* L-lysine producer strain utilized glucose (Table 2-3).

Promotion of fatty acid utilization by reducing intracellular H_2O_2. In the wild-type strain MG1655, no carbon source (glucose or oleate)-dependent change in carbonylated protein accumulation was observed (Fig. 2-1C), suggesting that the specific ROS stress was decreased only in the fatty acid-utilizing mutant FitnessOle strain. As shown in Fig. 3, the ROS consists of a single oxygen molecule, a superoxide anion ($O_2\cdot^-$), H_2O_2, and a hydroxyl radical (·OH) (González-Flecha and Demple 2003; Blanchard et al. 2007; Zheng et al. 1998). The two transcription factors reported to respond to $O_2\cdot^-$ and H_2O_2 are also shown (Blanchard et al. 2007; Zheng et al. 1998). SoxR is mainly involved in defense against $O_2\cdot^-$ and OxyR mainly against H_2O_2. Thus, I investigated the growth of the *soxR* deletion mutant (JW3933) and the *oxyR* deletion mutant (JW4024) derived from BW25113 (Baba et al. 2006) on

glucose or oleate as the sole carbon source. Both the Δ*soxR* and Δ*oxyR* strains showed no significant stationary phase optical density changes compared with their host strain BW25113 when they utilized glucose as the sole carbon source (Fig. 2-4A). However, the Δ*oxyR* strain showed an apparent cell growth defect and a stationary phase optical density decrease when grown on sodium oleate as the sole carbon source (Fig. 2-4B).

To determine which ROS has the greatest negative effect on fatty acid utilization in *E. coli*, I constructed expression plasmids harboring the *sodA* gene encoding the $O_2{\cdot}^-$ scavenger dismutase or the *oxyS* gene encoding an oxidative-stress regulator, and introduced them into the wild-type strain MG1655,respectively. The *oxyS* transcript might be involved in the excretion, rather than removal, of H_2O_2 by catalase peroxidases (González-Flecha and Demple 2003). The resultant strains (MG1655/ pTWV229-sodA and MG1655/ pTWV228-oxyS) were cultivated on glucose or sodium oleate as a carbon source (Fig. 2-5). The intracellular H_2O_2 concentration was significantly increased when the *E. coli* MG1655/pTWV228 strain utilized sodium oleate compared with glucose as the sole carbon source (Fig. 2-5A and 2-5B; $p<0.03$, Student's *t*-test). Furthermore, overexpression of the *sodA* gene resulted in an increase of intracellular H_2O_2 and a severe growth defect (Fig. 2-5B and 2-5D). Overexpression of the *oxyS* gene decreased intracellular H_2O_2 levels and promoted cell growth (Fig. 2-5B and 2-5D).

Effects of promotion of fatty acid utilization by reducing ROS stress on L-lysine production. To investigate the relationship between material production from fatty acids and reduction of ROS stress, I used the *E. coli* L-lysine-producing strain WC196LC/pCABD2 (Kikuchi et al. 1997). Overexpression of *oxyS* in WC196LC/pCABD2 resulted in increased cell growth and L-lysine accumulation (Table 2-4). This suggests that decreased ROS stress, assumed to be mainly caused by intracellular H_2O_2, promoted fatty acid utilization and L-lysine production. Next, I investigated the effect of the antioxidant reagent thiourea on fatty acid utilization in larger scale fermentation. Thiourea reduces damage caused by H_2O_2 (Blount et al. 1986), and was shown to decrease intracellular H_2O_2 concentrations both in glucose and sodium oleate utilization (Table 2-5). However, thiourea also reduced the cultivation times required to consume fatty acid, and increased cell and L-lysine accumulation when the *E. coli* L-lysine-producing strain utilized sodium oleate (Table 2-5). In contrast, no apparent difference in L-lysine production, cell growth, or glucose consumption was observed following thiourea addition when the *E. coli* L-lysine producer strain utilized glucose (Table 2-5).

Discussion

I predicted that test-tube adaptive evolution would shed light on fatty acid utilization in *E. coli* by comparing physiological phenotype differences between a mutant that can utilize fatty acids efficiently and a wild-type strain. Indeed, the mutant strain FitnessOle showed a higher ability to utilize various fatty acids, including oleic acid, elaidic acid (Table 2-2), stearic acid, sodium palmitate, myristic acid, and sodium oleate (data not shown), compared with wild-type.

The FitnessOle strain showed enhanced cell aggregation as well as lowered ROS stress (Fig. 2-2). Microorganism aggregation can be quantified by measurement of the aggregation index, and is positively correlated with membrane hydrophobicity (Malik et al. 2003). Thus, my results indicate that the FitnessOle strain possesses increased membrane hydrophobicity; I will examine this together with its relationship with fatty acid utilization in a future study.

My main focus here was the promotion of fatty acid utilization in *E. coli*. I discovered a novel fatty acid utilization promoting mutation, *rpsA*^{D210Y}. *rpsA* encodes the 30S ribosomal subunit protein. Introduction of the *rpsA*^{D210Y} mutation decreased intracellular H_2O_2 concentrations (Fig. 2-2D) but had no effect on cell aggregation (Fig. 2-2C). These results suggest that intracellular H_2O_2 concentrations can influence fatty acid utilization. I also found that a decrease in ROS stress, particularly that of H_2O_2, was important to enhance the ability to utilize fatty acid in *E. coli*. However, as the ROS was shown to change (Fig. 2-3), it is

difficult to identify which species affects fatty acid utilization. Nevertheless, my research revealed that it was mainly inhibited by H_2O_2 rather than $O_2^{\cdot -}$ (Fig. 2-4 and 2-5). There was no apparent change for the carbonylated protein accumulation in wild type *E. coli* cells grown in M9 media with glucose or oleate (Fig. 2-1C). On the other hand, the intracellular H_2O_2 concentration was significantly increased when the wild-type strain utilized sodium oleate compared with glucose as the sole carbon source (Fig. 2-5A and 2-5B). Carbonylated protein content indicates total ROS stress including H_2O_2, $O_2^{\cdot -}$ and ·OH (Fig. 2-3). These data show that the specific ROS stress is H_2O_2 stress when *E. coli* utilized sodium oleate among the various ROS. My preliminary microarray research revealed that *katG*, *ahpC*, *ahpF*, and *oxyR* transcripts were increased in FitnessOle strain compared with the wild type when they utilized sodium oleate. In addition, my preliminary microarray research also revealed that *sodA*, *sodB*, *soxS*, and *soxR* transcripts were decreased in FitnessOle strain compared with the wild type when they utilized sodium oleate (Doi, et al. unpublished data). These results indicate the independence of H_2O_2 and $O_2^{\cdot -}$. No significant phenotype was previously reported following the overexpression of *oxyS* when *E. coli* was cultivated on LB, in which the main carbon source was amino acids not fatty acids (González-Flecha and Demple 2003).

Similarly, no significant phenotype was observed by the overexpression of *oxyS* when *E. coli* utilized glucose as the main carbon source (Fig. 2-5A and 2-5C). However, I did observe the promotion of fatty acid utilization following *oxyS* overexpression, presumably

because of reduced H_2O_2 levels (Fig. 2-5B and 2-5D) and L-lysine production (Table 2-4). I assumed that this effect was a result of H_2O_2 excretion by the *oxyS* transcript (González-Flecha and Demple 2003). These results demonstrate a specific phenotype after *oxyS* overexpression, and suggest that more H_2O_2 is generated when utilizing fatty acid compared with glucose and amino acids supplied in LB medium. I presume that H_2O_2 is generated by flavin adenine dinucleotide ($FADH_2$) during the fatty acid β-oxidation pathway.

This autoxidation of $FADH_2$ is a well-known phenomenon that occurs, for example, in glucose concentration analysis by glucose oxidase (Raba and Mottola 1995). Free $FADH_2$ was previously shown to be reduced by cytosolic enzymes such as L-aspartate oxidase, and was autoxidized to generate endogenous *E. coli* H_2O_2 (Korshunov and Imlay 2010; Messner and Imlay 2002). I assumed that $FADH_2$ reduced by FadE, the acyl-CoA dehydrogenase in the fatty acid β-oxidation pathway, would be the endogenous H_2O_2 source in the present study. I am currently investigating the effects of $FADH_2$ oxidation by electron-transfer-flavoprotein (ETF) or ETF dehydrogenase (EC 1.5.5.1). Our preliminary research revealed that the overexpression of these homologous genes in *E. coli* results in the decrease of intracellular H_2O_2 and increased L-lysine accumulation during the utilization of fatty acid as a carbon source (Hoshino et al. unpublished data), supporting my hypothesis of endogenous H_2O_2 generation by $FADH_2$ autoxidation.

In jar fermentation, thiourea addition decreased intracellular H_2O_2 concentrations,

lowered cultivation time, and increased L-lysine production when *E. coli* utilized fatty acid (Table 2-5). However, when glucose was utilized, the total cultivation time and L-lysine production remained the same, even though intracellular H_2O_2 concentrations decreased (Table 2-5). This suggests that higher ROS stress was generated following fatty acid utilization, which inhibited growth. The addition of thiourea, a common antioxidant molecule, to reduce ROS stress is a promising approach for fatty acids used on an industrial scale as raw materials for fermentation. Thiourea is used as a building material because it is inexpensive compared with antioxidants such as vitamin C or tocopherol.

The present study focused only on the physiological phenotype of the FitnessOle strain and identified a novel mutation, *rpsA*^{D210Y}. I am currently using this mutation to understand the mechanism of decreasing intracellular H_2O_2 concentrations. My preliminary data revealed that superoxide dismutase SodB protein expression decreased following the introduction of the *rpsA*^{D210Y} mutation, as shown by 2-D electrophoresis and liquid chromatography–mass spectrometry analysis. However, the *rpsA*^{D210Y} mutation alone could not achieve the increased cell growth and decreased intracellular H_2O_2 concentration shown by the FitnessOle strain. Therefore, I am now investigating the other mutations of the FitnessOle genome, which should reveal more information concerning *E. coli* fatty acid utilization. I expect this to clarify the relationship between the reduction of ROS and changes in membrane hydrophobicity.

Fatty acids are a promising raw material for substance production, and I have shown that they can be used as such for amino acid fermentation by means of emulsification, despite their insolubility in water (Suzuki et al., unpublished data). This report is the first to show the bioconversion of fatty acid into L-lysine by obtaining a fatty acid-utilizing mutant, the FitnessOle strain. H_2O_2 generated by fatty acid β-oxidation was revealed to have a critical effect on growth and lysine production when *E. coli* utilized fatty acid as a carbon source. This will be useful for future industrial production using fatty acids as substrates, and I hope to identify further useful insights to help in the realization of this process.

Tables and Figures

Table 2-1 Strains and plasmids

Strain or plasmid	Description, genotype, or sequence	Reference
Strains		
MG1655	F- λ- *ilvG rfb-50 rph-1*	CGSC collection number 6300
MG1655 Δ*ycaI*::attR-cat-attL	MG1655 Δ*ycaI* deletion mutant constructed by λ red system	This study
MG1655 *rpsA*^{D210Y} Δ*ycaI*::attR-cat-attL	MG1655 containing *rpsA*^{D210Y} mutation	This study
FitnessOle	High performance fatty acid-utilizing mutant isolated by adaptive evolution	This study
FitnessOle Δ*ycaI*::attR-cat-attL	FitnessOle Δ*ycaI* deletion mutant constructed by λ red system	This study

BW25113	*rrnB3* Δ*lacZ4787 hsdR514* Δ(*araBAD*)*567* Δ(*rhaBAD*)*568 rph-1*	Baba et al. 2006, Keio collection
JW4024	BW25113 Δ*oxyR*::FRT-Kan-FRT; *oxyR* deletion mutant in BW25113	Baba et al. 2006, Keio collection
JW3933	BW25113 Δ*soxR*::FRT-Kan-FRT; *soxR* deletion mutant in BW25113	Baba et al. 2006, Keio collection
WC196LC	W3110 NTG mutant (S-aminoethyl- L-cysteine resistant mutant) Δ*ldc* Δ*cadA*	Kikuchi et al. 1997
WC196LC Δ*ycaI*::attR-cat-attL	WC196LC Δ*ycaI* deletion mutant constructed by λ red system	This study
WC196LC *rpsA*^{D210Y} Δ*ycaI*::attR-cat-attL	WC196LC containing *rpsA*^{D210Y} mutation	This study

Plasmids		
pTWV228	Cloning vector, Ap^r	Takara Bio Inc, Japan
pTWV229	Cloning vector, Ap^r	Takara Bio Inc, Japan
pTWV228-oxyS	*oxyS* gene on pTWV228	This study
pTWV229-sodA	*sodA* gene on pTWV229	This study
pCABD2	pRSF1010 carrying mutated *lysC*, mutated *dapA*, mutated *dapB*, and *C. glutamicum ddh*	Kojima et al. 1994
pKD46	λ red system helper plasmid	Datsenko and Wanner 2000
pMW118- λ attL-Cm^R- λ attR	λ red system vector containing Cm^R (cat) gene	Katashkina et al. 2005

Table 2-2 μ_{max} and ν_{max} values of the FitnessOle strain in flask cultivation with various carbon sources

Substrate (10 g/L)	μ_{max} of MG1655	μ_{max} of FitnessOle	ν_{max} of MG1655	ν_{max} of FitnessOle
Glucose	0.85	0.85	0.63	0.63
Glycerol	0.62	0.81	0.40	0.59
Maltose	0.44	0.41	0.30	0.29
Oleic acid	0.09	0.24	0.06	0.12
Elaidic acid	0.11	0.23	0.07	0.12
Acetate	0.09	0.11	0.07	0.08

μ_{max}: maximum specific growth rate; ν_{max}: maximum specific substrate-consumption rate.

Table 2-3 Effect of *rpsA*^{D210Y} mutation on L-lysine production in flask cultivation from fatty acid (sodium oleate)

Strain	Carbon Source	OD_{600}	L-lysine accumulation (g/L)	L-lysine yield (%)
WC196LC /pCABD2	Glucose	5.5	3.8	39.0
WC196LC Δ*ycaI*::attR-cat-attL /pCABD2	Glucose	5.5	3.8	39.2
WC196LC *rpsA*^{D210Y} Δ*ycaI*::attR-cat-attL /pCABD2	Glucose	5.5	3.8	39.0
WC196LC /pCABD2	Oleate	8.1	4.2	44.9

WC196LC Δ*ycaI*::attR-cat-attL /pCABD2	Oleate	8.3	4.2	44.8
WC196LC *rpsA*^{D210Y} Δ*ycaI*::attR-cat-attL /pCABD2	Oleate	9.3	4.5	47.2

Table 2-4 Effect of *oxyS* gene overexpression on L-lysine production in flask cultivation from fatty acid (sodium oleate)

Strain	OD_{600}	L-lysine accumulation (g/L)	L-lysine yield from oleate (%)	Intracellular H_2O_2 (μM / 10^6 cells)
WC196LC / pCABD2, pTWV228	4.3	3.8	40.9	0.52
WC196LC / pCABD2, pTWV228-oxyS	6.2	4.2	45.3	0.26

Table 2-5 Effects of ROS-scavenger addition on L-lysine production

Supplied carbon source and antioxidant	Cultivation time (h)	OD_{600}	L-lysine accumulation (g/L)	Intracellular H_2O_2 (μM / 10^6 cells)
Glucose 10 g/L	16.0	5.3	4.7	0.14
Glucose 10 g/L Thiourea 1 mM	16.0	5.3	4.7	0.11
Glucose 10 g/L Urea 1 mM (mock control)	16.0	5.2	4.6	0.14
Sodium oleate 10 g/L	41.5	6.8	4.8	0.17
Sodium oleate 10g/L Thiourea 1 mM	33.0	7.3	5.2	0.11
Sodium oleate 10 g/L Urea 1 mM (mock control)	41.5	6.8	4.8	0.17

The L-lysine producing strain, WC196LC/pCABD2, was cultivated in a jar fermenter, and the intracellular H_2O_2 concentration was measured immediately after the exhaustion of carbon sources.

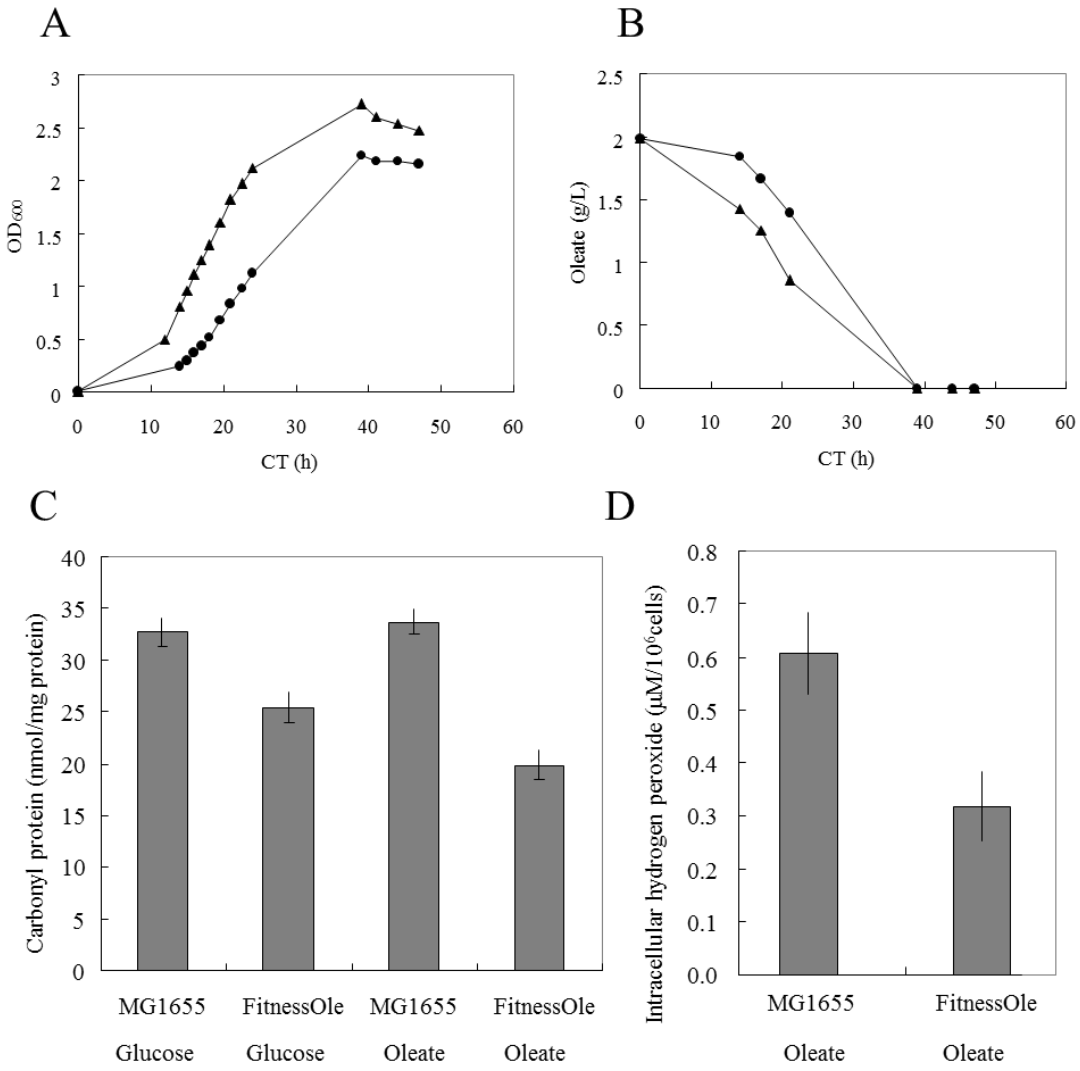

Figure 2-1 The physiological phenotypes of the FitnessOle strain. Cell growth (A) and residual oleate concentration (B) profiles were measured for MG1655 (●) and FitnessOle strains (▲). Carbonylated protein content (C) and intracellular hydrogen peroxide concentration (D) were also measured. Values are the mean of more than three independent samples. SE bars represent the standard error of the mean calculated with Excel software.

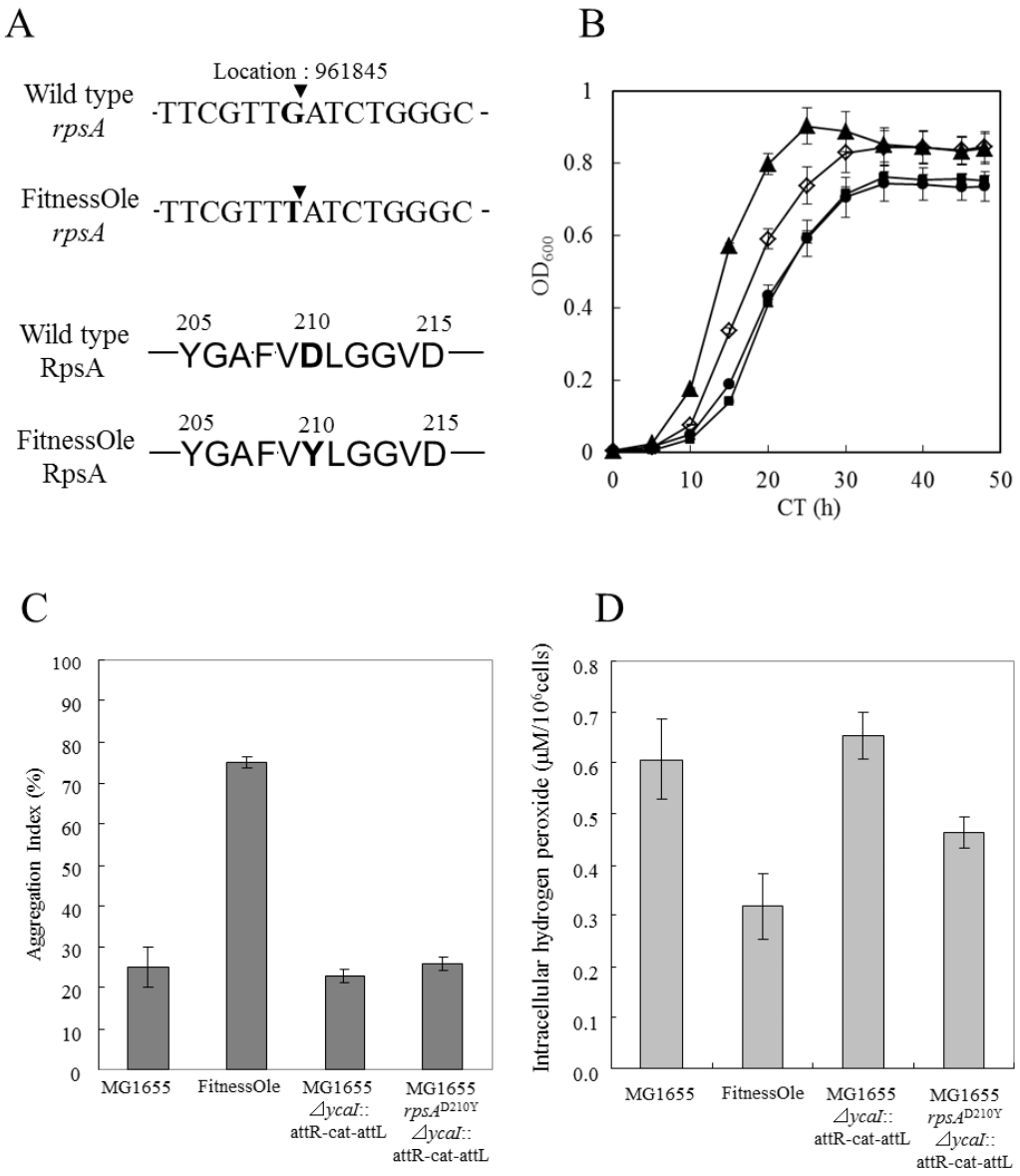

Figure 2-2 DNA and amino acid sequence of *rpsA*^{D210Y} mutation (A) and its effect on fatty acid utilization. (B) Growth of the *rpsA*^{D210Y} mutant strain in M9 medium test tube cultivation supplemented with sodium oleate as the sole carbon source. Parental strain MG1655 (●), FitnessOle strain (▲), MG1655 Δ*ycaI*::attR-cat-attL strain (■) and MG1655 *rpsA*^{D210Y} Δ*ycaI*::attR-cat-attL strain (◇)were monitored. Aggregation index (C) and intracellular hydrogen peroxide concentration (D) of cells cultivated in M9 medium

supplemented with sodium oleate as a sole carbon source were also measured. Values are the mean of more than three independent samples. SE bars represent the standard error of the mean calculated with Excel software.

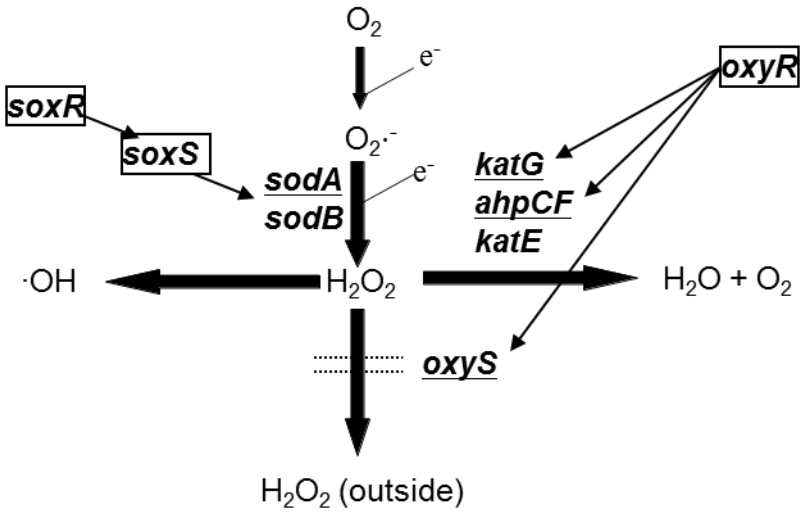

Figure 2-3 Schematic representation of ROS generation and elimination, and transcriptional regulation of ROS elimination systems in *E. coli*. Ordinary electron transfer to an oxygen molecule converting into a water molecule is catalyzed by cytochrome oxidases, but incomplete electron transfer to an oxygen molecule generates $O_2^{\cdot -}$, H_2O_2, and OH^-. These ROS molecules cause cell damage so *E. coli* possesses various ROS scavenger genes. Superoxide dismutases (SodA and SodB) convert $O_2^{\cdot -}$ into H_2O_2, which decomposes into harmless H_2O and O_2 with the aid of catalases KatG, KatE, and the alkyl hydroxiperoxide reductase AhpCF. Intracellular H_2O_2 excretion is promoted by small RNA *oxyS*. These ROS-scavenger genes are regulated by SoxR and OxyR. SoxR detects intracellular $O_2^{\cdot -}$ and upregulates SoxS expression. SoxR and SoxS activate $O_2^{\cdot -}$ decomposing genes such as *sodA* and *sodB*. OxyR is an intracellular H_2O_2 sensor and H_2O_2 removal-associated gene regulator. OxyR activates *oxyS* and H_2O_2-decomposing genes such as *katG*, *katE* and *ahpCF*.

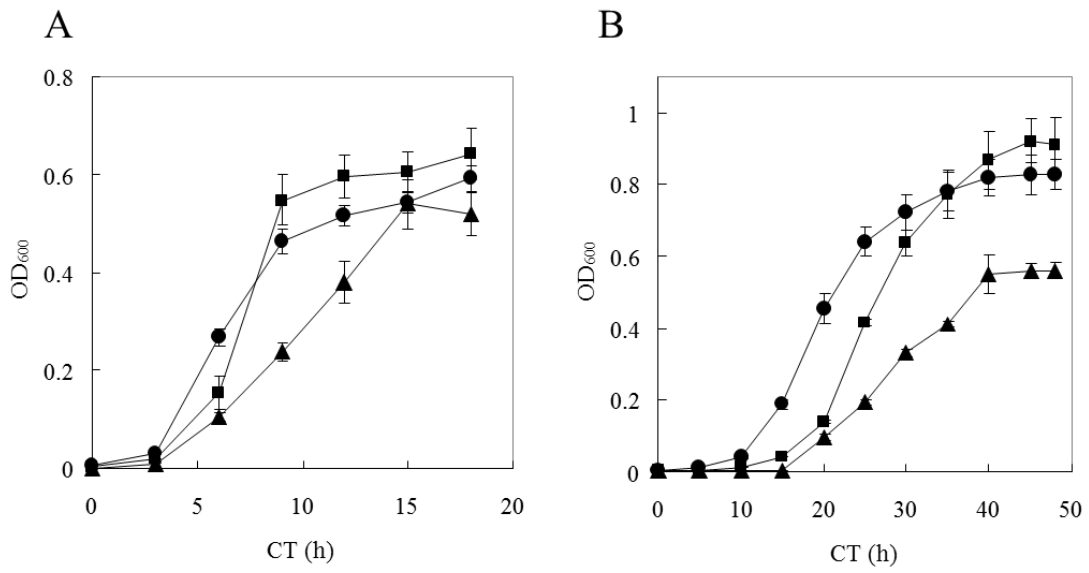

Figure 2-4 The effects of antioxidant transcription factor gene deletion. The growth of Δ*soxR* and Δ*oxyR* strains in M9 medium test tube cultivation supplemented with sodium glucose (A) or oleate (B) as the sole carbon source. Parental strain BW25113 (●), Δ*oxyR* strain (▲), and Δ*soxR* strain (■) were monitored. Values are the mean of more than three independent samples. SE bars represent the standard error of the mean calculated with Excel software.

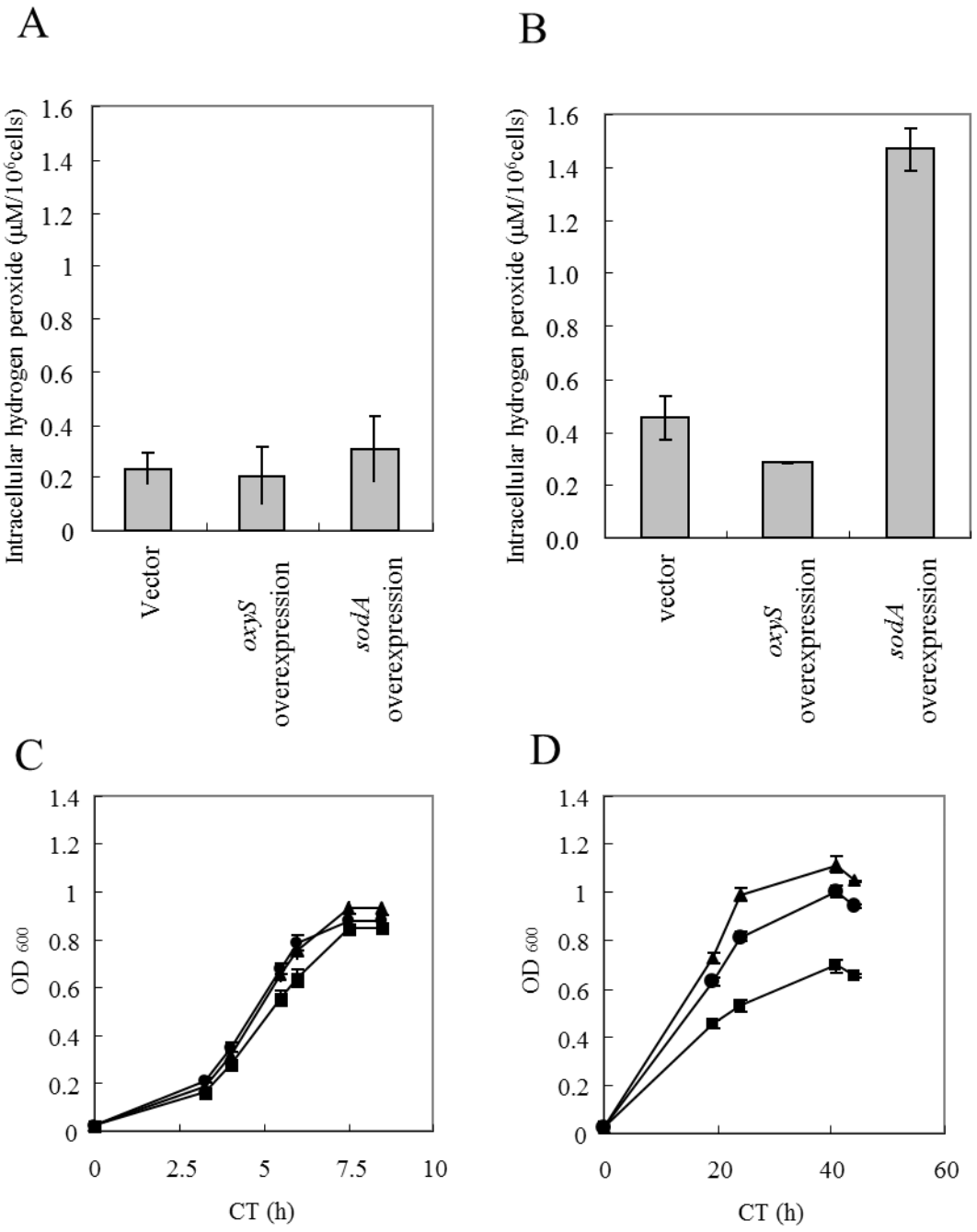

Figure 2-5 Effects of overexpression of *sodA* or *oxyS* genes. Intracellular hydrogen peroxide concentration of cells grown in M9 medium supplemented with glucose (A) or sodium oleate (B) as the sole carbon source. Cell growth using glucose (C) or sodium oleate (D) as the sole carbon source. Vector control MG1655/pTWV228 (●), *oxyS* overexpressing strain

MG1655/pTWV228-oxyS (▲) and *sodA* overexpressing strain MG1655/pTWV229-sodA (■) were studied. Values are the mean of more than three independent samples. SE bars represent the standard error of the mean calculated with Excel software. The Student's *t*-test between the intracellular hydrogen peroxide concentration of vector control samples and that of *oxyS* overexpression samples when grown on sodium oleate gave a *p*-value of 0.024.

Chapter 3 *Vibrio algivorus* sp. nov., an alginate and agarose assimilating bacterium isolated from the gut flora of a turban shell marine snail.

Abstract

An agarose and alginate assimilating, Gram-negative, non-motile, rod-shaped bacterium, designated strain SA2^T, was isolated from the gut of a turban shell sea snail (*Turbo cornutus*) collected near Noto Peninsula, Ishikawa Prefecture, Japan. The 16S rRNA sequence of strain SA2^T was 99.59 % identical to that of *Vibrio rumoiensis* DSM 19141^T, 98.19 % identical to that of *Vibrio litoralis* DSM 17657^T. This suggested that strain SA2^T could be a subspecies of *V. rumoiensis* or *V. litoralis*. However, DNA-DNA hybridization results showed only 37.5 % relatedness to DSM 19141^T and 44.7 % relatedness to DSM 17657^T, which was far lower than the 70 % widely accepted to define common species. Strain SA2^T could assimilate agarose as a sole carbon source, whereas strains DSM 19141^T and DSM 17657^T could not assimilate it at all. Furthermore, results using API 20NE and API ZYM kits indicated that their enzymatic and physiological phenotypes were also different. These results suggested that strain SA2^T represented a novel species within the genus *Vibrio*. The major isoprenoid quinone in SA2^T was Q-8 and its major polar lipids were phosphatidylethanolamine and phosphatidylglycerol. The major fatty acids were summed feature 3, (comprising $C_{16:1\omega6c}$ and/or $C_{16:1\omega7c}$), $C_{16:0}$, and summed feature 8 (comprising

$C_{18:1\omega6c}$ and/or $C_{18:1\omega7c}$). The DNA G + C content of SA2^T was 40.7 mol%. The name proposed for this novel *Vibrio* species is *Vibrio algivorus* sp. nov., with the type strain designated SA2^T (= DSM 29824^T = NBRC 111146^T).

Introduction

The genus *Vibrio* is part of the family *Vibrionaceae* (Baumann & Schubert, 1984), which belongs to the class *Gammaproteobacteria* (Baumann & Baumann, 1984). Members of the genus *Vibrio* are widespread, but are mainly found in the ocean and its inhabitants. At the time of writing, 114 species are recognized in the genus *Vibrio* (http://www.bacterio.net/vibrio.html). *Vibrio* spp. are known to decompose and assimilate components of seaweed, with reports of red algal agarose being degraded by some *Vibrio* agarases (Dong *et al*., 2006; Fu *et al*., 2008; Liao *et al*., 2011) and brown algal alginate being degraded and/or assimilated by some *Vibrio* alginate lyases (Sawabe *et al*., 1998; Kim *et al*., 2013; Badur *et al*., 2015). *Vibrio halitiocoli* is such an alginate-utilizing *Vibrio* species that was first isolated from the gut of the Japanese abalone, *Haliotis discus* (Sawabe *et al*., 1998). Further research has shown that *V. halitiocoli* also lives in the gut of the Japanese turban shell, *Turbo cornutus* (Sawabe *et al*., 2003). Recent studies have suggested that red algal agarose and brown algal alginate are candidates for novel sustainable resources for fermentative production processes (Wargacki *et al*., 2012; Youngdeuk *et al*., 2013). I therefore initiated studies to isolate novel *Vibrio* strains that can degrade and assimilate both agarose and alginate from the gut of the Japanese turban shell, *T. cornutus* and isolated a novel strain which can utilize both alginate and agarose (Table 3-1).

Material and Methods

Isolation of SA2^T strain

I purchased a live turban shell caught near the Noto Peninsula, Japan (N: 37°09’ E: 137°05’). I broke the outer shell and diluted about 10 μl of the gut microflora in 20 ml of autoclaved artificial seawater (Daigo’s Artificial Seawater SP for Marine Microalgae Medium; Wako Pure Chemical Industries, Japan). I then diluted it 10^6-fold with autoclaved artificial seawater and spread 50 μl of the diluted solution on a minimal medium plate containing alginate and agar (Table 3-2). After incubation for 75 h at 25 °C, I obtained more than 100 colonies. Each colony was transferred into 10 ml of 0.85 % NaCl, spread onto minimal medium plates and incubated for 50 h at 37 °C. I then picked the largest colony, spread it on a minimal medium plate, and incubated it for 15 h at 37 °C. I then picked the fastest growing colony and named it strain SA2^T.

Pysiological and Biochemical properties tests For physiological phenotyping, I used API 20NE and API ZYM kits (bioMérieux, Marcy l'Etoile, France). I checked the other physiological characteristics of strain SA2^T following the method for bacterial identification reported by Barrow & Feltham (1993). I checked the carbon sources utilizable by SA2^T, *V. rumoiensis* DSM 19141^T and *V. litoralis* DSM 17657^T by expanding cell numbers on LB plates supplemented with 30 g/l NaCl for 20 h at 30 °C. Approximately 5 μl of these cell

cultures were then inoculated into 5 ml M9 minimal medium supplemented with 1 mM $MgSO_4$, 0.1 mM thiamine, 30g/l NaCl and either sodium alginate or sucrose or D-xylose or D-galactose at 3 g/l as a carbon source, in L-shaped test tubes. These cultures were grown for 72 h at 30 °C with constant shaking at 70 r.p.m. using a TVS062CA rocking incubator (Advantec, Tokyo, Japan). If the optical density at 600 nm exceeded 0.1 after 72 h, the bacterium was classed as able to use a carbon source. To assess agarose utilization, I prepared M9 plates supplemented with 1 mM $MgSO_4$, 0.1 mM thiamine and 30 g/l NaCl, with 10 g/l agarose as the only carbon source. I streaked about 5 μl of cells on these plates and cultured them for 72 h at 30 °C. If it was able to form colonies over 1 mm in diameter, the bacterium was classed as able to use agarose.

To clarify the temperature conditions in which $SA2^T$ could grow, I cultured it in LB medium containing 15 g/l NaCl in static culture for one week at different temperatures. To clarify the pH conditions in which $SA2^T$ could grow, I cultured $SA2^T$ in a test tube in 4 mL of LB medium containing 15 g/l NaCl and 45 mM MES (2-Morpholinoethanesulfonic acid) buffer sterilized with filtration for 2 days at 30 °C with shaking 120 rpm, at different pHs, which were established by adding HCl or NaOH. I measured the pH before and after cultivation with pH meter F-52 (HORIBA, Kyoto, Japan) to check that the pHs are maintained. To assess NaCl tolerance, I grew $SA2^T$ in LB medium containing different concentrations of NaCl in static culture for one week. I analysed the motility of $SA2^T$ by

observing colony edges on LB plates containing 15 g/l NaCl at 30 °C (Perry, 1973) and hanging drops in marine broth 2216 cultures at 30 °C (Bernardet *et al*., 2002) using a BX50F4 optical microscope (Olympus, Japan).

Molecular Phylogenetic analysis

I expanded SA2^T on LB medium supplemented with 15 g/l NaCl for 15 h at 37 °C and extracted genomic DNA using the PurElute Bacterial Genomic Kit (Edge BioSystems, MD, USA). Genomic DNA was analysed by whole-genome sequencing using an Illumina Genome Analyzer II (GAII; Illumina Inc., CA, USA). I identified the 16S rRNA gene sequence and its housekeeping gene sequences within the draft whole-genome sequence using a BigDye terminator v3.1 Cycle Sequencing kit and an ABI PRISM 3130 x1 Genetic Analyzer System (Applied Biosystems, CA, USA). The *rpoD* sequences are amplified by PCR using 70F and 70R primers and *Taq* polymerase (repeating 30 amplification cycles: the amplification cycle at 94 °C for 60 seconds for denaturing, at 59 °C for 45 seconds for annealing, at 72 °C for 2 minutes for extension) and identified (Table 3-3, Yamamoto & Harayama, 1998). I constructed phylogenetic trees based on *Vibrio* housekeeping genes (Table 3-3) by the neighbour joining method (Fig. 3-1; Saitou *et al*., 1987) using MEGA ver. 5.0 software (Tamura *et al*. 2011). The genes were jointed in the order of *atpA*, *pyrH*, *recA*, *rpoA*, *rpoD* and 16S rRNA. DNA substitution was performed using the Jukes Cantor model (Jukes and

Cantor 1969). Confidence levels of each branch are indicated by bootstrap percentages, which are calculated using 1000 repetitions (Felsenstein, 1985). Next, I constructed another phylogenetic tree based on genus *Vibrio* housekeeping genes by the maximum parsimony method (Fig. 3-2; Eck & Dayhoff, 1966; Fitch, 1971; Nei & Kumar, 2000) using MEGA ver. 5.0 software (Tamura *et al*., 2011) and the parameter: Min-Mini Heuristic model. Confidence levels of each branch are indicated by bootstrap percentages, which are calculated using 1000 repetitions (Felsenstein, 1985). I constructed the third phylogenetic tree based on *Vibrio* housekeeping genes by the maximum likelihood method (Fig. 3-3; Felsenstein, 1981) using MEGA ver. 5.0 software (Tamura *et al*., 2011) and the parameter: General Time Reversible model (+I +G). Confidence levels of each branch are indicated by bootstrap percentages, which are calculated using 1000 repetitions (Felsenstein, 1985). I finally constructed phylogenetic trees based on individual *Vibrio* housekeeping genes using the neighbour joining method (Fig. 3-4, 3-5, 3-6, 3-7, 3-8 and 3-9) using MEGA ver. 5.0 software (Tamura *et al*., 2011) and the Jukes Cantor model (Jukes & Cantor, 1969). Confidence levels of each branch are indicated by bootstrap percentages, which are calculated using 1000 repetitions (Felsenstein, 1985).

DNA-DNA hybridization test

I performed DNA-DNA hybridization tests using a published method (Ezaki *et al*.,

1989). Briefly, I expanded the cells on LB medium supplemented with 15 g/l NaCl for 30 h at 30 °C and extracted genomic DNA using the PurElute Bacterial Genomic Kit (Edge BioSystems, MD, USA). Probe genomic DNA was diluted to 100mg/L and sonicated. After sonication, the probe DNA was heated for 10 minutes at 99.5 °C to denature to single-strand DNA.100µl of the probe DNA was immobilized on each well of NUNC-IMMUNO PLATE (Catalog Number:439454, Thermo Fisher Scientific, Waltham, MA, USA).Sample genomic DNA was sonicated and denatured on the same condition after labelling by photobiotin solution (Sigma-Aldrich, St. Louis, MO, USA). The denatured DNA was diluted in DNA hybridization solution (2 x SSC solution, 1 x Denhard's solution, 0.1mg/L denatured salmon DNA, 50 % formamide, 3 % dextran sulfate) and added on each immobilezed probe DNA. DNA sample was hybridized for 180 minutes at 41°C. D-galactosidase-streptavidin solution at 100µl was added after washing and incubated for 10 minutes at 37°C. 4-methylumbelliferyl-beta-D-galactopyranoside (in 0.1% PBS) at 100µl was added after washing and incubated for 15 minutes at 37 °C. The fluorescence intensity was measured with the GENios plate reader (Tecan, Switzerland). The fluorescence intensity to Calf thymus DNA (Sigma-Aldrich, St. Louis, MO, USA) was used as the negative control (0%). The fluorescence intensity to the same strain's genomic DNA was used as the positive control (100%).

Average Nucleotide Identity (ANI) test

I calculated ANI values with the online calculation tool at the EzGenome (http://www.ezbiocloud.net/ezgenome/ani , Goris *et al*., 2007). I calculated OrthoANI values with the published algorithm (Lee *et al*., 2015).

The Digital DNA-DNA hybridization test

Digital DNA-DNA hybridization tests were performed with GGDC 2 (http://ggdc.dsmz.de/distcalc2.php, Meier-Kolthoff *et al*. 2013).

Electron microscopy

For scanning electron microscopy (SEM), $SA2^T$ was fixed using the t-butyl alcohol freeze-drying method (Inoué & Osatake, 1998) and scanned with a JSM-6340F electron microscope (JEOL, Tokyo, Japan).

Analysis of Quinone, Fatty acids and Polar lipids

I extracted and purified isoprenoid quinones using a previously reported method (Collins, 1994), after growing $SA2^T$ on marine broth 2216 plates at 30 °C for 24 h. When the extract was analysed by HPLC and the quinone species were identified using previously reported method (Tamaoka *et al*., 1983). For fatty acid extractions and measurements, I used

the methodology described in the Sherlock^{TM} Microbial Identification System, version 6.0 manual (MIDI Inc., DE, USA) after growing SA2^{T}, *V. rumoiensis* DSM 19141^{T}, *V. litoralis* DSM 17657^{T} and *V. casei* DSM 22364^{T} on marine broth 2216 plates at 30 °C for 24 h. To determine the predominant polar lipids in SA2^{T}, I extracted them using the method reported by Bligh & Dyer (1959), after growing SA2^{T} on marine broth 2216 plates at 30 °C for 24 h. I identified the predominant polar lipids using liquid chromatography quadrupole time-of-flight mass spectrometry (LC-QTOF/MS; Mal & Wong S, 2011) with previously reported identification method (Mazzella *et al*., 2004). I also performed thin layer chromatography analysis (Minnikin *et al*., 1979) to determine the predominant polar lipids in SA2^{T}.

Results

Strain SA2^T could grow on marine broth 2216 medium (Becton Dickinson, MD, USA), LB medium containing 15 g/l NaCl or M9 medium (Miller,1992) containing 5 g/l sodium alginate and 15 g/l NaCl. It also showed a Gram-negative phenotype on LB plates containing 15 g/l NaCl. In my analysis, strain SA2^T was catalase- and oxidase-positive, glucose-fermenting and susceptible to 150 μg of the vibriostatic agent O/129 (2,4-diamino-6,7-diisopropylpteridine). In the oxidative-fermentative test, strain SA2^T showed both oxidative and fermentative phenotypes.

I looked for bacterial species closely related to SA2^T by using the EzTaxon server (http://www.ezbiocloud.net/eztaxon; Kim *et al*., 2012). On the basis of 16S rRNA similarity, the closest bacterial species were *Vibrio rumoiensis* DSM 19141^T (= S -1^T; Yumoto *et al*., 1999), which was 99.59 % similar to strain SA2^T, and *Vibrio litoralis* DSM 17657^T (= MANO22D^T; Nam *et al*., 2007), which was 98.19 % identical (Table 3-4). Most of the phylogenetic trees, with the exception of those based on 16S rRNA and *pyrH* genes, indicated that strain SA2^T was phylogenetically closer to *V. litoralis* DSM 17657^T than to *V. rumoiensis* DSM 19141^T (Fig. 3-1, 3-2, 3-3, 3-5, 3-7, 3-8 and 3-9) and confirmed that it belonged to the genus *Vibrio*. Strain SA2^T is phylogenetically close to *V. litoralis* DSM 17657^T, *V. rumoiensis* DSM 19141^T and *Vibrio casei* DSM 22364^T (Bleicher *et al.*, 2010).

It has been proposed that two bacterial strains should be considered to belong to different species if the identity of their 16S rRNA gene sequences is below 98.7 % (Stackebrandt & Goebel, 2006). A more recent study has shown that a 98.65 % 16S rRNA gene sequence similarity can be used as the threshold for differentiating two species (Kim *et al*., 2014). Therefore, *Vibrio* sp. strain SA2^T could belong to the *V. rumoiensis* species (Table 4). To clarify the relatedness of SA2^T and *V. rumoiensis* DSM 19141^T, three independent DNA-DNA hybridization tests were performed using a published method (Ezaki *et al*., 1989). The DNA-DNA relatedness between SA2^T and *Vibrio rumoiensis* DSM 19141^T was only 37.5 %, compared to the 70 % DNA-DNA relatedness by hybridization, which has been suggested as the level below which two bacterial strains can be defined as belonging to different species (Wayne *et al*., 1987). Three independent DNA-DNA hybridization tests were also performed between SA2^T and *V. litoralis* DSM 17657^T. The DNA-DNA relatedness between them was only 44.7 %. Thus, I concluded that SA2^T strain should be classified as a different species from both *V. rumoiensis* and *V. litoralis.* The results from the DNA-DNA hybridization test also showed that SA2^T was most closely related to *V. litoralis* phylogenetically, as had the phylogenetic tree analysis. Preliminary ANI values between SA2^T and *Vibrio litoralis* DSM17657^T were 88.02-88.12%. Preliminary ANI values between SA2^T and *V. rumoiensis* DSM 19141^T were 76.76-76.92%. These preliminary ANI results also supported that SA2^T strain should be classified as a different species from both *V.*

rumoiensis and *V. litoralis.* And OrthoANI values between SA2^T and *Vibrio litoralis* DSM17657^T were 88.06-88.46%. OrthoANI values between SA2^T and *V. rumoiensis* DSM 19141^T were 76.78-77.63%. In addition, the preliminary digital DNA-DNA hybridization tests were performed with GGDC 2 (Meier-Kolthoff *et al*. 2013). All of the digital DNA-DNA hybridization values among these species were less than 70% and the value between SA2^T strain and *V. litoralis* was higher than that between SA2^T strain and *V. rumoiensis*.

Electron micrographs showed that *Vibrio* sp. SA2^T was a slightly curved, rod-shaped bacterium with no blebs (Fig. 3-10). In contrast, *V. rumoiensis* DSM 19141^T showed some clear blebs on its cell surface in electron micrographs (Yumoto *et al.*, 1999). I observed colony edges (Perry, 1973) and hanging drops (Bernardet *et al*., 2002). Both tests were unable to detect any motility in SA2^T.

V. rumoiensis DSM 19141^T and *V. litoralis* DSM 17657^T have differential characteristics with respect to the carbon sources they can utilize (Yumoto *et al.*, 1999 & Nam *et al*., 2007). I therefore checked the carbon sources utilizable by SA2^T, *V. rumoiensis* DSM 19141^T and *V. litoralis* DSM 17657^T. Both *V. rumoiensis* DSM 19141^T and *V. litoralis* DSM 17657^T could utilize D-xylose as a sole carbon source, but SA2^T could not (Table3-1). Only SA2^T could grow on the plates containing agarose as the only carbon source (Table3-1). The predominant isoprenoid quinone in SA2^T was Q-8 (Fig. 3-11). Q-7 and MK-8 were also detected (Fig. 3-11). The other ubiquinones and the other menaquinones were not

determined.

The predominant fatty acids in all four species were summed feature 3 (comprising $C_{16:1\omega6c}$ and/or $C_{16:1\omega7c}$), $C_{16:0}$ and summed feature 8 (comprising $C_{18:1\omega6c}$ and/or $C_{18:1\omega7c}$; Table 3-5). This result suggested that SA2^T was closely related to *V. litoralis*, *V. rumoiensis* and *V. casei***.** The LC-QTOF/MS results showed that the major phospholipids of SA2^T were phosphatidylethanolamine and phosphatidylglycerol (Fig. 3-13). The thin layer chromatography analysis results also showed that the major polar lipids in SA2^T were phosphatidylethanolamine and phosphatidylglycerol (Fig. 3-12).

SA2^T showed different enzymatic and physiological characteristics from those previously reported for *V. rumoiensis* DSM 19141^T and *V. litoralis* DSM17657^T with APIZYM kit and API 20 NE kit (Table 3-1). Among these three phylogenetically related *Vibrio* strains, β-galactosidase activity was observed only in *Vibrio* sp. SA2^T (Table 3-1). Esterase lipase (C8) activity was negative only in *Vibrio* sp. SA2^T (Table 3-1).

Discussion

I showed that SA2^T is a Gram negative, oxidative, and fermentative phenotypes. This spectrum of characteristics was specific to the genus *Vibrio*. The similarity of the 16S rRNA and the housekeeping genes of SA2^T also supported that SA2^T belongs to the genus *Vibrio*. MLSA analysis results showed that SA2^T belongs to the *V. rumoiensis* clade (Sawabe et al., 2013)

DNA-DNA hybridization results showed only 37.5 % relatedness to DSM 19141^T and 44.7 % relatedness to DSM 17657^T, which was far lower than the 70 % widely accepted to define common species. It suggested that SA2^T strain can be classified as a different species from both *V. rumoiensis* and *V. litoralis*. The predicted DNA-DNA hybridization results (ANI, OrthoANI and GGDC) also supported it. In conclusion, strain SA2^T belongs to no previously reported *Vibrio* species. Therefore, I named it *Vibrio algivorus* sp. nov. as the novel alginate-utilizable *Vibrio* species. I prepared the physiological and biochemical characteristics data for the Description of *Vibrio algivorus* sp. nov. following a standardized format for the description of the genus *Vibrio* and proposed it.

Description of *Vibrio algivorus* sp. nov.

Vibrio algivorus [al.gi.vo'rus]. (L. fem. n. *alga*, seaweed and also a botanical name, Algae; L. suff. -*voro* (from L. vorare, to devour); *algivorus*, algae-devouring.).

Cells are Gram-negative, slightly curved rods that are 0.7 – 0.8 μm wide and 1.5 – 2.5 μm long. They do not have blebs and are not motile on marine broth 2216 plates (Becton Dickinson, MD, USA) or in liquid media. Colonies on marine broth 2216 plates are pale yellow, smooth, round in shape and measure 2.0 – 3.0 mm in diameter after 24 h culture at 30 °C. Cells can grow at 4 - 40 °C and pH 5.5 – 9.5. Optimal growth is observed at 25 - 30 °C and pH 7 – 8. Cells can grow in the presence of 1 – 14 % NaCl, but not in the absence of NaCl or at a concentration of 15 %. Cells are susceptible to the vibriostatic agent O/129. They are oxidase-positive and catalase-positive. They are facultatively anaerobic and reduce nitrate to nitrite. Indole production is not observed. Using API 20NE tests (bioMérieux, Marcy l'Etoile, France), glucose, gluconate, and malate can be used as sole carbon and energy sources, but arabinose, mannose, mannitol, N-acetylglucosamine, maltose, n-capric acid, dipic acid and citrate cannot. API ZYM tests show alkaline phosphatase, esterase (C4), leucine arylamidase, valine arylamidase, acid phosphatase, naphthol-AS-BI-phosphohydrolase, β-galactosidase, and N-acetyl-β-glucosaminidase activities. Esterase lipase (C8), arginine dihydrolase, lipase (C14), cystine arylamidase, trypsin, chymotrypsin, α-galactosidase, β-glucuronidase, α-glucosidase, β-glucosidase, α-mannosidase and α-fucosidase activities are not present. On M9 minimal medium supplemented with 15g/l NaCl, glucose, agarose, alginate and D-galactose can be used as sole carbon and energy sources. The

DNA G + C content of the strain is 40.7 %. The predominant isoprenoid quinone is Q-8. Q-7 (below 5%) and MK-8 (below 20%) are also contained. The major polar lipids are phosphatidylethanolamine and phosphatidylglycerol. The major fatty acids are summed feature 3 (comprising $C_{16:1\omega6c}$ and/or $C_{16:1\omega7c}$), $C_{16:0}$ and summed feature 8 (comprising $C_{18:1\omega6c}$ and/or $C_{18:1\omega7c}$).

The type strain, $SA2^T$ (= $DSM29824^T$, = $NBRC111146^T$) was isolated from the gut of a turban shell, *Turbo cornutus*, caught near Noto Peninsula, Ishikawa Prefecture, Japan.

Tables and Figures

Table 3-1. Differential physiological characteristics of strain SA2^T from relate species. Strains: 1, SA2^T (= DSM 29824^T,= NBRC 111146^T); 2, *V. litoralis* DSM 17657^T; 3, *V. rumoiensis* DSM 19141^T; 4, *V. casei* DSM 22364^T**.** All data were obtained in this study where indicated *.

Characteristic	1	2	3	4
Growth at 39℃	+	+	−	−
Growth in 12% NaCl	+	+	−	−
Utilization (on Minimal medium) of:				
Agarose	+	−	−	−
Sodium Alginate	+	+	−	−
Sucrose	−	−	+	+
D-Xylose	−	+	+	+
D-Glucose Fermentation	+	+	−	−
Aesculin hydrolysis	−	−	+	+
Esterase lipase (C8) activity	−	+	+	+

Valine arylamidase activity	+	+	−	−
β-Galactosidase activity	+	−	−	+
The DNA G + C content (mol%)	40.7	41.9	41.1	41.8*

*: this G + C content result of *V. casei* DSM 22364^T obtained from Bleicher *et al*., 2010

Table 3-2. The composition of minimal medium plates containing alginate and agar.

Component	Final Concentration
Sodium Alginate	5 g/L
Na_2HPO_4	6 g/L
KH_2PO_4	3 g/L
NaCl	0.5 g/L
NH_4Cl	1 g/L
NaCl	21.247 g/L
$MgSO_4 \cdot 7H_2O$	0.246 g/L
Thiamine•HCl	10 mg/L
$MgCl_2 \cdot 6H_2O$	9.474 g/L
$CaCl_2 \cdot 2H_2O$	1.328 g/L
Na_2SO_4	3.505 g/L
KCl	0.597 g/L
$NaHCO_3$	0.171 g/L
KBr	0.085 g/L
$Na_2B_4O_7 \cdot 10H_2O$	0.034 g/L
$SrCl_2$	0.012 g/L

NaF	3 mg/L
LiCl	1 mg/L
KI	0.07 mg/L
$CoCl_2 \cdot 6H_2O$	0.0002 mg/L
$AlCl_2 \cdot 6H_2O$	0.008 mg/L
$FeCl_3 \cdot 6H_2O$	0.006 mg/L
$Na_2WO_4 \cdot 2H_2O$	0.0002 mg/L
$(NH_4)_6Mo_7O_{24} \cdot 4H_2O$	0.0008 mg/L
Bacto Agar	15 g/L

Table 3-3. Sequences used for phylogenetic analysis.

Species	Accession No. (GenBank/DDBJ/EMBL)					
	atpA	*pyrH*	*recA*	*rpoA*	*rpoD*	16S rRNA
Vibrio algivorus sp. nov, SA2^T (=DSM 29824^T, =NBRC 111146^T)	LC060681*	LC060682*	LC060683*	LC060684*	LC060685*	LC060680*
Vibrio alginolyticus LMG 4409^T	EF601231	GU266285	AJ842373	AJ842558	FM202535	X56576
Vibrio brasiliensis LMG 20546^T	EF601320	HM771374	AJ842376	HM771384	AEVS01000072	HM771338
Vibrio campbellii DSM 19270^T	EF601232	EF596641	AJ842377	AJ842564	FM202508	X56575
Vibrio casei DSM 22364^T	FJ968711	FJ968720	FJ968714	FJ968717	LC060686†	FJ968722
Vibrio chagasii LMG 21353^T	EF601280	EU118252	AJ842385	AJ842572	AY751356	AJ316199

Vibrio cholerae						
	EF601300	EF990257	AJ842386	AJ842573	AM942060	X76337
LMG 21698^{T}						
Vibrio coralliilyticus						
	JN039158	GU266292	AJ842402	AJ842587	ACZN01000013	AJ440005
LMG 20984^{T}						
Vibrio gigantis						
	EU541556	EU871951	EU541593	EU541573	AY751347	EF094888
LMG 22741^{T}						
Vibrio halioticoli						
	EF601260	EU871952	EU871966	AJ842617	BAUJ01000027	AB000390
LMG 18542^{T}						
Vibrio harveyi						
	BAOD01000015	EU118238	AJ842440	AJ842627	FM202498	X74706
ATCC 14126^{T}						
Vibrio ichthyoenteri						
	EF601262	HM771375	AJ842446	HM771385	HF679140	AJ437192
LMG 19664^{T}						
Vibrio lentus						
	EU541558	JX401842	AJ842452	AJ842639	AY751358	AJ278881
LMG 21034^{T}						
Vibrio litoralis						
	FJ968710	AUFZ01000011	FJ968713	FJ968716	LC060687 †	DQ097523
DSM 17657^{T}						
Vibrio mediterranei						
	EF601242	GU266288	AJ842459	AJ842644	HF542043	X74710
ATCC 43341^{T}						

Vibrio orientalis LMG 7897^{T}	EF601341	EU118243	AJ842485	AJ842672	HF542105	X74719
Vibrio parahaemolyticus ATCC 17802^{T}	EF601274	EU118240	AJ842490	AJ842677	FM202531	AF388386
Vibrio proteolyticus LMG 3772^{T}	EF601259	BATJ01000010	AJ842499	AJ842686	HE805638	X74723
Vibrio rotiferianus LMG 21460^{T}	EF601340	EF596722	AJ842501	AJ842688	FM202525	AJ316187
Vibrio rumoiensis DSM 19141^{T}	EF601329	‡	AJ842503	AJ842690	LC060688 †	AB013297
Vibrio scophthalmi LMG 19158^{T}	EF601261	HM771376	AJ842505	HM771386	HF679141	U46579
Vibrio tapetis LMG 19706^{T}	HE795159	HE795189	HE795219	AJ842730	HF542104	Y08430
Vibrio vulnificus LMG 13545^{T}	AMQV01000037	GQ382226	AJ842523	AJ842737	HE805634	X76333

Enterovibrio						
norvegicus	EF601330	JF739391	AJ842348	AJ842531	AM942062	AJ316208
LMG 19839^{T}						
Grimontia hollisae						
	EF601247	JF739393	AJ842351	AJ842535	AM942061	AJ514909
LMG 17719^{T}						

* Identified by whole genome sequencing and Sanger DNA sequencing in this study.

† Identified by degenerate PCR (Yamamoto & Harayama, 1998) in this study.

‡ Sequence of *pyrH* of *Vibrio rumoiensis* retrieved from The Taxonomy of the Vibrios website (http://www.taxvibrio.lncc.br/).

Table 3-4. Comparison of 16S rRNA sequences from *Vibrio algivorus* sp. nov. SA2^T(= DSM29824^T, = NBRC111146^T) and other *Vibrio* species.

Species (Type strain GenBank/EMBL/DDBJ Accession Number)	% Pairwise Similarity
Vibrio algivorus SA2^T (LC060680)	100.00
Vibrio rumoiensis DSM 19141^T (AB013297)	99.59
Vibrio litoralis DSM 17657^T (DQ097523)	98.19
Vibrio casei DSM22364^T (FJ968722)	98.02

Table 3-5. Fatty acid content after growth for 24 h at 30 °C on marine broth 2216 plates. Strains: 1, SA2^T strain (= DSM 29824^T,= NBRC 111146^T); 2, *V. litoralis* DSM 17657^T; 3, *V. rumoiensis* DSM 19141^T; 4, *V. casei* DSM 22364^T; n.d.: not determined. All data were obtained in this study.

Fatty acid content (%)	1	2	3	4
$C_{12:0}$	3.9	3.9	3.9	4.3
$C_{12:0\ 2OH}$	n.d	n.d	n.d	0.3
$C_{12:0\ 3OH}$	0.1	n.d	n.d	3.6
$C_{14:0}$	1.7	1.8	4.7	2.1
$C_{14:0\ iso\ 3OH}$	n.d	n.d	n.d	0.1
$C_{15:0}$	n.d	n.d	n.d	n.d
$C_{16:0}$	28.0	23.2	26.0	22.6
$C_{16:0\ iso}$	n.d	0.5	0.2	0.3
$C_{16:0\ 3OH}$	1.2	0.6	1.1	n.d
$C_{16:1\ \omega 9c}$	0.0	n.d	0.0	0.9
$C_{17:0}$	0.6	1.1	0.4	0.7
$C_{17:1\ \omega 8c}$	n.d	0.5	0.3	0.7

$C_{18:0}$	2.0	3.2	1.6	2.2
$C_{18:0\ iso}$	n.d	0.4	n.d	0.4
$C_{18:1\ \omega 9c}$	0.9	0.9	1.2	2.3
$C_{20:1\ \omega 7c}$	0.2	0.4	n.d	0.4
Summed feature 2*	9.0	9.5	8.8	3.9
Summed feature 3†	38.2	40.1	38.2	39.4
Summed feature 8‡	14.3	14.1	13.5	15.3

*Summed feature 2 comprising one of more of $C_{12:0\ aldehyde}$, $C_{14:0\ 3OH}$ and/or $C_{16:1\ iso}$

†Summed feature 3 comprising $C_{16:1\omega 6c}$ and/or $C_{16:1\omega 7c}$,.

‡Summed feature 8 comprising $C_{18:1\omega 6c}$ and/or $C_{18:1\omega 7c}$.

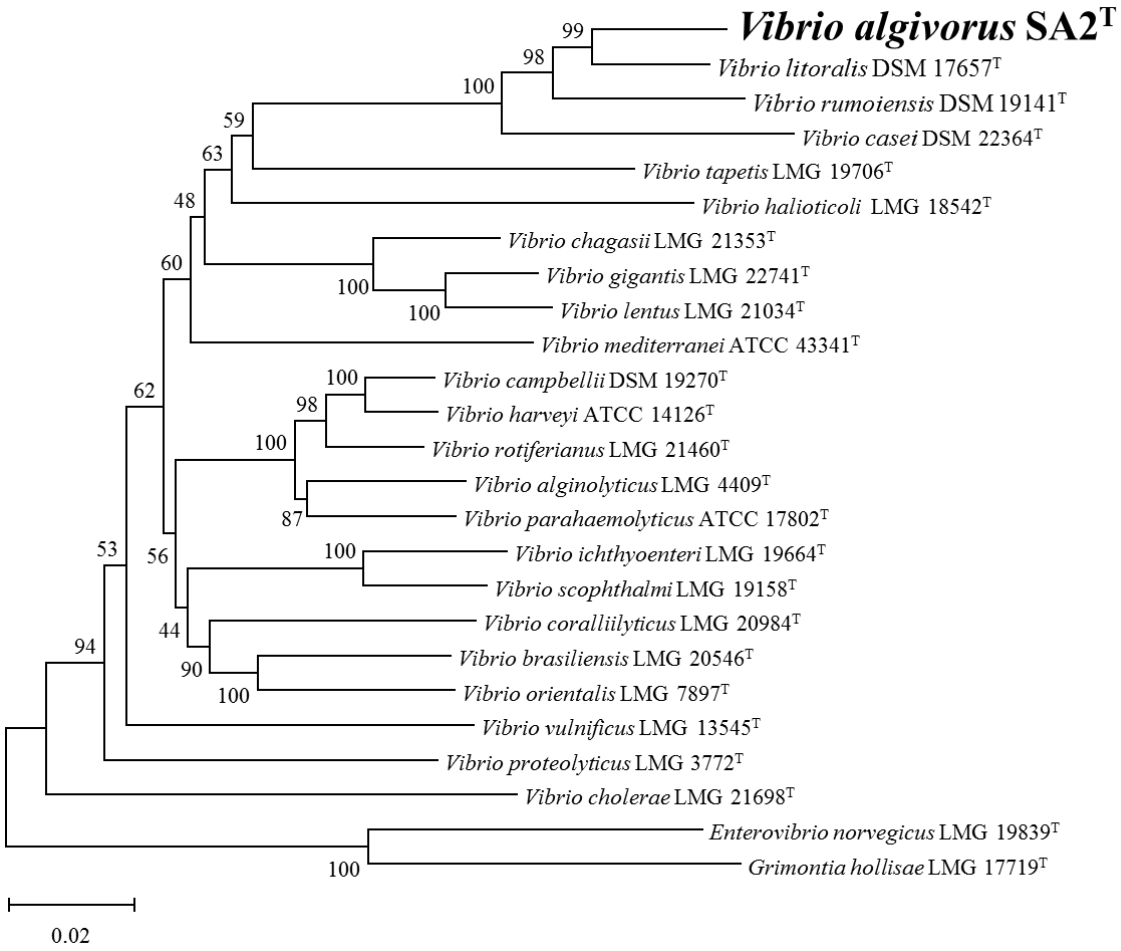

Figure 3-1.

Phylogenetic tree showing the relationships of *Vibrio algivorus* sp. nov. SA2^T using multi-locus sequence analysis (MLSA) based on *Vibrio* housekeeping genes, *atpA*(1542 bp), *pyrH* (735 bp), *recA* (1047 bp), *rpoA* (993 bp), *rpoD* (1842 bp) and 16S rRNA (1492 bp). Bar, 2 substitutions per 100 nucleotide positions.

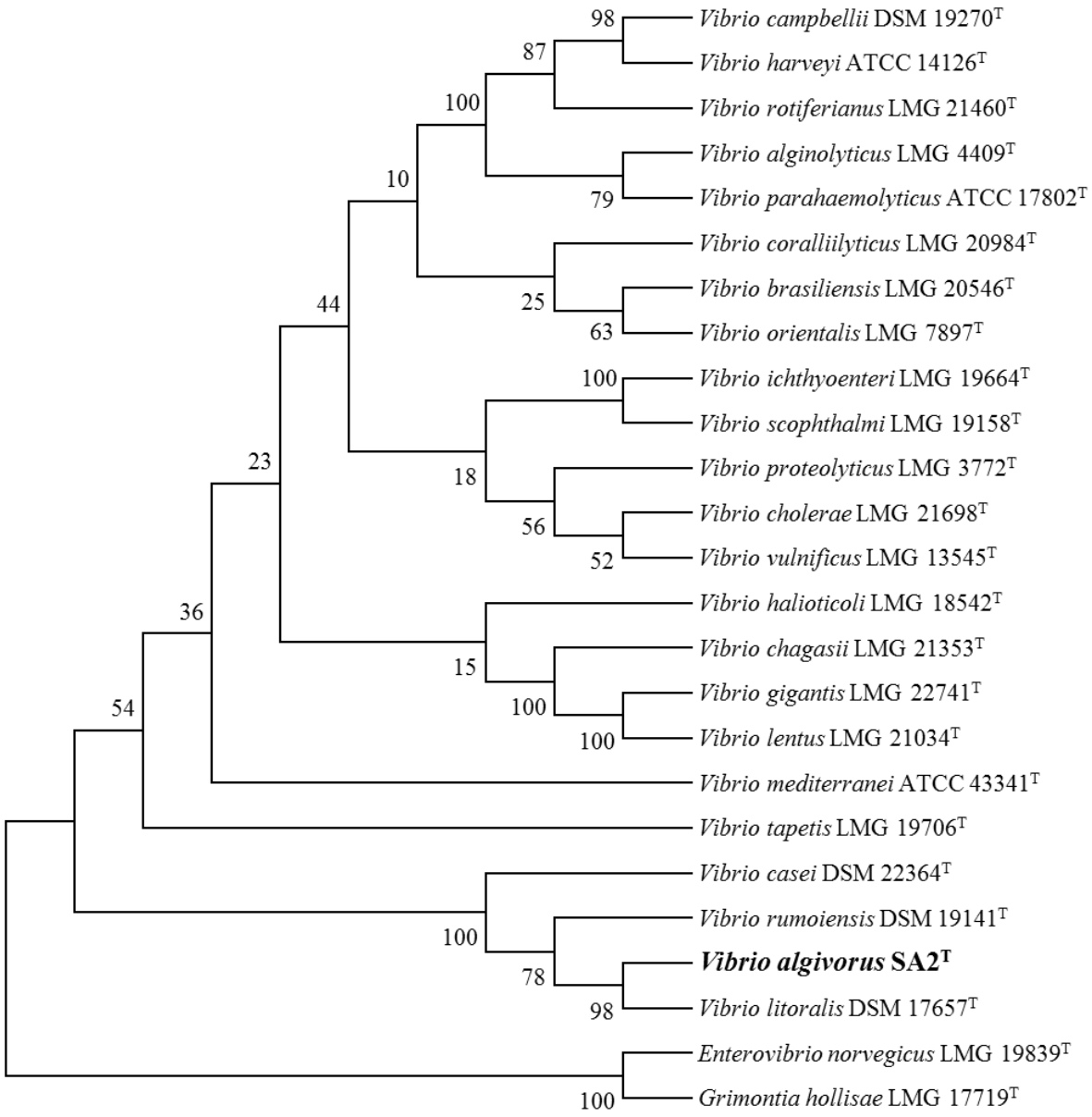

Figure 3-2. Phylogenetic tree showing the relationships of *Vibrio algivorus* sp. nov. SA2^T using MLSA) based on *Vibrio* housekeeping genes withthe maximum parsimony method (Eck & Dayhoff ,1966; Fitch, 1971; Nei & Kumar,2000). Bar, 2 substitutions per 100 nucleotide positions.

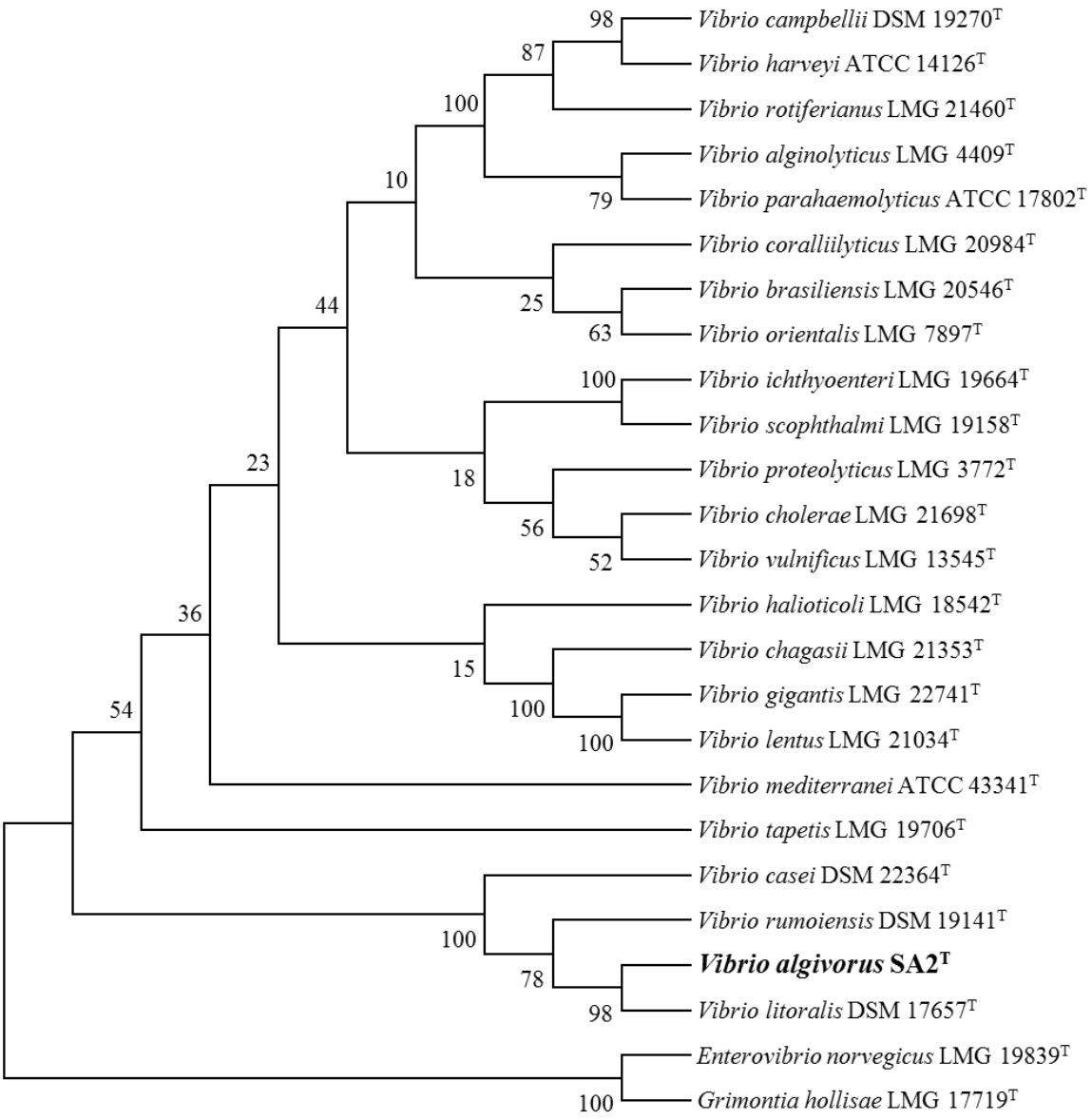

Figure 3-3. Phylogenetic tree showing the relationships of *Vibrio algivorus* sp. nov. SA2^T using Multi-locus Sequence Analysis (MLSA) based on *Vibrio* housekeeping genes, *atpA* (1542 bp), *pyrH* (735 bp), *recA* (1047 bp), *rpoA* (993 bp), *rpoD* (1842 bp) and 16S rRNA (1492 bp). Bar, 2 substitutions per 100 nucleotide positions.

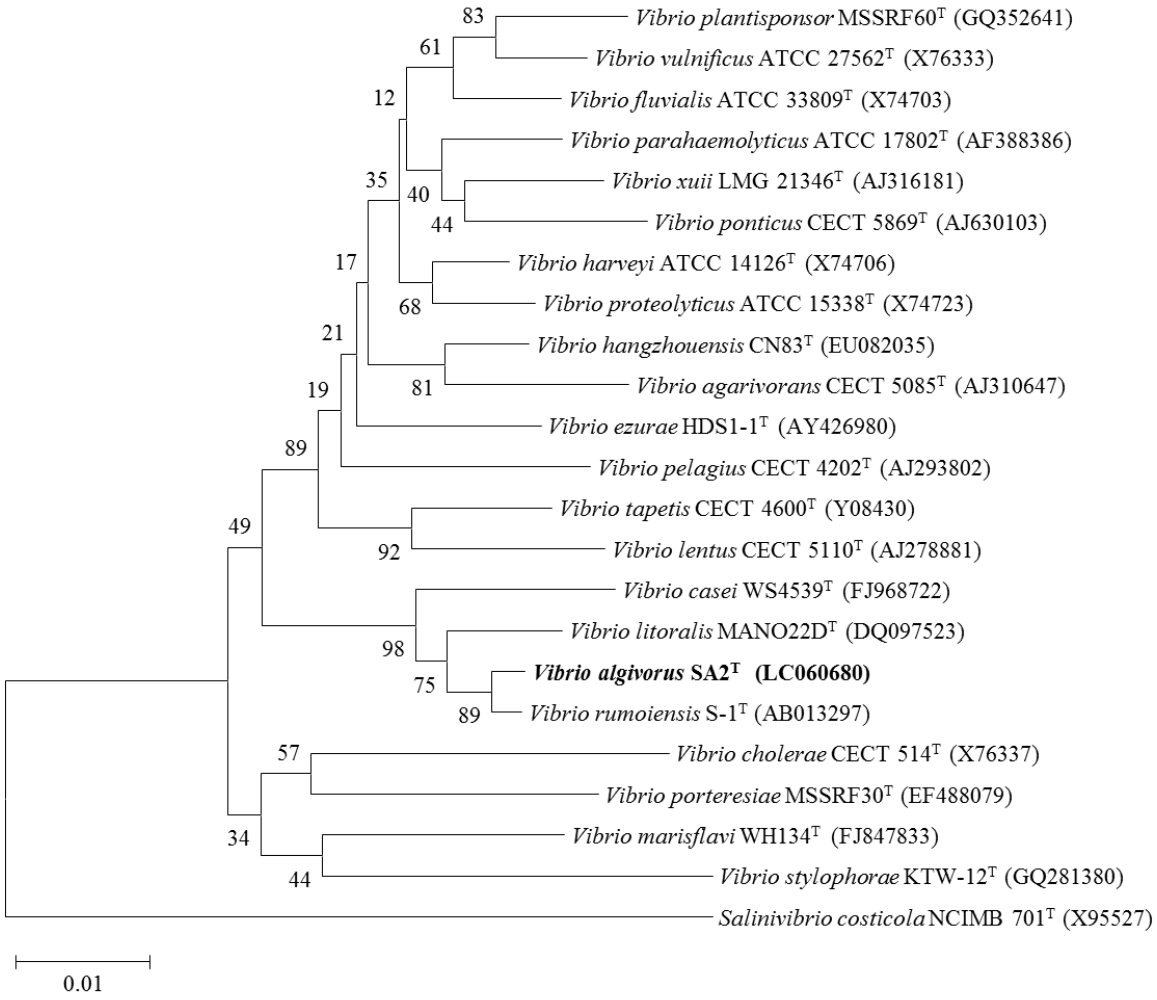

Figure 3-4. Phylogenetic tree showing the relationships of *Vibrio algivorus* sp. nov. SA2^T based on 16S rRNA genes (see Table 3-3). Bar, 1 substitution per 100 nucleotide positions.

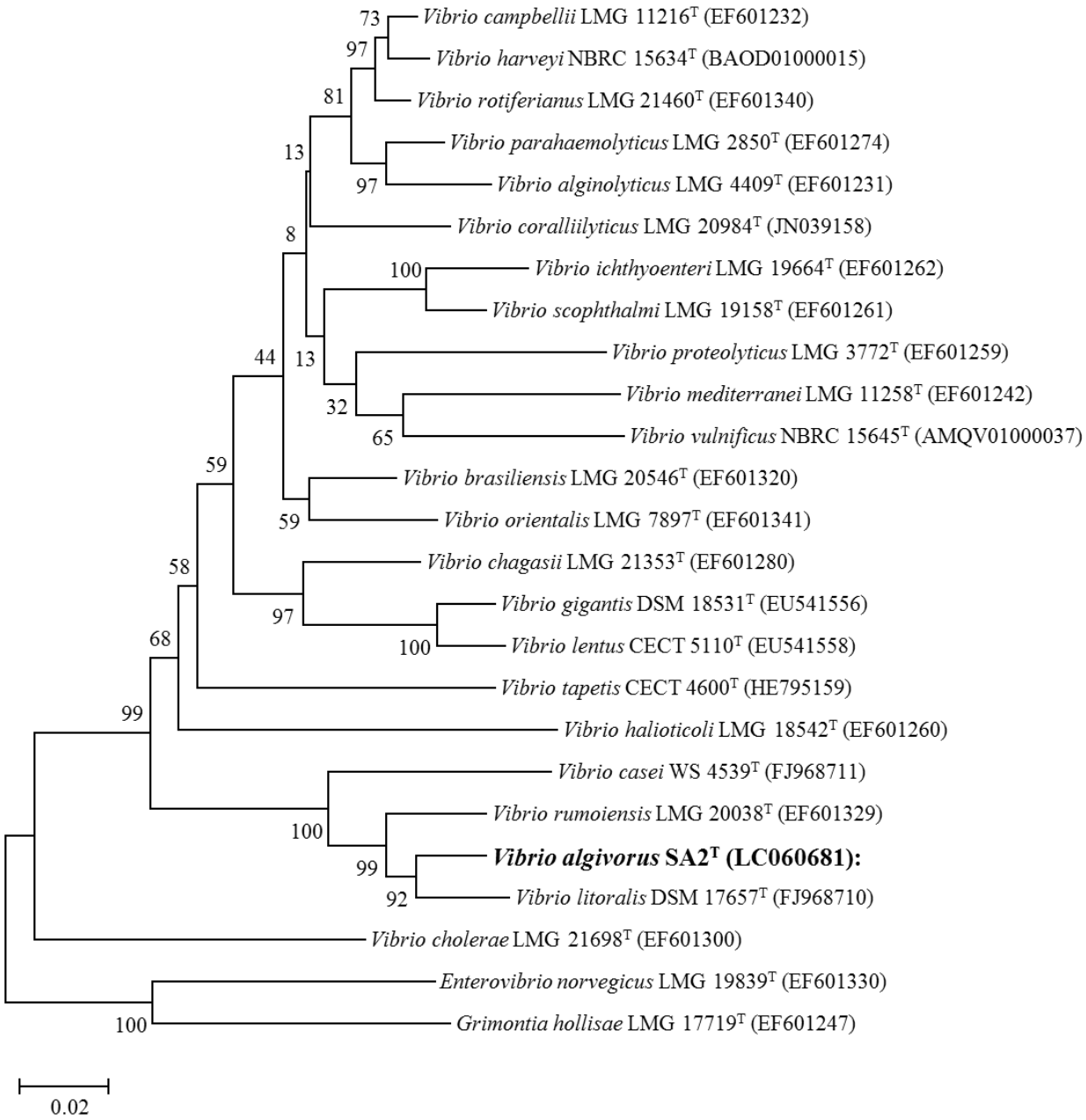

Figure 3-5. Phylogenetic tree showing the relationships of *Vibrio algivorus* sp. nov. SA2^T based on *atpA* genes (see Table 3-3). Bar, 2 substitutions per 100 nucleotide positions.

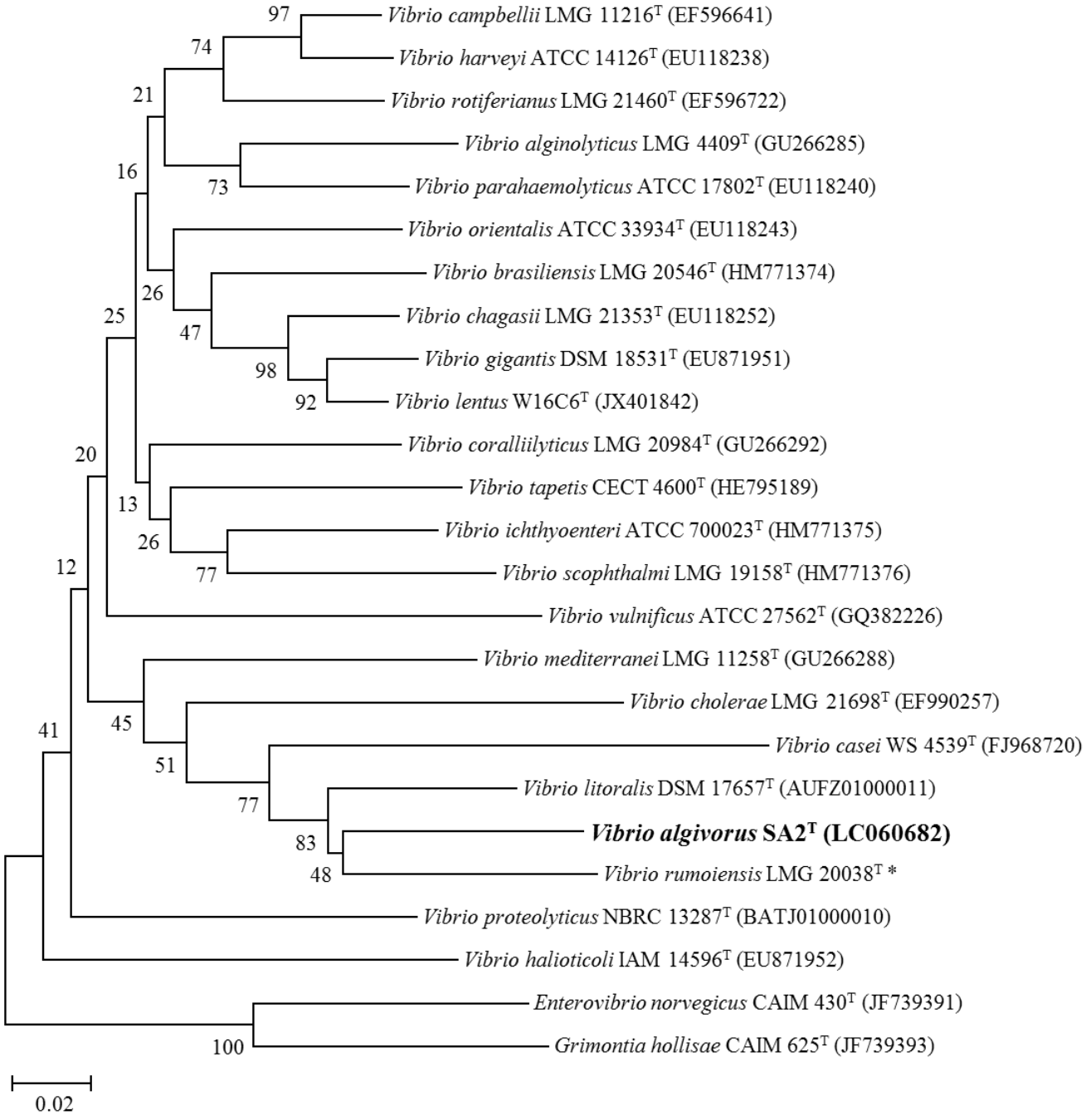

Figure 3-6. Phylogenetic tree showing the relationships of *Vibrio algivorus* sp. nov. SA2^T based on *pyrH* genes (see Table 3-3). Bar, 2 substitutions per 100 nucleotide positions.

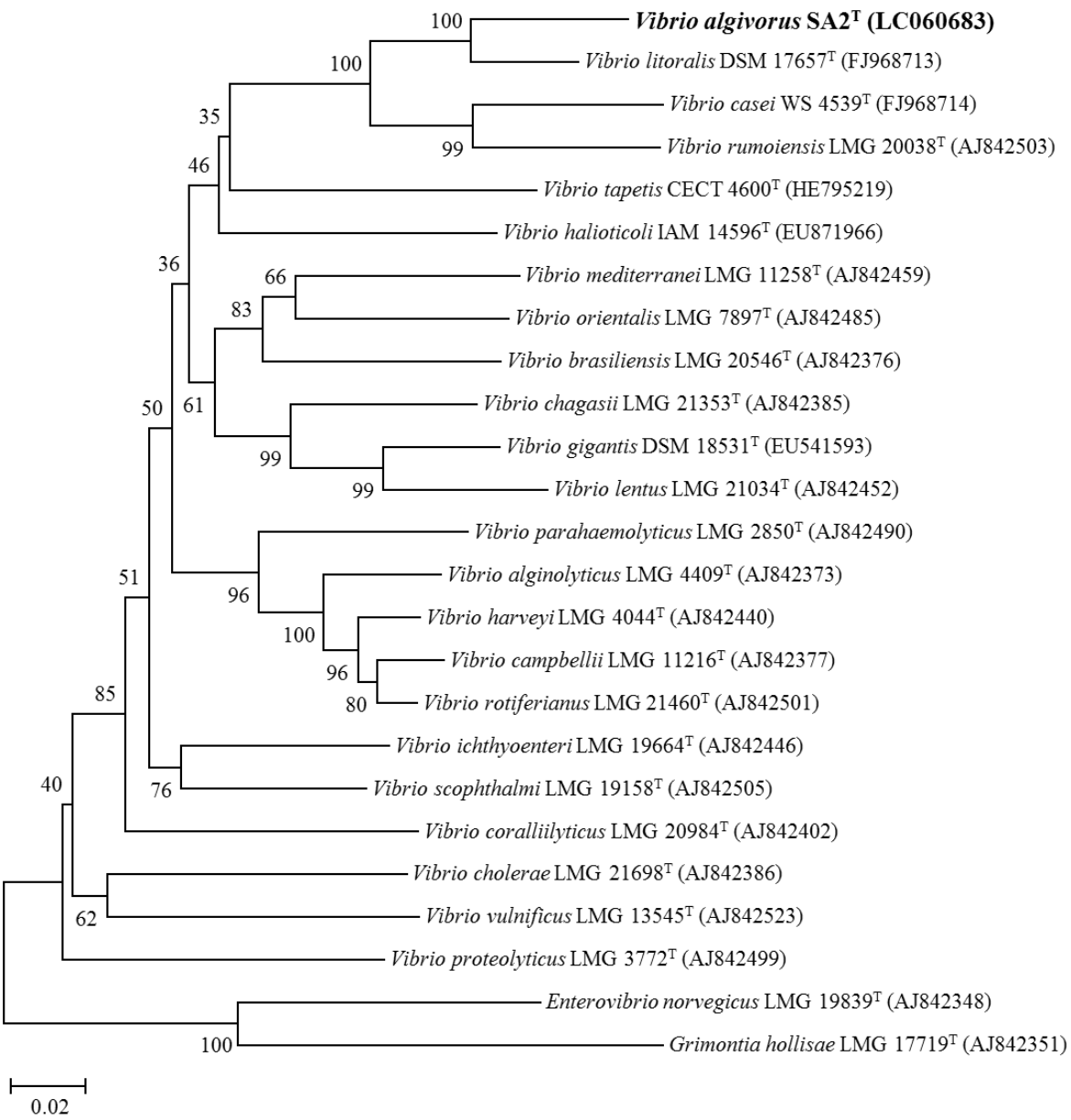

Figure 3-7. Phylogenetic tree showing the relationships of *Vibrio algivorus* sp. nov. SA2^T based on *recA* genes (see Table 3-3). Bar, 2 substitutions per 100 nucleotide positions.

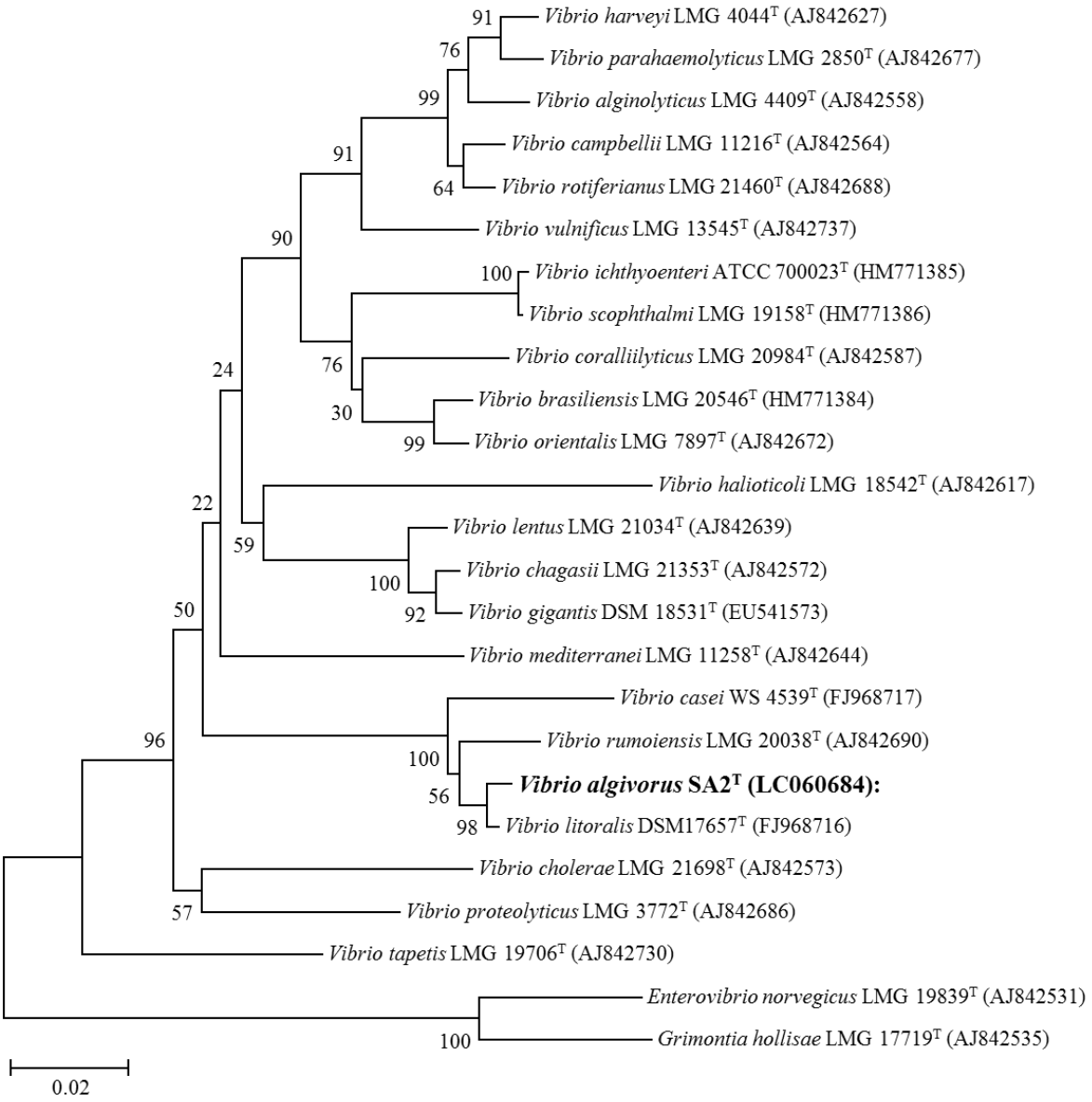

Figure 3-8. Phylogenetic tree showing the relationships of *Vibrio algivorus* sp. nov. SA2^T based on *rpoA* genes (see Table 3-3). Bar, 2 substitutions per 100 nucleotide positions.

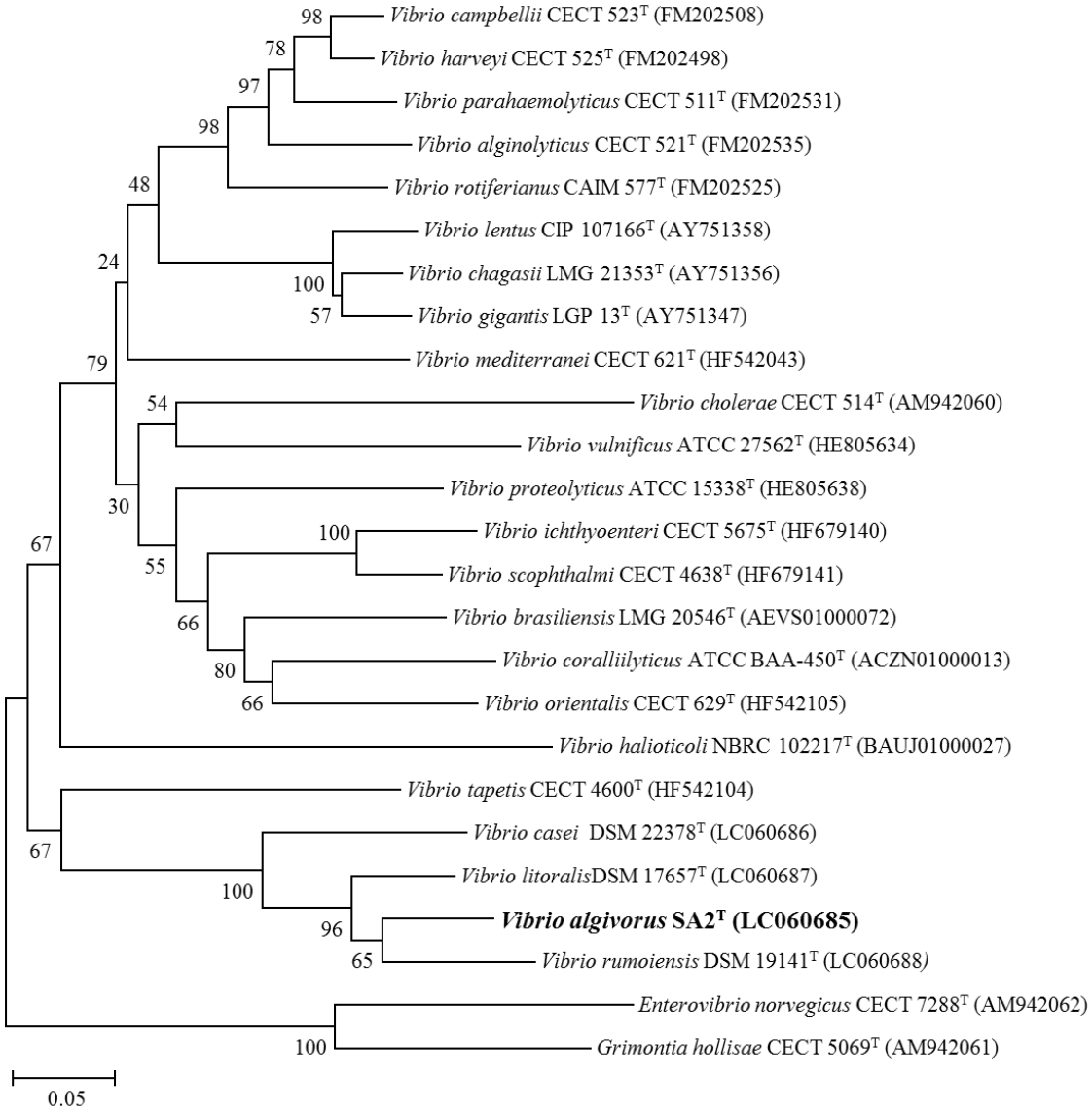

Figure 3-9. Phylogenetic tree showing the relationships of *Vibrio algivorus* sp. nov. SA2^T based on *rpoD* genes (see Table 3-3). Bar, 5 substitutions per 100 nucleotide positions.

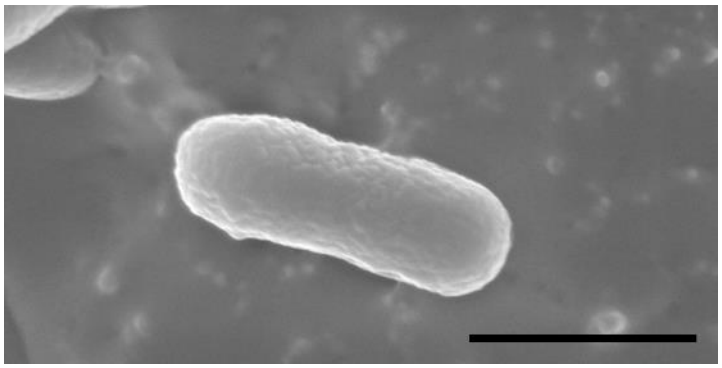

Figure 3-10. Scanning electron micrographs of fixed and freeze-dried cells of *Vibrio algivorus* sp.nov. strain SA2^{T}, 30000 x magnification; bar , 1 μm.

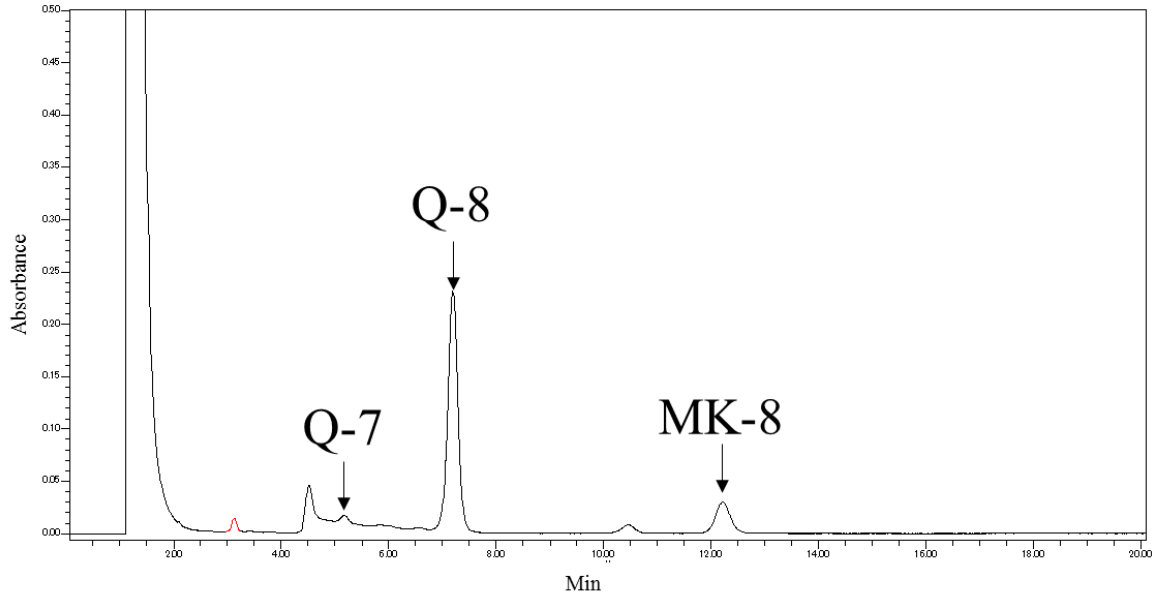

Figure 3-11. HPLC of isoprenoid quinones extracted from *Vibrio algivorus* sp. nov. SA2^T strain (= DSM29824^T,= NBRC111146^T)

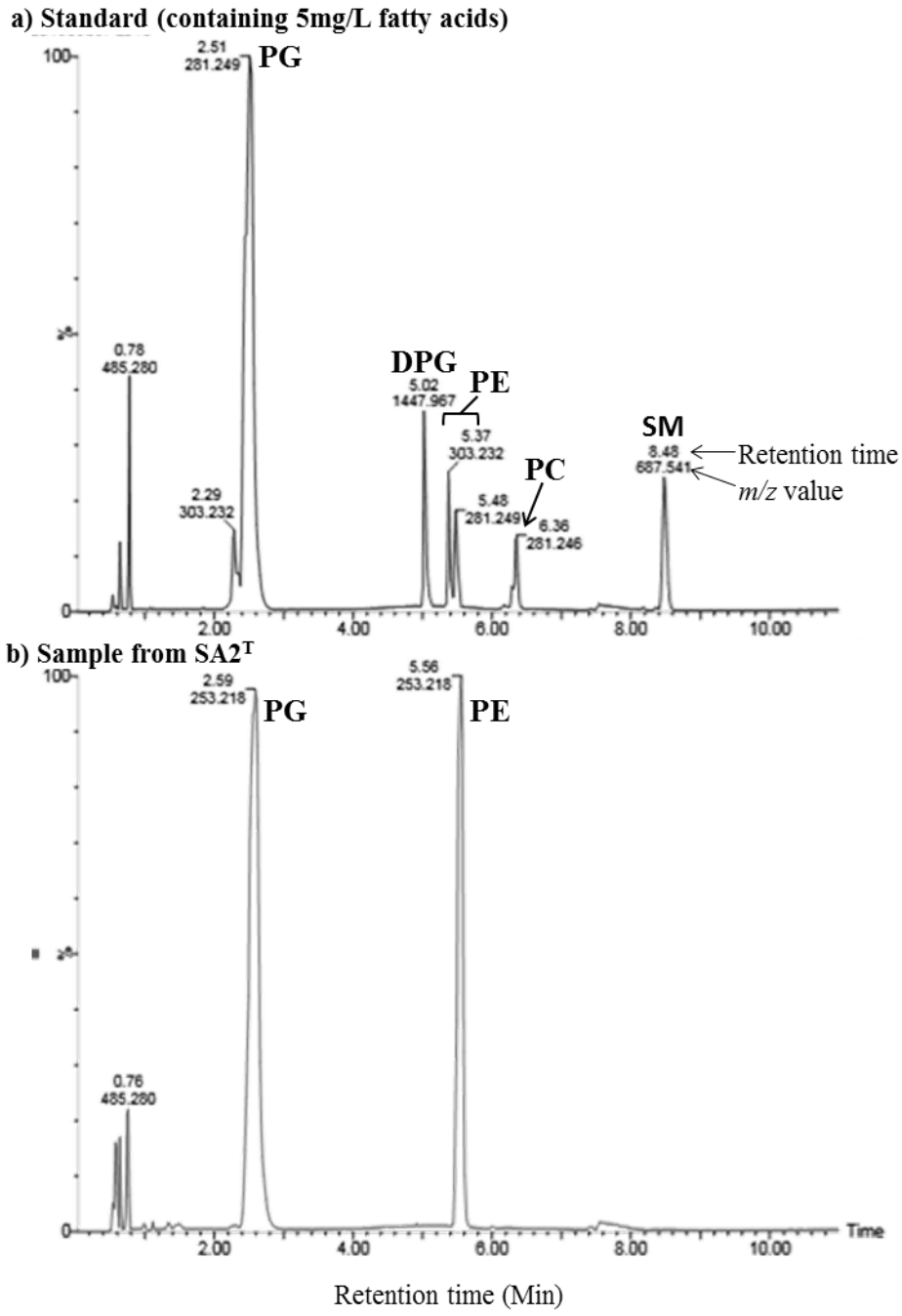

Figure 3-12. LC-QTOF/MS of polar lipid fractions from the *Vibrio algivorus* sp. nov. SA2^{T}.

TLC analysis used a previously reported procedure (Mal & Wong S, 2011). Polar species identification were performed with the standard chromatogram and the previously reported method (Mazzella *et al*., 2004). PE, phosphatidylethanolamine; PG, phosphatidylglycerol;

DPG, diphosphatidylglycerol; Lyso-PE, lysophosphatidylethanolamine; AP, unidentified aminophospholipid; AL, unidentified amino-lipid.

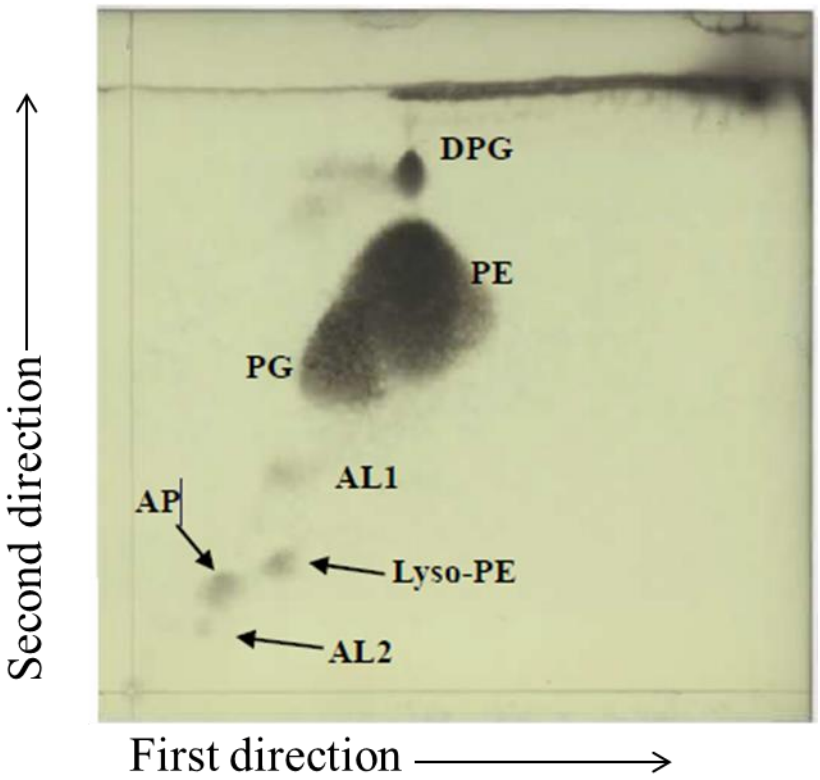

Figure 3-13. Two-dimensional TLC of polar lipid fractions from the *Vibrio algivorus* sp. nov. SA2^{T}. TLC analysis used a previously reported procedure (Minnikin *et al*., 1979). Staining with 5% phosphomolybdic acid in ethanol was at 180 °C for 20 min. PE, phosphatidylethanolamine; PG, phosphatidylglycerol; DPG, diphosphatidylglycerol; Lyso-PE, lysophosphatidylethanolamine; AP, unidentified aminophospholipid; AL, unidentified amino-lipid.

Chapter 4 Identification of enzymes responsible for extracellular alginate depolymerization and alginate metabolism in *Vibrio algivorus*

Abstract

Alginate is a marine non-food-competing polysaccharide that has potential applications in biorefinery. Owing to its large size (molecular weight > 300,000 Da), alginate cannot pass through the bacterial cell membrane. Therefore, bacteria that utilize alginate are presumed to have an enzyme that degrades extracellular alginate. I isolated *Vibrio algivorus* sp. SA2^T as a novel alginate-decomposing and -utilizing species. To address the mechanism of alginate degradation and metabolism in this species, I screened the *V. algivorus* genomic DNA library for genes encoding polysaccharide-decomposing enzymes using a novel double-layer plate screening method and identified *alyB* as a candidate. Most identified alginate-decomposing enzymes (i.e., alginate lyases) must be concentrated and purified before extracellular alginate depolymerization. AlyB of *V. algivorus* heterologously expressed in *Escherichia coli* depolymerized extracellular alginate without requiring concentration or purification. I found seven homologs in the *V. algivorus* genome (*alyB*, *alyD*, *oalA*, *oalB*, *oalC*, *dehR*, and *toaA*) that are thought to encode enzymes responsible for alginate transport and metabolism. Introducing these genes into *E. coli* enabled the cells to assimilate soluble alginate depolymerized by *V. algivorus* AlyB as the sole carbon source. The alginate was bioconverted

into L-lysine (43.3 mg/l) in *E. coli* strain AJIK01. These findings demonstrate a simple and novel screening method for identifying polysaccharide-degrading enzymes in bacteria and provide a simple alginate biocatalyst and fermentation system with potential applications in industrial biorefinery.

Introduction

Alginate is an abundant sugar in marine brown macroalgae (Chapman, 1970) that is considered as an efficient candidate for a non-food-competing raw material of biorefinery. Sugars from cane or corn starch are currently the major raw materials of biorefinery; however, an ethical challenge associated with their production is that it competes with food production. In contrast, the cultivation of marine brown macro algae does not require arable land, fresh water, pesticide, or fertilizer (John et al., 2011), and has the advantage of rapid growth (Stephens et al., 2013).

Alginate consists of a long-chain polymer of α-L-guluronic acid and β-D-mannuronic acid that form a high-molecular weight macromolecule (> 300,000 Da) that is poorly soluble in water (Gacessa, 1988). Raw alginate is too large to import through the cell membrane. As such, most microorganisms cannot degrade and utilize alginate. However, novel alginate-utilizing microbial species have recently been discovered (Kita et al., 2015; Doi et al., 2016), while various fermentation processes using alginate as raw material have been proposed. For example, ethanol for biofuel production has been derived from alginate by fermentation using metabolically engineered *Sphingomonas* sp. A1 strain (Takeda et al., 2011), *Escherichia coli* (Wargacki et al., 2012), and *Saccharomyces cerevisiae* (Enquist-Newman et al., 2014), while pyruvate has been produced by *Sphingomonas* sp. A1 (Kawai et al., 2014). These studies exploit specific alginate-assimilating species and/or their enzymes. However, there are certain

challenges for the industrialization of alginate fermentation, including the need to pretreat alginate for degradation and ensuring efficient bioconversion of alginate into products. These can potentially be circumvented by identifying novel alginate-degrading and -utilizing enzymes, which could be used for the production of commodity chemicals such as L-lysine, a food and feed additive. To date there have been no report of L-lysine production from alginate as a carbon source, although the bioconversion of D-glucose to L-lysine in *E. coli* strain AJIK01 has been described (Doi et al., 2015).

In Chapter 3, I isolated *Vibrio algivorus* sp. strain SA2^T from the gut flora of the turban shell marine snail (Doi et al., 2016), which can depolymerize and assimilate alginate as a sole carbon source, although the underlying mechanisms are unclear. To address this issue, in the present study I developed a novel system to screen for genes encoding extracellular active alginate-degrading enzymes and identified *V. algivorus alyB* as a candidate. The protein was expressed in *E. coli* and exhibited extracellular alginate-depolymerizing activity. I also identified seven putative alginate utilization pathway genes in *V. algivorus* (*toaA*, *alyB*, *alyD*, *oalA*, *oalB*, *oalC*, and *dehR*) that were expressed in wild-type *E. coli* and conferred the cells with the capacity to convert depolymerized alginate into L-lysine. This is the first report identifying genes encoding enzymes for alginate degradation and utilization in *V. algivorus* and demonstrating the bioconversion of alginate into L-lysine.

MATERIALS AND METHODS

Bacterial strains and plasmids

All strains and plasmids used in this study are listed in Table 4-1. Primers used for the construction of plasmids and strains are listed in Table 4-2. DNA fragments were PCR-amplified and purified with the Wizard SV Gel and PCR Clean-up system (Promega, Madison, WI, USA). To construct plasmids, purified insert DNA was cloned into the linearized vector with the In-Fusion HD PCR cloning system (Clontech, Mountain View, CA, USA). To express *V. algivorus* sp. SA2^T genes (*dehR*, *alyB*, *alyD*, *oalA*, *oalB*, and *oalC*) in *E. coli*, the genes were PCR-amplified and inserted downstream of the chloramphenicol resistance marker gene *cat* and the promoter sequence attR-cat-attL-P_{14} using the plasmid shown in Table 4-1 as a template (i.e., pM08, pM03, pM09, pM10, pM11, and pM12) and the λ-red system (Datsenko and Wanner, 2000). The *cat* gene was excised from the genome as previously described (Katashikina et al., 2009). To express the *V. algivorus* sp. SA2^T *toaA* gene in *E. coli*, I carried out crossover PCR amplification of *toaA* (using *V. algivorus* sp. SA2^T genomic DNA as the template) and inserted the amplicon downstream of attR-cat-attL-$P_{tac1000}$, which was amplified using a chemically synthesized DNA template (Katashikina et al., 2005) and the λ-red system. The *cat* gene was then excised from the genome as described above.

Screen for extracellular active alginate lyase

I prepared sheared 40–50 kb DNA fragments of *V. algivorus* sp. SA2^T genomic DNA using HydroShear (Gene Machines, San Carlos, CA, USA) followed by gel purification. *E. coli* EPI300 cells were transformed with the sheared fragments as previously described (Wargacki et al., 2012). *E. coli* EPI300 colonies expressing the fragments were covered with M9 minimal medium (Miller, 1992) containing 4 g/l agar and 10 g/l sodium alginate (300–400 cP, CAS no. 9005-38-3; Wako Pure Chemical Industries, Osaka, Japan) (Fig. 4-1A). After a 16h incubation at 37°C, I observed an indentation over the colonies (Fig. 4-1B), which were transferred to a Luria-Bertani (LB) plate containing 12.5 mg/l chloramphenicol (Cm), 1 mM isopropyl β-D-1-thiogalactopyranoside, and 40 μg/l X-gal. Colonies were then cultured in liquid LB medium containing 12.5 mg/l Cm at 37°C with constant shaking at 120 rpm until the optical density at 600 nm (OD_{600}) was 0.8. I added 0.1% (v/v) of Copy Control Induction Solution (Epicentre, Madison, WI, USA) and incubated the cultures at 37°C for 6 h with constant shaking at 120 rpm. Cells were collected by centrifugation for 20 min at 3000 × *g* and fosmid DNA was extracted using the Plasmid Midi kit (Qiagen, Hilden, Germany). The terminal sequences of extracted fosmids were determined by Sanger sequencing using EPI forward and reverse primers (Table 4-2). The whole insert sequence of the extracted fosmid was determined based on the draft genome of SA2^T (Doi et al., 2016).

In vitro determination of alginate lyase activity

V. splendidus ATCC33125^T and *V. algivorus* sp. SA2^T cells were grown on LB plates with 15 g/l NaCl for 16 h at 30°C. The cells were scraped and crude cell lysates were obtained using BugBuster Master Mix (Merck Millipore, Billerica, MA, USA). A similar procedure was used to obtain crude cell lysates of *E. coli* grown on LB plates with 40 mg/l Cm for 16 h at 30°C. Protein concentration of the lysates was measured as previously described (Chial and Splittgerber, 1993) using Coomassie Brilliant Blue (CBB) G (Nacalai Tesque, Kyoto, Japan). Alginate lyase activity was measured using a published protocol (Iwamoto et al., 2001; Tang et al., 2009). Briefly, 180 µl of the reaction mixture (0.08 g/l protein sample, M9 minimal medium, and 2 g/l sodium alginate) were transferred to a 96-well microplate (Greiner Bio One, Frickenhausen, Germany) followed by incubation at different temperatures (34°C, 37°C, 40°C, and 44°C). After 18 min, the increase in absorbance at 235 nm (Abs_{235}) was measured with a Spectra Max190 microplate reader (Molecular Devices, Sunnyvale, CA, USA). One unit of alginate lyase activity was defined as an increase in Abs_{235} of 0.100 per minute (Iwamoto et al. 2001).

Alginate viscosity test for detecting in vivo extracellular alginate decomposing activity

E. coli cells were cultured in 5 ml of LB with 40 mg/l Cm at 37°C for 16 h with shaking at 120 rpm. Sodium alginate (0.25 g) was added to the test tubes, which were placed at an angle of 45°, and the cultures were incubated with shaking for 72 h. I waited for 5 s after placing the

tubes upright to assess the angle of the liquid surface (Fig. 4-3). If alginate depolymerization was insufficient, the liquid surface remained at an angle of 45° (Fig. 4-4A); conversely, upon alginate depolymerization the liquid loses its viscosity and the liquid surface would be horizontal (Fig. 4-4B). I analysed the depolymerized liquid by gel permeation chromatography (GPC) and confirmed that the alginate peak was reduced (Fig. 4-4B and data not shown for the other results in Table 4-4).

Preparation of supernatant and washed cell samples

E. coli strains were grown overnight at 37°C on LB plates. Cells were then inoculated into 40 ml of fermentation medium composed of 20 g/l glucose, 5 g/l tryptone, 2.5 g/l yeast extract, 5 g/l NaCl, 40 mg/l Cm, and 0.3 M 3-(N-morpholino)propanesulphonic acid (MOPS; adjusted to pH 7.0 with NaOH) in a Sakaguchi flask at an initial OD_{600} of 0.05 at 37°C for 20 h with shaking at 120 rpm. The cultures were centrifuged at 5000 rpm (7830 × *g*) and 4°C for 10 min (CR20GIII; Hitachi, Tokyo, Japan). The pellet was washed three times with 5 ml of 0.85% NaCl followed by centrifugation at 5000 rpm and 4°C for 10 min.

Determination of protein concentration in the supernatant

The supernatant from the above-described cultures was concentrated using the Amicon Ultra-15 centrifugal filter unit with an Ultracel-50 membrane (Merck Millipore). Protein

concentration was measured with the CBB assay using bovine serum albumin (Bio-Rad, Hercules, CA, USA) as a standard.

Preparation of alginate depolymerized with commercial alginate lyase

Sodium alginate (2.5 g) and 50 ml distilled water were mixed in a Sakaguchi flask (500 ml) at 120 rpm and 37°C for 16 h to obtain a uniformly dispersed, clear alginate gel containing 50 g/l sodium alginate. I added 40 ml of 0.85% NaCl and 1 mg/l commercial alginate lyase (A1603; Sigma-Aldrich, St. Louis, MO, USA) with shaking at 120 rpm and 37°C for 25 h. Depolymerized alginate solution was sterilized using Nalgene Rapid-flow filters (pore size: 0.2 μm; Thermo Fisher Scientific, Waltham, MA, USA).

Preparation of alginate depolymerized with alginate lyase purified from *E. coli*

E. coli strain JM109/pM03 was grown at 37°C on LB plates containing 40 mg/l Cm for 16 h. Colonies were inoculated into 40 ml of fermentation medium composed of 20 g/l glucose, 5 g/l tryptone, 2.5 g/l yeast extract, 5 g/l NaCl, 40 mg/l Cm, and 0.3 M MOPS (adjusted to pH 7.0 with NaOH) in a Sakaguchi flask at an initial OD_{600} of 0.05 and incubated at 37°C for 20 h with shaking at 120 rpm. Cells were collected by centrifugation at 5000 rpm and 4°C for 10 min, then inoculated in 0.85% NaCl such that the total volume was 40 ml. The mixture was combined with the uniformly dispersed clear alginate gel containing 50 g/l sodium alginate and

incubated at 37°C for 25 h with shaking at 120 rpm. After centrifugation at 5000 rpm and 4°C for 10 min, the supernatant containing depolymerized alginate was recovered and sterilized using Nalgene Rapid Flow filters (pore size 0.2 μm; Thermo Fisher Scientific) before addition of minimal medium.

Test tube cultivation with minimal medium

For test-tube cultivation on minimal medium, *E. coli* MG1655 and its derivative strains were grown overnight at 37°C on LB plates. Colonies were inoculated into 5 ml M9 minimal medium supplemented with 1 mM $MgSO_4$, 0.001% thiamine, and different carbon sources in L-shaped test tubes at an initial OD_{600} of 0.05 and incubated at 37°C for 96 h with constant shaking at 70 rpm on a TVS062 CA rocking incubator (Advantec, Tokyo, Japan).

Test tube cultivation for L-lysine bioconversion

Test-tube cultivation for l-lysine bioconversion was carried out by growing *E. coli* AJIK01 and its derivative strains overnight at 37°C on LB plates. Colonies were inoculated into 5 ml of medium composed of 0.25 g/l yeast extract, 4 g/l $(NH_4)_2SO_4$, 0.01 g/l $FeSO_4 \cdot 7H_2O$, 0.01 g/l $MnSO_4 \cdot 7H_2O$, 0.246 g/l $MgSO_4 \cdot 7H_2O$, 0.001% thiamine,10 g/l piperazine-N,N'-bis(2-ethanesulphonic acid) (adjusted to pH 7.0 with NaOH) and different carbon sources in test tubes at an initial dry cell weight of 0.05 g/l. Cells were cultured at

34°C for 90 h with constant shaking at 120 rpm.

Analytical procedures

Molecular weights and amounts of commercial alginate were determined by GPC under the conditions described in Table 4-3. Pullulan (CAS no. 9057-02-7) was used as the molecular weight standard. OD_{600} was measured with a U-2900 spectrophotometer (Hitachi). The standard error of the mean was calculated and a two-tailed unpaired Student's t test was carried out using Excel software (Microsoft Corporation, Redmond, WA, USA) from more than three independent samples.

Western blotting

Affinity-purified rabbit polyclonal antibody recognizing a chemically synthesized peptide sequence of *V. algivorus* AlyB (AAQKEARKDLRK) (Eurofins Genomics, Tokyo, Japan) was prepared as previously described (Iwai et al., 2015). Rabbit polyclonal anti-AlyB antibody (1:400) and horseradish peroxidase-linked anti-rabbit IgG (3:2000; Cell Signaling Technologies, Danvers, MA, USA; catalog no. 7074) were used to detect AlyB. Two independent repeats were carried out for western blot analyses, for which 2 μg of each sample were used. Sodium dodecyl sulphate polyacrylamide gel electrophoresis was carried out using XV Pantera pre-cast gels (DRC Co., Tokyo, Japan) and SimplyBlue SafeStain solution

(Thermo Fisher Scientific).

RESULTS

Screen for an extracellular alginate-decomposing enzyme in *V. algivorus* sp. SA2^T genome and phenotypic analysis of mutant AlyB

I used a plate assay method to screen colonies with extracellular alginate-decomposing activity (Fig. 4-1 A, B). A colony of the SA2^T strain (Doi et al., 2016) was first prepared and covered with a layer of alginate-containing gel. A visible indentation in the gel formed over the colony (data not shown), which was presumed to result from the decomposition of alginate by the underlying colony. Over 3000 *E. coli* EPI300 colonies harboring a fosmid containing a 40- to 50-kb fragment of SA2^T genomic DNA were inoculated on LB plates and covered with a layer of gel. After 16 h, three indentations appeared; the corresponding colonies were harvested and the fosmid DNA was extracted and sequenced. All three colonies harbored the same polysaccharide lyase family gene that showed high similarity to *alyB* of *V. splendidus* (Bardur et al., 2015); I therefore named the gene *alyB* of *V. algivorus*. The gene was inserted into an expression plasmid (pM03), which was introduced into *E. coli* JM109 (Table 4-1). The in vitro alginate lyase activity of *V. algivorus* SA2^T, *V. splendidus*, and *E. coli* JM109/pM03 whole cell lysates was analysed. *V. algivorus* SA2^T and *V. splendidus* lysates showed alginate lyase activities; the activities in the JM109/pM03 lysate were significantly higher than those in the *V. algivorus* SA2^T and *V. splendidus* lysates (Fig. 4-2). I also constructed a vector control strain (*E. coli* JM109/pM01) and a strain expressing *alyB* of *V. splendidus* (*E. coli*

JM109/pM02) (Table 4-1). JM109/pM03 but not JM109/pM01 and JM109/pM02 grown on LB medium lowered the viscosity of alginate in the alginate viscosity test (Figs. 4-3 and 4-4A).

Alginate was added to the supernatants of JM109/pM01 and JM109/pM03 cultures, followed by incubation; the supernatants were then analysed by GPC (Fig. 4-4B). Alginate exhibited a single peak within the retention time of 7.7–10 min; the centre of the peak was at 8.7 min (Fig. 4-4B). The alginate peak was lower for the supernatant of JM109/pM03, although the peak was retained in the supernatant of JM109/pM01 (Fig. 4-4B).

The domain structure of *V. algivorus* AlyB was modelled with SignalP 4.0 (http://www.cbs.dtu.dk/services/SignalP/; Petersen et al., 2011) and Pfam 25.0 (http://pfam.xfam.org; Finn et al., 2014) software. AlyB had a 17-amino acid (a.a.) signal peptide (SP) for secretion, a 123-a.a. CBM32 domain, and a 265-a.a. PL7 domain (Fig. 4-5A, B). I constructed plasmids harboring AlyB sequences lacking each of these domains (Fig. 4-5C); the plasmids were then introduced into *E. coli* JM109 and the alginate viscosity test was performed (Fig. 4-3). The viscosity-reducing activity was lost in the supernatant of cells expressing *alyB* lacking the N-terminal SP (Table 4-4), while the cell lysate of the SP deletion mutant retained this activity. PL7 deletion also caused the loss of viscosity-lowering activity in the supernatant, washed cells, cell lysate, and whole broth (Table 4-4). Deletion of the CBM32 domain had no effect on viscosity, which was similar to that observed with wild-type *alyB* expression.

I assessed the alginate depolymerization potential of the filtered and concentrated supernatants. The protein concentration of the supernatant was measured with the CBB protein assay, and the same amount of protein from each sample was incubated with alginate. The decrease in the amount of alginate and average molecular weights were evaluated by GPC (Fig. 4-6). I found that deletion of SP or PL7 reduced alginate-decomposing activity (Fig. 4-6A, B). A similar observation was made upon deletion of the CBM domain, although in this case half of the activity remained (Fig. 4-6A, B). A western blot analysis of the supernatants revealed a band of the same size as AlyB (57 kDa), which disappeared upon deletion of the SP domain (Fig. 4-6C).

Artificial alginate assimilation by *E. coli* expressing alginate metabolism pathway genes of *V. algivorus*

I searched the draft whole-genome sequence of $SA2^T$ (Doi et al., 2016) for genes with sequences homologous to those encoding alginate utilization-related enzymes of *V. splendidus* 12B01 (Wargacki et al., 2012) using GENETYX v.10 software (GENETYX, Osaka, Japan). Seven such genes were identified (Table 4-5): *alyB*, *alyD*, *oalA*, *oalB*, *oalC*, *dehR*, and *toaA* were introduced into wild-type *E. coli* MG1655 cells, which were then cultured in M9 minimal medium with depolymerized alginate as the sole carbon source. Expression of the seven genes along with *alyB* enabled *E. coli* MG1655 cells to utilize the alginate that was depolymerized

by AlyB activity (Fig. 4-7B, D).

Bioconversion of alginate to L-lysine

E. coli strain AJIK01 can utilize D-glucose and accumulate L-lysine (Doi et al., 2015). The introduction of the seven genes homologous to *V. algivorus* alginate metabolism genes (*alyB*, *alyD*, *oalA*, *oalB*, *oalC*, *dehR*, and *toaA*) into *E. coli* strain AJIK01 enabled the cells to utilize the alginate depolymerized by AlyB activity and accumulate L-lysine (Fig. 4-8A4, B4). There was no L-lysine accumulation in the absence of depolymerized alginate (Fig. 4-8B2) and without expression of all seven genes (Fig. 4-8B3).

DISCUSSION

Macroalgal utilization requires viscous polysaccharide decomposition. Brown macroalgae contain alginate, whereas red macroalgae contain carrageenan, xylan, and agarose (Chapman, 1970); these are all high-molecular weight polysaccharides that cannot pass through the cell membrane. It is therefore important to identify enzymes that can decompose these molecules. In this study, I used a simple double-layer screening procedure to identify AlyB, an extracellular polysaccharide-decomposing enzyme in *V. algivorus*, an alginate-assimilating strain. Like alginate, most polysaccharides are viscous; therefore, this double-layer screening procedure can be used to identify other polysaccharide-decomposing enzymes by adding a polysaccharide other than alginate to the upper layer gel.

Alginate degradation is important for its industrial applications (Wang et al., 2014) and is necessary for microbial alginate assimilation. Many *Vibrio* species are presumed to have enzymes for extracellular alginate degradation; indeed, several *Vibrio* alginate lyases such as AlyVI from *Vibrio* sp. QY101 (Han et al., 2004) and OalA, OalB, OalC, AlyA, AlyB, AlyD, and AlyE from *V. splendidus* 12B01 (Jagtap et al., 2014; Bardur et al., 2015) have been purified and characterized. *V. algivorus* AlyB exhibited alginate-depolymerizing activity when expressed in *E. coli* EPI300 and JM109 cells without requiring any purification or concentration.

I found that *V. algivorus* AlyB contained three predicted functional domains—i.e., SP,

CBM32, and PL7. *V. splendidus* AlyB (Genbank accession no. EAP94922.1, Bardur et al., 2015) also has these domains in the same order.

Deletion of PL7 resulted in the loss of alginate-depolymerizing activity, suggesting that the PL7 domain is the active centre of this enzyme, similar to the alginate lyase of *V. splendidus* (Bardur et al., 2015).

Deleting the SP domain caused the alginate-decomposing activity to be lost in the supernatant and washed cells but not in the cell lysate. The GPC analysis confirmed that the lysate from cells expressing the SP deletion mutant showed a reduced peak corresponding to alginate (data not shown). However, a western blot analysis showed that the AlyB signal in the supernatant was undetectable upon deletion of SP. The most recent study of *V. splendidus* alginate lyase used a mutant AlyB protein in which a His tag replaced the N-terminal SP for all the experiments, and did not discuss the function of the SP (Bardur et al., 2015). My results show that wild-type AlyB of *V. splendidus* is not released into the supernatant irrespective of the presence of the SP; in contrast, in *V. algivorus* the release of AlyB into the extracellular medium is dependent on this domain.

The CBM32 domain of *V. splendidus* AlyB is essential for its alginate lyase activity (Bardur et al., 2015). In this study, deletion of the CBM32 domain of *V. algivorus* AlyB reduced the extracellular alginate depolymerization potential by 50%, whereas extra- and intracellular alginate-decomposing activity was not lost completely. These results suggest that

the function of the CBM32 domain differs in the two species.

Alginate depolymerized by Aly enzymes has many uses, including as an ingredient of fish jelly food products (Sato et al., 2005), an agent that promotes plant growth (Yonemoto et al., 1995), and as an antioxidant (Falkeborg et al., 2014). However, these require alginate concentration and purification prior to depolymerization, which is unsuitable for large-scale applications due to the high cost. The fact that *V. algivorus* AlyB does not require purification makes it a good candidate for industrial production.

Uptake of alginate oligomer and its metabolism are required for alginate assimilation. Alginate-assimilating microbial species are presumed to have enzymes for degradation, uptake, and metabolism of this polysaccharide. Indeed, these have been reported for *V. splendidus* 12B01; expression of *toaA*, *toaB*, *eda*, *kdgK*, *oalA*, *oalB*, *oalC*, and *dehR* in *E. coli* strain ATCC8739 enabled the cells to utilize alginate depolymerized by alginate lyase derived from *Pseudoalteromonas* sp. SM0524 and expressed in another strain of *E. coli* (Wargacki et al., 2012). However, there is no report describing the depolymerization of extracellular alginate for assimilation by alginate lyase of a specific *Vibrio* strain; the above-mentioned study used alginate lyase from a different species (*Pseudoalteromonas* sp. SM0524, not *V. splendidus*) for assimilation. In the present study, I expressed seven alginate utilization pathway genes derived from *V. algivorus* in *E. coli* MG1655; the cells began utilizing extracellular alginate depolymerized by the activity of *V. algivorus* AlyB as a sole carbon source, suggesting that

AlyB has the same function in *V. algivorus*.

ToaA expression in *E. coli* increased alginate utilization and cell growth, although the import of depolymerized soluble alginate into the cytosol by *V. algivorus* ToaA was a rate-limiting step. *E. coli* cells expressing ToaA solely were unable to grow using enzymatically decomposed extracellular alginate as the sole carbon source (data not shown). I therefore speculate that other enzymes involved in alginate metabolism (*alyB, alyD, oalA, oalB, oalC,* and *dehR*) also function in alginate utilization. My results suggest that *V. algivorus* assimilates depolymerized alginate via a single uronic acid molecule (beta-D-mannuronate and 4-deoxy-l-erythro-5-hexoseulose urinate), similar to what has been predicted for *V. splendidus* (Wargacki et al., 2012) and *Sphingomonas* sp. strain A1 (Takeda et al., 2011). I propose a model of alginate degradation and metabolism in *V. algivorus* $SA2^T$ based on my findings (Fig. 4-9).

In this study, I evaluated the potential for producing alginate derivatives using engineered *E. coli*. One possible derivative is L-lysine, a commodity chemical that is commercially produced by fermentation in the order of over 1,500,000 metric tons per year (Doi et al., 2014). To date, there is no report describing the bioconversion of alginate to L-lysine. I observed here that the alginate depolymerized by AlyB turned into cell biomass and L-lysine.

L-lysine productivity of *E. coli* in this study is still low. There are some technologies for improving L-lysine productivity, such as the introduction of feedback-resistant L-lysine

biosynthesis genes (Kojima et al., 1994), the introduction of heterologous *ddh* gene of *Corynebacterium glutamicum* and the attenuation of the meso-α,ε-diaminopimelic acid synthesis pathway (Doi and Ueda 2010). By using of these technologies, L-lysine production from alginate can be further developed.

Metabolically engineered *E. coli* fermentation can be used to produce other commodity chemicals such as L-glutamate (Nisiho et al., 2013), L-tryptophan (Wang et al., 2013), L-phenylalanine (Báez-Viveros et al., 2007), lactic acid (Niu et al., 2014), and succinic acid (Zhu et al., 2013). My results indicate that expressing *V. algivorus* genes in *E. coli* is a suitable alginate degradation and utilization system that can be used in combination with fermentation to produce commercially valuable chemicals.

A higher bioconversion efficiency is necessary for the industrialization of alginate fermentation. This requires optimizing the expression levels of alginate metabolism enzymes. A recent study reported that a high-throughput method for constructing recombinant variants known as recombinase-assisted genome engineering (RAGE) system cotributed to the improvement of bioconversion of alginate into ethanol (Santos et al., 2013). Other efficient high-throughput engineering technologies have also been reported for *E. coli* (Esvelt and Wang, 2013; Ronda et al., 2016). These approaches can broaden the industrial applications of *V. algivorus* AlyB and other enzymes involved in alginate depolymerization and metabolism.

Tables and Figures

Table 4-1. Strains and plasmids

Strain	Description or genotype	Reference
MG1655	*Escherichia coli*, F⁻λ⁻*ilvG rfb-50 rph-1*	CGSC (no. 6300)
Vibrio algivorus SA2^T	Alginate-utilizing strain	DSM 29824^T; Doi et al., 2016
Vibrio splendidus ATCC33125^T	Alginate-utilizing strain	Le Roux et al., 2009
JM109	*E. coli*, *recA1*, *endA1*, *gyrA96*, *thi-1*, *hsdR17*(r_K^- m_K^+), *e14*⁻ (*mcrA*⁻), *supE44*, *relA1*, *Δ*(*lac-proAB*)/F'*traD36*, *proAB*⁺, *lac I*^{q}, *lacZΔ*M15	Takara Bio,Kyoto, Japan
EPI300	*E. coli*, F⁻ *mcrAΔ*(*mrr-hsdRMS-mcrBC*) *Φ80dlacZΔ*M15*ΔrecA1 endA1 araD139 lacX74Δ*(*ara, leu*)*7697 galU galK* λ⁻ *rpsL nupG trfA tonA dhfr*	Epicentre Biotechnologies, Madison, WI, USA
D2964	MG1655*ΔnarI*::P_{14}-*dehR*, *ΔycgV*::P_{14}-*alyB*, *Δ*ycgG::P_{14}-*alyD*, *ΔyegQ*::P_{14}-*oalA*, *ΔybdN*::P_{14}-*oalB*, *ΔyggW*::P_{14}-*oalC*	This study
D2978	MG1655*ΔnarI*::P_{14}-*dehR*, *ΔycgV*::P_{14}-*alyB*, *Δ*ycgG::P_{14}-*alyD*, *ΔyegQ*::P_{14}-*oalA*, *ΔybdN*::P_{14}-*oalB*, *ΔyggW*::P_{14}-*oalC*, *ΔyegD*::P_{tac6}-*toaA*	This study
AJIK01	*E. coli* strain capable of L-lysine bioconversion	Doi et al. 2015; NITE-BP1520

D3000	AJIK01*Δnar*I::P_{14}-*dehR*, *ΔycgV*::P_{14}-*alyB*, *Δ*ycgG::P_{14}-*alyD*, *ΔyegQ*::P_{14}-*oalA*, *ΔybdN*::P_{14}-*oalB*, *ΔyggW*::P_{14}-*oalC*, *ΔyegD*::P_{tac6}-*toaA*	This study
pCC1FOS	Fosmid vector for preparing the *V. algivorus* genomic library	Epicentre Biotechnologies
pM01	Plasmid for cloning and serving as a vector control, pMW119-attR-*cat*-attL-P_{14}	Doi et al., 2015
pM02	Plasmid expressing *alyB* of *V. splendidus*, pMW119-attR-*cat*-attL-P_{14}-*alyB*	This study
pM03	Plasmid expressing *alyB* of *V. algivorus*, pMW119-attR-*cat*-attL-P_{14}-*alyB*	This study
pM04	Plasmid expressing SP-deficient *alyB* mutant of *V. algivorus*, pMW119-attR-*cat*-attL-P_{14}-*alyBΔ*SP	This study
pM05	Plasmid expressing CBM32-deficient *alyB* mutant of *V. algivorus*, pMW119-attR-*cat*-attL-P_{14}-*alyBΔ*CBM32	This study
pM06	Plasmid expressing PL7-deficient *alyB* mutant of *V. algivorus*, pMW119-attR-*cat*-attL-P_{14}-*alyBΔ*PL7	This study
pM07	Plasmid expressing SP- and CBM32-deficient *alyB* mutant of *V. algivorus*, pMW119-attR-*cat*-attL-P_{14}-*alyBΔ*SP*Δ*CBM32	This study
pM08	Plasmid expressing *dehR* of *V. algivorus*, pMW119-attR-*cat*-attL-P_{14}-*dehR*	This study

pM09	Plasmid expressing *alyD* of *V. algivorus*, pMW119-attR-*cat*-attL-P_{14}-*alyD*	This study
pM10	Plasmid expressing *oalA* of *V. algivorus*, pMW119-attR-*cat*-attL-P_{14}-*oalA*	This study
pM11	*oalB* of *Vibrio algivorus* expressing plasmid,pMW119-attR-*cat*-attL-P_{14}-*oalB*	This study
pM12	*oalC* of *Vibrio algivorus* expressing plasmid,pMW119-attR-*cat*-attL-P_{14}-*oalC*	This study
pKD46	λ Red system helper plasmid	Datsenko and Wanner, 2000
pMW-intxis-ts	λ Red system marker excision plasmid, temperature sensitive	Katashkina et al., 2009
pMW118-attR-cat-attL-P_{tac6}	Template plasmid for cloning of attR-cat-attL-P_{tac6}-*toaA* by crossover PCR	Katashkina et al., 2005

CGSC, Coli Genetic Stock Center.

Table 4-2. Primers used in this chapter

Primer	Sequence	Description
EPI for	GGA TGT GCT GCA AGG CGA TTA AGT TGG	For sequencing pCC1FOS
EPI rev	CTC GTA TGT TGT GTG GAA TTG TGA GC	For sequencing pCC1FOS
L47	AGA TAT AAA ACC CTT ATA TAT TAA TAC GAT T	For amplifying pMW119- attR-cat-attL-P_{14} linear fragment
L48	gtc gac tct aga gga tcc ccg ggt acc gag c	For amplifying pMW119- attR-cat-attL-P_{14} linear fragment
N73	TAA GGG TTT TAT ATC TAT GAA ACA TAT TTT TCT AAA AAG CTT GCT AGC TTC	For amplifying *V. algivorus alyB* linear fragment
N74	atc ctc tag agt cga cTT ATT TAC CTG TGT ATG TAC CGT GCG ATT TTT CTA	For amplifying *V. algivorus alyB* linear fragment
N75	TAA GGG TTT TAT ATC TAT GTT AAA AAA ATT CCT CTG CAT GTC GGT TAT CCT	For amplifying *V. algivorus alyD* linear fragment
N76	atc ctc tag agt cga cCT ATT TTT TAT GCG ATG TTA ATT CTA ACT TAG AGA	For amplifying *V. algivorus alyD* linear fragment
N77	TAA GGG TTT TAT ATC TAT GAT GAC TAA ACC TGT TAT TGG TTT TAT CGG CCT	For amplifying *V. algivorus dehR* linear fragment

N78	atc ctc tag agt cga cTT ACT TTT TCA AAC CCA TGA AGT AAT CAA AGA TAA	For amplifying *V. algivorus dehR* linear fragment
O55	TAA GGG TTT TAT ATC Tat gac aga cca aaa atc tct tga tgc gat cag gaa	For amplifying *V. algivorus oalA* linear fragment
O56	ATC CTC TAG AGT CGA Ctt aca gcg taa taa caa cac ttt cac cat caa ca	For amplifying *V. algivorus oalA* linear fragment
O57	TAA GGG TTT TAT ATC Tat gaa aaa tga agt atc agc tgt att gct taa cac	For amplifying *V. algivorus oalB* linear fragment
O58	ATC CTC TAG AGT CGA Ctt att tca ctt gta ctt cta atg aat aga agc cat	For amplifying *V. algivorus oalB* linear fragment
O59	TAA GGG TTT TAT ATC Tat gaa tta cca acc att att aat gaa ttt tga aga	For amplifying *V. algivorus oalC* linear fragment
O60	ATC CTC TAG AGT CGA Ctt ata act gag ccg ttg ctc ccg tcc att ggt att	For amplifying *V. algivorus oalC* linear fragment
H69	TAA GGG TTT TAT ATC TAT GAA ACA AAT TAC TCT AAA AAC TTT ACT	For amplifying *Vibrio splendidus alyB* linear fragment
H70	atc ctc tag agt cga cTT ACT TTT TGT ATT GAT CGT GCG ATA CAT	For amplifying *Vibrio splendidus alyB* linear fragment

Q03	AAT GAA CAG TTG ACT GCT GCT GCA ACA CGC GGG CCT TCT TGT TTT GC	For amplifying pMW119-attR-*cat*-attL-P_{14}-*alyB⊿*CBM32 linear fragment
Q04	GCA GCA GTC AAC TGT TCA TTG AAC TCT	For amplifying pMW119-attR-*cat*-attL-P_{14}-*alyB⊿*CBM32 linear fragment
Q05	GGT ACA TAC ACA GGT AAA TAA	For amplifying pMW119-attR-*cat*-attL-P_{14}-*alyB⊿*PL7 linear fragment
Q06	ACC TGT GTA TGT ACC GTT TTG GCT TGG CTT ATT GCC	For amplifying pMW119-attR-*cat*-attL-P_{14}-*alyB⊿*PL7 linear fragment
Q07	aac agt tga ctg ctg cCA TAG ATA TAA AAC CCT TAT ATA TTA A	For amplifying pMW119-attR-*cat*-attL-P_{14}-*alyB⊿*SP*⊿*CBM32 linear fragment (used with Q10)
Q09	TAA GGG TTT TAT ATC TAT GGG CTG TTC ATC TAA TGG CGC CGA	For amplifying pMW119-attR-*cat*-attL-P_{14}-*alyB⊿*SP linear fragment
Q10	AGA TAT AAA ACC CTT ATA TAT TAA TA	For amplifying pMW119-attR-*cat*-attL-P_{14}-*alyB⊿*SP linear fragment
O01	ATA GCC GGG GCG GTC TTC CTG ATT GGT AGC TGG CTG CGT TAT GAC TAC GGT CTA GAC GCT CAA GTT AGT ATA AAA AAG CT	For introduction of *⊿narI*::P_{14}-*dehR*

O04	CGG TAC GCT CCA GAT GTG TAT CAG ACG CGA GAA CGG GAA CAG CAG GAA TAT TAC TTT TTC AAA CCC ATG AAG TAA TCA AA	For introduction of *⊿narI*::P_{14}-*dehR*
O20	gat ggt gac aga att aca gga gat acc gcc gat cca tca gga aac ctc taT CTA GAC GCT CAA GTT AGT ATA AAA AAG CT	For introduction of *⊿narI*::P_{14}-*alyB*
O38	CCG TTA TTC CAG CCA TTA CCT TTG AAA CTG TAC TTC TCC Ctt att tac ctg tgt atg tac cgt gcg att ttt cta gtt ta	For introduction of *⊿narI*::P_{14}-*alyB*
O32	tta ccg gtg tcg cta ttt tga aca tcc agc tct ggt att ccg caa aag caT CTA GAC GCT CAA GTT AGT ATA AAA AAG CT	For introduction of *⊿narI*::P_{14}-*alyD*
O35	ggg tct gcg ttt acg cgg cca acg aaa ctg tga tca att ttg ata taa tcC TAT TTT TTA TGC GAT GTT AAT TCT AAC TT	For introduction of *⊿narI*::P_{14}-*alyD*
O70	gtt acg ctt tcg ctt atg gcg cag atg ctg ttt atg cgg gcc agc TCT AGA CGC TCA AGT TAG TAT AAA AAA GCT GAA CG	For introduction of *⊿narI*::P_{14}-*oalA*

O72	cac agt ata acc atc gcc tgg tgc tat cgg cat agc ttc gcc ttt tta cag cgt aat aac aac act ttc acc atc aac a	For introduction of *⊿narI*::P_{14}-*oalA*
O65	CAG ACT TAT CTC ACT GAT CAC CCT GTA ACG TTC AGA GAG CGT CTT TCT AGA CGC TCA AGT TAG TAT AAA AAA GCT GAA CG	For introduction of *⊿ybdN*::P_{14}-*oalB*
O67	cgc tga tag ttc ttc gat ttt gtg ggg cta aat gat aat gcc cga TTA TTT CAC TTG TAC TTC TAA TGA ATA GAA GCC AT	For introduction of *⊿ybdN*::P_{14}-*oalB*
O75	ATT CAC ATC CCG TGG TGC GTG CAG AAA TGC CCG TAC TGC GAT TTC TCT AGA CGC TCA AGT TAG TAT AAA AAA GCT GAA CG	For introduction of *⊿yggW*::P_{14}-*oalC*
O77	aac agc ttc cca tgt tcc gtt atc tgc cag taa tcc gca cat tcg tta taa ctg agc cgt tgc tcc cgt cca ttg gta tt	For introduction of *⊿yggW*::P_{14}-*oalC*
K01	TCG CGA CGG CAA CAT TTC GCT AAA GTC ACG CCC CTT CTT CAC CGG CAT GGG GAT TAT TTC TCT AGA CGC TCA AGT TAG TA	For construction of ⊿yegD::P_{tac6}-*toaA* fragment (crossover PCR) and its introduction
K02	GGC AGC AAC AAC AAT AGT ATC GAC AGT CAT agc tgt tTC CTG TGT GAA ATT GTT ATC CGC	For construction of ⊿yegD::P_{tac6}-*toaA* fragment (crossover PCR) and its introduction

K03	GCG GAT AAC AAT TTC ACA CAG GAa aca gct ATG ACT GTC GAT ACT ATT GTT GTT GCT GCC	For construction of ⊿yegD::P_{tac6}-*toaA* fragment (crossover PCR) and its introduction
K04	gca gca gaa aaa ctg gct cag gcg cag gca gat tta agc cgc tgc tga gcc att ttt caa TTA CGA TTC TGA AAC CGT TT	For construction of ⊿yegD::P_{tac6}-*toaA* fragment (crossover PCR) and its introduction

Table 4-3. Analytical conditions for GPC analysis

System:	SHIMADZU Prominence L C20A UFLC
Column:	Asahipak GS-520 HQ, 7.5 × 300 mm, 7 μm
Solvent:	100 mM KH_2PO_4
Flow rate:	0.6 ml/min
Injection volume:	60 μl
Detection wavelength:	200 nm

Table 4-4. Results of the alginate viscosity test for detecting in vivo extracellular alginate-decomposing activity

	1	2	3	4	5	6	7
Whole broth	−	−	+	−	−	+	−
Supernatant	−	−	+	−	−	+	−
Washed cells	−	−	+	−	−	+	−
Cell lysate	−	+	+	+	−	+	+

1, JM109/pM01 (vector control); **2**, JM109/pM02 (expressing wild-type AlyB of *V. splendidus*); **3**, JM109/pM03 (expressing wild-type AlyB of *V. algivorus*); **4**, JM109/pM04 (SP deletion mutant); **5**, JM109/pM06 (PL7 deletion mutant); **6**, JM109/pM05 (CBM32 deletion mutant); **7**, JM109/pM07 (SP and CBM32 deletion mutant).

Table 4-5. Candidate genes of *V. algivorus* encoding enzymes related to alginate degradation and metabolism

Assigned gene name	Annotated function of homologous genes of *V. splendidus* (Wargacki et al., 2012)	DNA similarity to homologous genes of *V. splendidus* (%)	GenBank/EMBL/DDBJ accession no.
alyB	Alginate lyase	69	LC175806
alyD	Alginate lyase	65	LC175802
kdgN	Porin	53	LC175810
toaA	Symporter	75	LC175801
oalA	Oligoalginate lyase	81	LC175805
oalB	Oligoalginate lyase	69	LC175803
oalC	Oligoalginate lyase	74	LC175804
dehR	DEHU reductase	81	LC175807

DEHU, 4-deoxy-l-erythro-5-hexoseulose urinate.

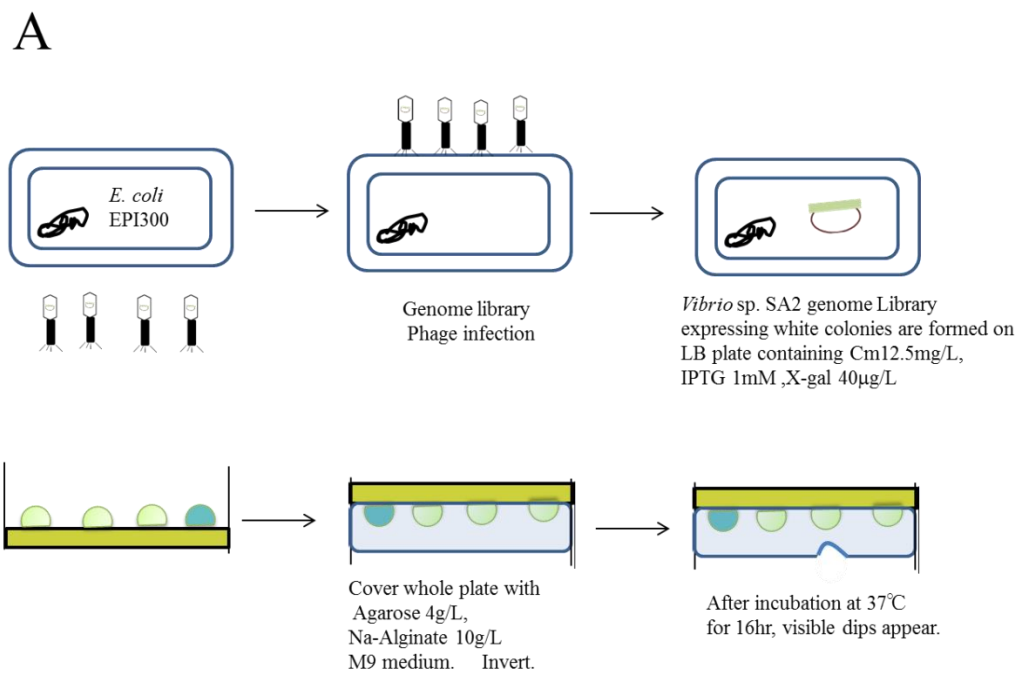

B

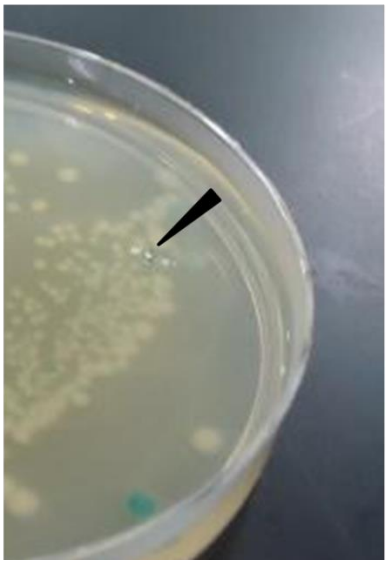

Figure 4-1. Screen for extracellular active alginate lyase.

A) Schematic representation of the double-layer screening method, B) A visible dip (arrowhead) appeared above the colony expressing the candidate alginate lyase.

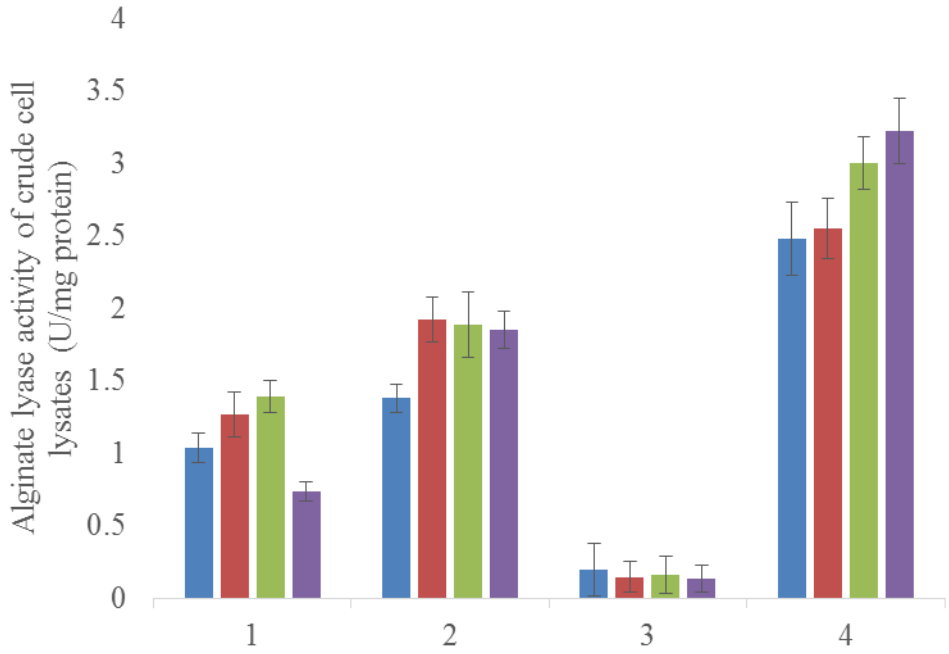

Figure 4-2. Results of alginate lyase enzyme activity assay.

1, Crude lysate of *V. splendidus* ATCC33125^{T}; **2**, crude lysate of *V. algivorus* SA2^{T}; **3**, crude lysate of *E. coli* JM109/pM01 (vector control); **4**, crude lysate of *E. coli* JM109/pM03 (harbouring *alyB* of *V. algivorus*). Blue, red, green, and purple bars represent activity at 34°C, 37°C, 40°C, and 44°C, respectively.

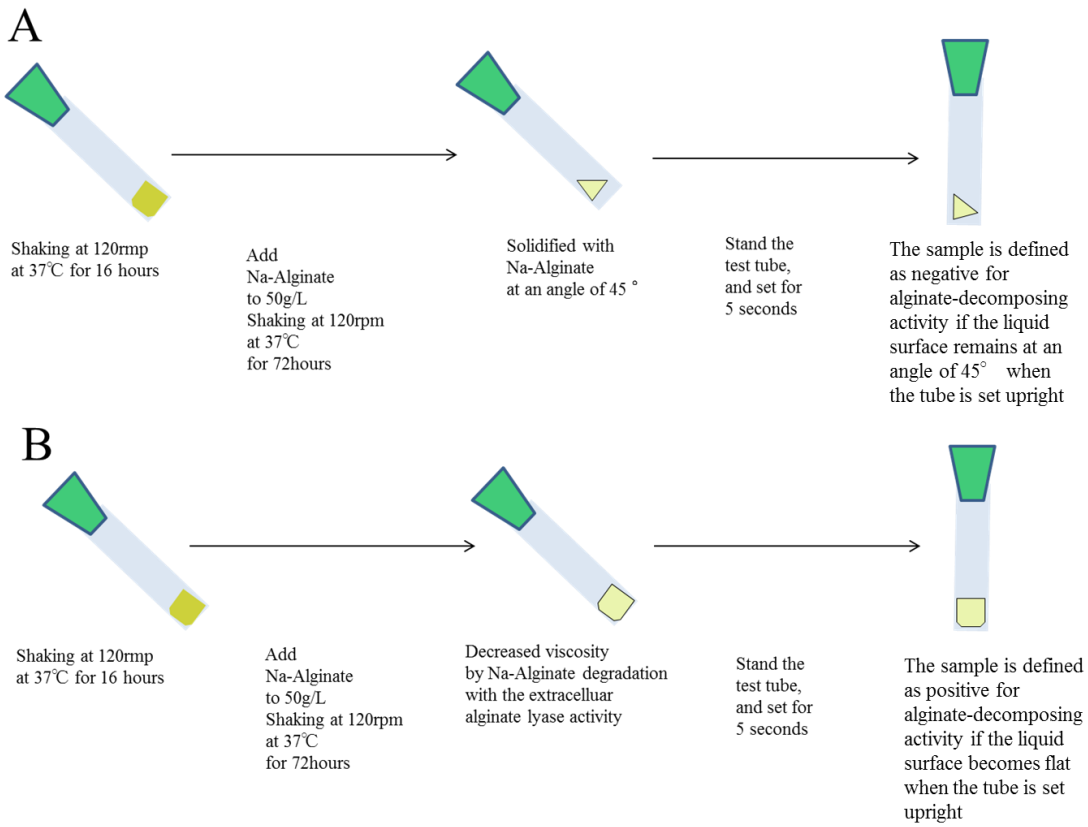

Figure 4-3. Schematic representation of the alginate viscosity test for detecting the in vivo extracellular alginate-decomposing activity.

A, B) Schematic representation of negative (A) and positive (B) results.

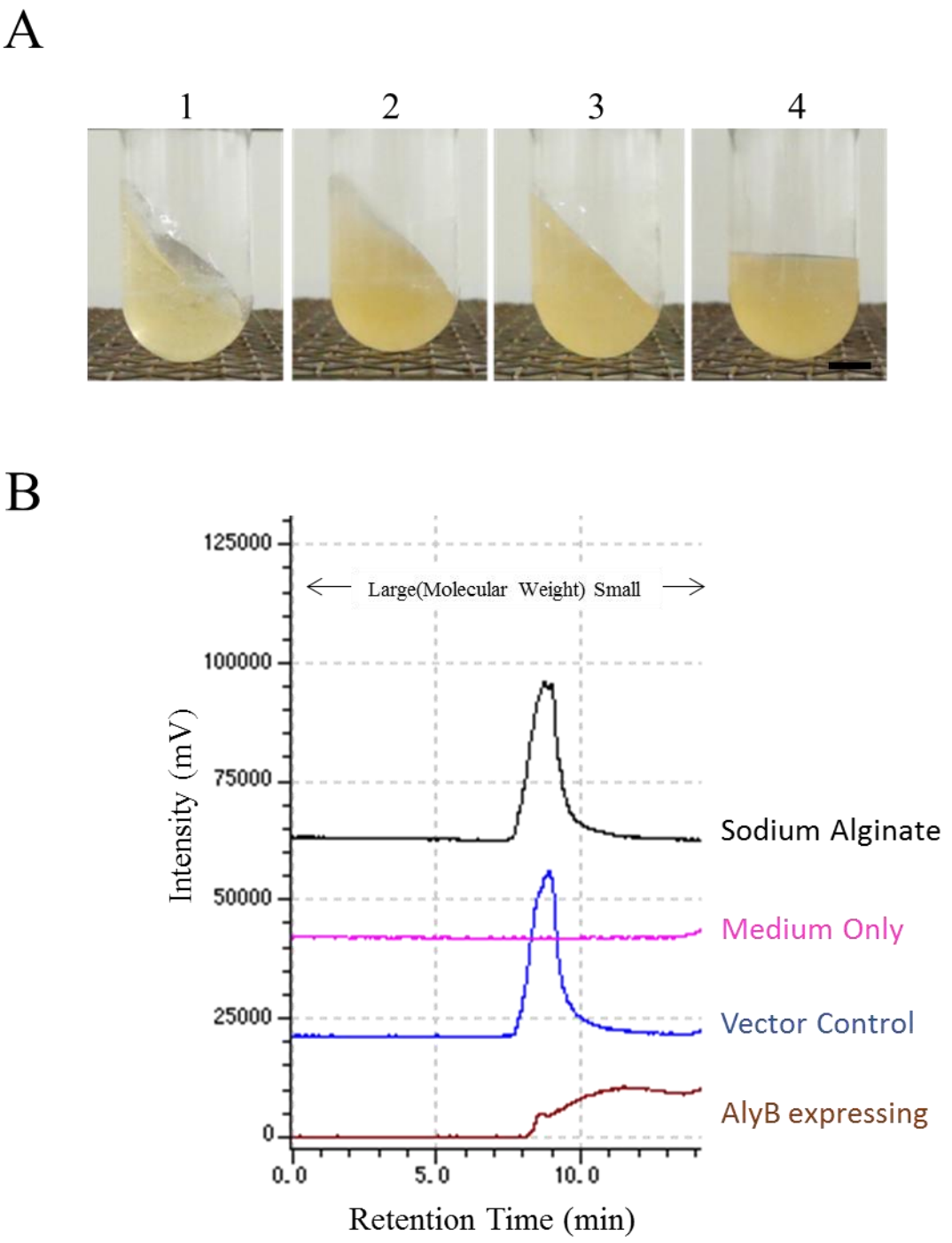

Figure 4-4. Extracellular alginate depolymerization by AlyB of *V. algivorus*.

A) Liquefaction of alginate-containing medium. **1**, LB medium with 50 g/l sodium alginate; **2**, JM109/pM01 broth with 50 g/l sodium alginate (vector control); **3**,

JM109/pM02 broth with 50 g/l sodium alginate (whole broth of cells expressing *alyB* of *V. splendidus*); **4**, JM109/pM03 broth with 50 g/l sodium alginate (whole broth of cells expressing *alyB* of *V. algivorus*). B) Results of GPC analysis. Black, 2 g/l sodium alginate standard; pink, LB medium; blue, 2 g/l sodium alginate after processing with the supernatant of JM109/pM01; brown, 2 g/l sodium alginate after processing with the supernatant of JM109/pM03.

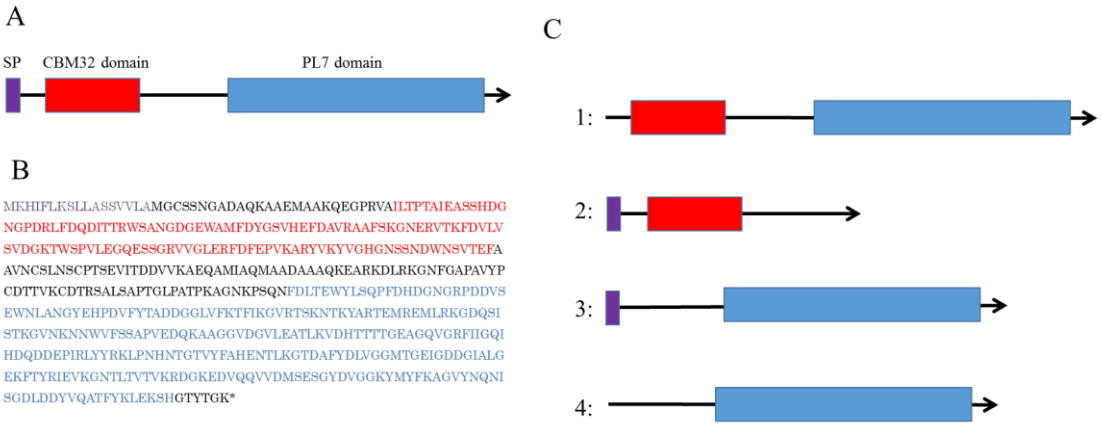

Figure 4-5. Predicted domain structure of *V. algivorus* AlyB.

A) The model was established using SignalP 4.0 (http://www.cbs.dtu.dk/services/SignalP/) (Petersen et al., 2011) and Pfam 25.0 (http://pfam.xfam.org) (Finn et al., 2014) software. B) Amino acid sequence of *V. algivorus* AlyB. Purple, red, and blue letters denote the SP, CBM32, and PL7 domains, respectively. C) Model of AlyB domain deletion mutants. **1**, SP deletion; **2**, PL7 deletion; **3**, CBM32 deletion; **4**, SP and CBM32 deletion.

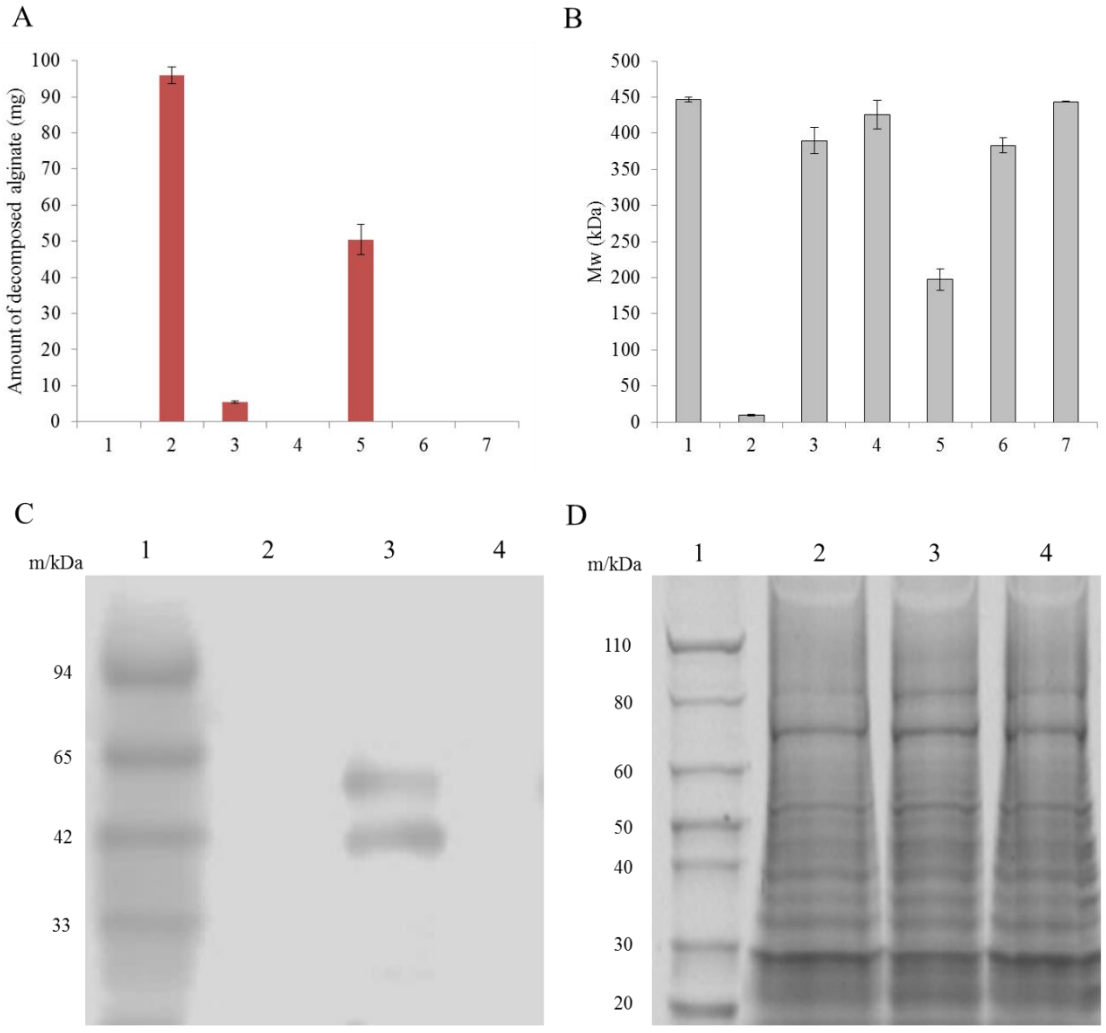

Figure 4-6. SP-dependent extracellular alginate decomposition.

A) Quantification of decomposed alginate in concentrated supernatant samples (with 100 mg sodium alginate added to 5 ml concentrated supernatant protein samples; protein concentration: 0.24 g/l). GPC analysis was carried out after shaking at 120 rpm and 37°C for 20 h. **1**, JM109/pM01 (vector control); **2**, JM109/pM03 (expressing wild-type AlyB of *V. algivorus*); **3**, JM109/pM04 (SP deletion mutant); **4**, JM109/pM06 (PL7 deletion

mutant); **5**, JM109/pM05 (CBM32 deletion mutant); **6**, JM109/pM07 (SP and CBM32 deletion mutant); **7**, JM109/pM02 (expressing wild-type AlyB of *V. splendidus*). B) Average molecular weights after processing concentrated supernatant samples. Samples 1–7 are as described for panel A. C) Western blot analysis of alginate in concentrated supernatants. **1**, XL-Western Marker SP-2170 (Aproscience, Tokushima, Japan); **2**, JM109/pM01 (vector control); **3**, JM109/pM03; **4**, JM109/pM04 (SP deletion mutant). D) Sodium dodecyl sulphate polyacrylamide gel electrophoresis analysis alginate in concentrated supernatants. Lane 1, Novex Sharp Unstained Protein Standard (Thermo Fisher Scientific, Waltham, MA, USA); Lanes 2–4 are as described for panel C.

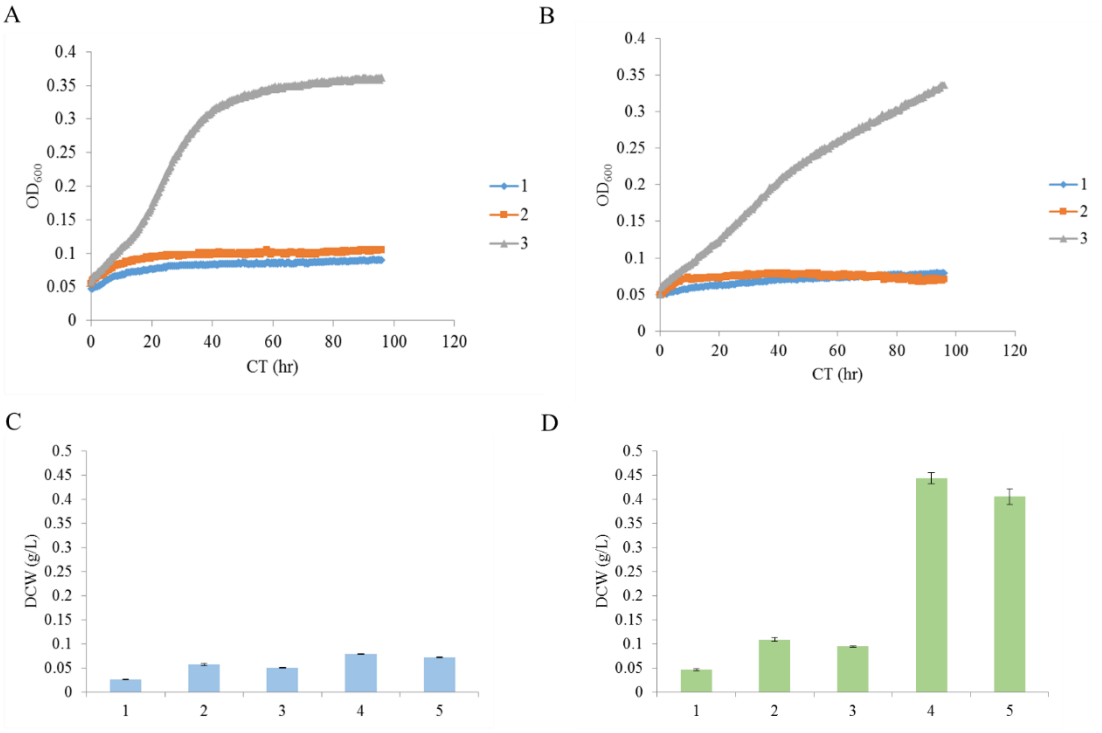

Figure 4-7. Results of test tube cultivation on minimal medium.

A) Cell growth on minimal medium using alginate depolymerized with commercial alginate lyase as the sole carbon source. **1**, MG1655; **2**, D2964; **3**, D2978. B) Cell growth on minimal medium using alginate depolymerized with AlyB (JM109/pM03) as the sole carbon source. **1**, MG1655; **2**, D2964; **3**, D2978. C) MG1655 accumulation on M9 medium, presented as dry cell weight (DCW). **1**, M9 medium only (no carbon added); **2**, supernatant of JM109/pM03 cells (without alginate added); **3**, sodium alginate (without preprocessing); **4**, depolymerized alginate with AlyB-expressing cells (JM109/pM03); **5**, depolymerized alginate with commercial alginate lyase. D)

59 Accumulation of D2978 on M9 medium, presented as DCW. Samples 1–5 are as

60 described for panel C.

A B

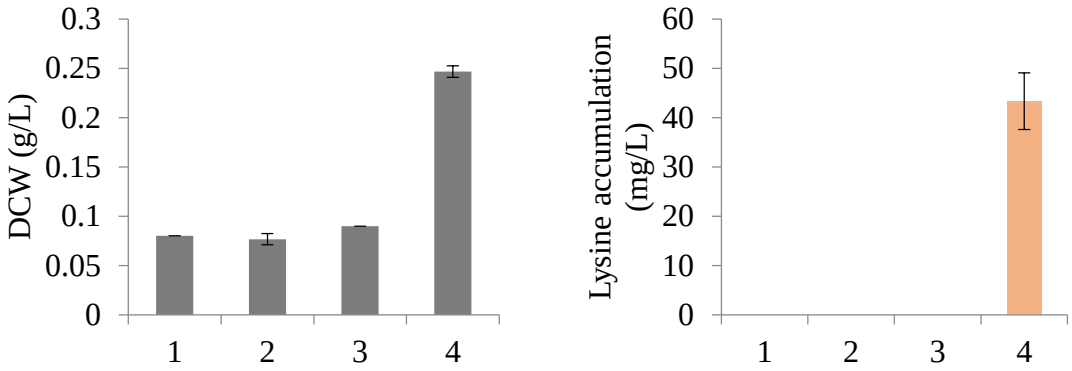

Figure 4-8. Results of test tube cultivation for L-lysine bioconversion.

A) Dry cell weight (DCW) accumulation. B) L-Lysine accumulation. **1**, AJIK01 strain without depolymerized soluble alginate; **2**, D3000 strain without depolymerized soluble alginate; **3**, AJIK01 strain with alginate depolymerized by AlyB of *V. algivorus* expressed in *E. coli*; **4**, D3000 strain with alginate depolymerized by AlyB of *V. algivorus* expressed in *E. coli*.

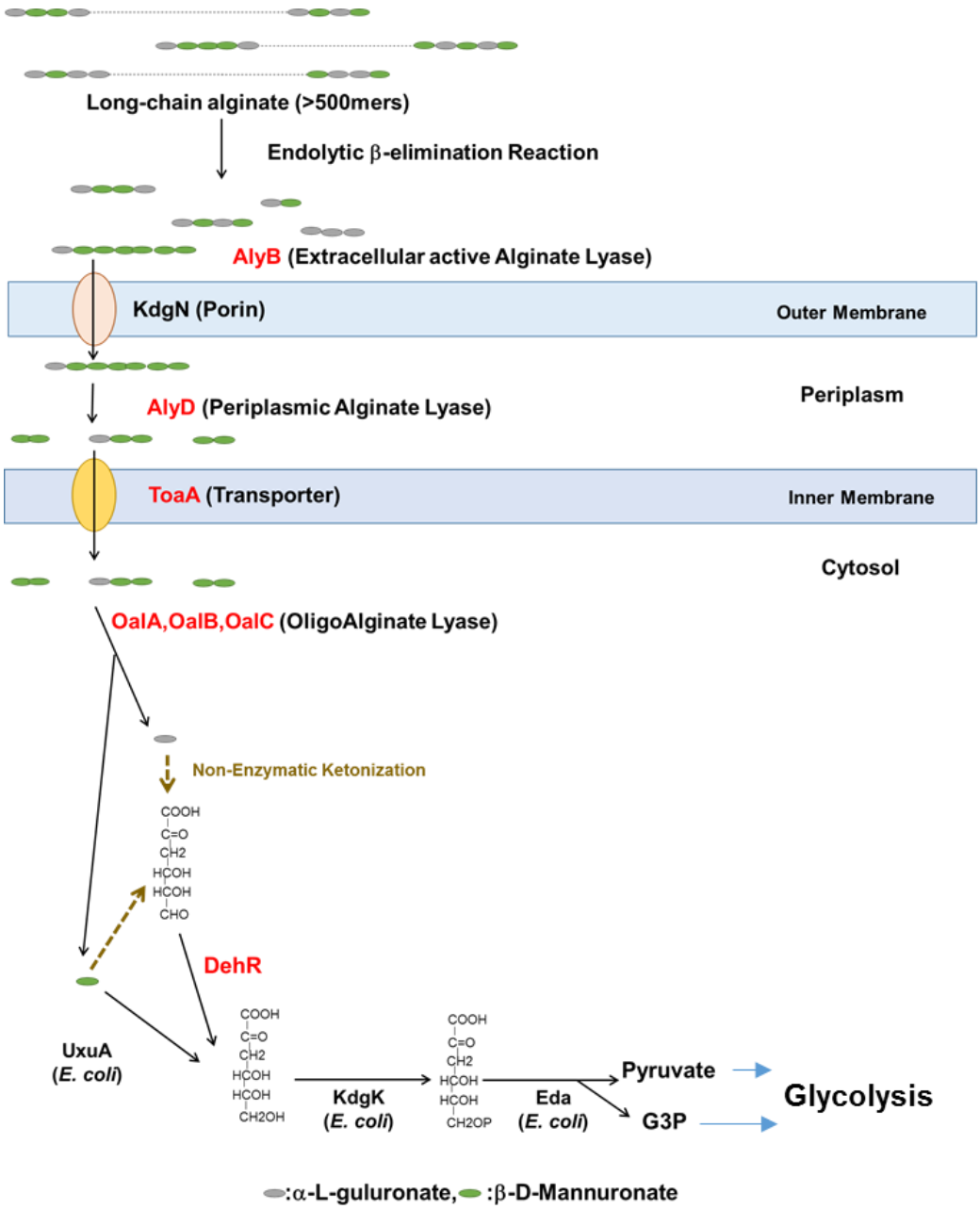

70

71 **Figure 4-9.** Model of alginate degradation and metabolism in *V. algivorus* Proteins

72 denoted in red letter are heterologously expressed in *E. coli* MG1655 and fulfilled their

73 functions for alginate utilization in this study.

74

Chapter 5 Conclusions and Perspectives

Considering the supply and demand balance of food resources expected to be tight, it would be desire for human being to utilize algae as an alternative fermentation resource for large scale production. In view of large scale cultivation of algae, artificial large scale farming of microalgae has been actively invested in various countries including Japan (Chirsti et al., 2007 and Chen et al., 2011), and the industrial large scale cultivation of macroalgae has also been established in China and Indonesia (http://www.fao.org/3/a-i3720o.pdf). Therefore, the remaining important problem was efficient utilization of main components of large scale-cultured algae. In particular, efficient enzymatic degradation of fattay acids and aliginate from algae has been a big target for large scale of production of argae materials.

The major compounds of algal biomass are fatty acids in microalgae and alginate in macroalgae. In this study, threrefore, I atempted to establish *E. coli* systems for biocoverstion of fatty acid and alginate into L-lysine, and to understand the mechanism underlying the systems. As a result, I succeeded in producing *E. coli* systems for efficient bioconversion of fatty acids and alginine from alage. My findings are summarized as follows. 1) I found that the regression of hydrogen peroxide stress promotes fatty-acid utilization and L-lysine production. 2) I digignated a novel *Vibrio*

93 species name as *Vibrio algivorus* sp. nov., with the type strain designated SA2^{T}. 3) I
94 found that AlyB of *Vibrio algivorus* SA2^{T} expressed in *E. coli* depolymerized
95 extracellular alginate without requiring concentration or purification. 4) Introduction of
96 seven genes of the *V. algivorus* genome (*alyB, alyD, oalA, oalB, oalC, dehR,* and *toaA*)
97 into *E. coli* enabled the cells to assimilate soluble alginate depolymerized by *V.*
98 *algivorus* AlyB as the sole carbon source, and bioconverte into L-lysine. These findings
99 greatly contributed to bioconverstion of two alagal biomass, fatty acids and alginate
100 with. *E. coli.* In addition, I provided a new insight into mechanism suppressing fatty
101 acid bioconverstion and into extracellular degradation of alginate. Therefore my results
102 provided simple biocatalyst and fermentation systems for both fatty acids and alginate
103 with potential applications in industrial biorefinery.
104 For future more practical utilization of algal biomass, there reamins some
105 problems such that fatty acids are difficult to be mixed in water and alginate is
106 inevitably viscous just after extraction. These problems will be approached extensively
107 through the establsihsement of a large scale surfactant application system including
108 recovery and reuse for fatty acids and a new large scale device to solve the viscosity for
109 alginate. Such new methods might take additional cost to utilize algal biomass.
110 However, algal biomass often contains other valuable ingredients such as pigments,

111 proteins and raw metals. Therefore, future development of a multiproducts biorefinery
112 system for algal components can help the practical application of sustainable algal
113 biomass utilization.

References

Baba T, Ara T, Hasegawa M, Takai Y, Okumura Y, Baba M, Datsenko KA, Tomita M, Wanner BL, Mori H (2006) Construction of *Escherichia coli* K-12 in-frame, single-gene knockout mutants: the Keio collection. *Mol. Syst. Biol*. 2:2006.0008.

Badur AH, Jagtap SS, Yalamanchili G, Lee JK, Zhao H, Rao CV (2015) Alginate lyases from alginate-degrading *Vibrio splendidus* 12B01 are endolytic. *Appl Environ Microbiol*. 81:1865–1873.

Báez-Viveros JL, Flores N, Juárez K, Castillo-España P, Bolivar F, Gosset G (2007) Metabolic transcription analysis of engineered *Escherichia coli* strains that overproduce L-phenylalanine. *Microb Cell Fact* 6:30. doi: 10.1186/1475-2859-6-30

Barrow GI, Feltham RKA (1993).*Cowan and Steel's Manual for the Identification of Medical Bacteria*, 3rd edition. Cambridge: Cambridge University Press.

Baumann P, Baumann L (1984). Genus II. *Photobacterium* Beijerinck 1889, 401^{AL}. In *Bergey's Manual of Systematic Bacteriology*, N. R. Krieg & J. G. Holt edition.

Baltimore: Williams & Wilkins.

Baumann P, Schubert RHW (1984). Genus II. *Vibrionaceae* Veron 1965, 5245^{AL}. In *Bergey's Manual of Systematic Bacteriology*, N. R. Krieg & J. G. Holt editon. Baltimore: Williams & Wilkins.

Bernardet JF, Nakagawa Y, Holmes B (2002). Proposed minimal standards for describing new taxa of the family Flavobacteriaceae and emended description of the family. *Int J Syst Evol Microbiol* 52, 1049–1070.

Blanchard JL, Wholey WY, Conlon EM, Pomposiello PJ (2007). Rapid changes in gene expression dynamics in response to superoxide reveal SoxRS-dependent and independent transcriptional networks. *PLoS ONE*. 11:e1186.

Bleicher A, Neuhaus K, Scherer S (2010). *Vibrio casei* sp. nov., isolated from the surfaces of two French red smear soft cheeses. *Int J Syst Evol Microbiol* 60, 1745–1749.

Bligh EG, Dyer WJ (1959). A rapid method of total lipid extraction and purification.

Canadian Journal of Biochemistry and Physiology 37, 911–917.

Blount S, Griffiths HR, Lunec J (1989). Reactive oxygen species induce antigenic changes in DNA. *FEBS Lett*. 245:100–104.

Bruinsma J (2003). World Agriculture: Towards 2015/2030: An FAO Perspective (Earthscan, London and Food and Agriculture Organization, Rome)

Chapman VJ (1970). *Seaweeds and Their Uses,* 2nd edition, London:The Camelot Press.

Chen CY, Yeh KL, Aisyah R, Lee DJ, Chang JS (2011). Cultivation, photobioreactor design and harvesting of microalgae for biodiesel production: a critical review. *Bioresource Technol*. 102:71-81.

Chial HJ, Splittgerber AG (1993). A comparison of the binding of Coomassie brilliant blue to proteins at low and neutral pH. *Anal Biochem* 213:362–369.

Chisti Y (2007). Biodiesel from microalgae. *Biotechnol. Adv*. 25:294–306.

Collins MD (1994). Isoprenoid quinones. In *Chemical Methods in Prokaryotic Systematics*, M. Goodfellow & A. G. O'Donnell edtion. Chichester: Wiley.

Cronan JE Jr, Subrahmanyam S (1998). FadR, transcriptional co-ordination of metabolic expediency. *Mol. Microbiol*. 29:937–943.

Datsenko KA, Wanner BL (2000). One-step inactivation of chromosomal genes in *Escherichia coli* K-12 using PCR products. *Proc. Natl. Acad. Sci. U. S. A.* 97:6640–6645.

Dellomonaco C, Rivera C, Campbell P, Gonzalez R (2010). Engineered respiro-fermentative metabolism for the production of biofuels and biochemicals from fatty acid-rich feedstocks. *Appl. Environ. Microbiol.* 76:5067–5078.

Doi H, Chinen A, Fukuda H, Usuda Y (2016). *Vibrio algivorus* sp. nov., an alginate and agarose assimilating bacterium isolated from the gut flora of a turban shell marine

snail. *Int J Syst Evol Microbiol*. 66:3164–3169.

Doi H, Hoshino Y, Nakase K, Usuda Y (2014). Reduction of hydrogen peroxide stress derived from fatty acid beta-oxidation improves fatty acid utilization in *Escherichia coli*. *Appl Microbiol Biotechnol*, 98:629–639.

Doi H, Matsudaira A, Usuda Y (2015). Treaty Patent WO2015/186749. International Patent Cooperation.

Doi H, Ueda T (2009). Treaty Patent WO2009/014117. International Patent Cooperation.

Dong J, Hashikawa S, Konishi T, Tamaru Y, Araki T (2006). Cloning of the Novel Gene Encoding β-Agarase C from a Marine Bacterium, *Vibrio* sp. Strain PO-303, and Characterization of the Gene Product. *Appl Environ Microbiol*, 72, 6399–6401.

Eck RV, Dayhoff MO (1966). *Atlas of Protein Sequence and Structure*. The 1 st edition, Maryland:Silver Springs.

Enquist-Newman M, Faust AM, Bravo DD, Santos CN, Raisner RM, Hanel A, Sarvabhowman P, Le C, Regitsky DD, Cooper SR, Peereboom L, Clark A, Martinez Y, Goldsmith J, Cho MY, Donohoue PD, Luo L, Lamberson B, Tamrakar P, Kim EJ, Villari JL, Gill A, Tripathi SA, Karamchedu P, Paredes CJ, Rajgarhia V, Kotlar HK, Bailey RB,Miller DJ, Ohler NL, Swimmer C, Yoshikuni Y (2014). Efficient ethanol production from brown macroalgae sugars by a synthetic yeast platform. *Nature,* 505:239–243.

Esvelt K, Wang HH (2013). Genome-scale engineering for systems and synthetic biology. *Mol Syst Biol,* 9: 641. doi: 10.1038/msb.2012.66.

Ezaki T, Hashimoto Y, Yabuuchi E (1989). Fluorometric deoxyribonucleic acid-deoxyribonucleic acid hybridization in microdilution wells as an alternative to membrane filter hybridization in which radioisotopes are used to determine genetic relatedness among bacterial strains. *Int J Syst Bacteriol*, 39, 224–229.

Falkeborg M, Cheong LZ, Gianfico C, Sztukiel KM, Kristensen K, Glasius M, Xu X, Guo Z (2014) Alginate oligosaccharides: enzymatic preparation and antioxidant

property evaluation. *Food Chem,* 164,185–194.

Felsenstein J (1981). Evolutionary trees from DNA sequences: a maximum likelihood approach. *J Mol Evol,* 17, 368–376.

Felsenstein J (1985). Confidence Limits on Phylogenies: An Approach Using the Bootstrap. *Evolution,* 39, 783-791.

Fitch WM (1971). Toward defining the course of evolution: minimum change for a specific tree topology. *Syst Zool,* 20, 406–416.

Finn RD, Bateman A, Clements J, Coggill P, Eberhardt RY, Eddy SR, Heger A, Hetherington K, Holm L, Mistry J, Sonnhammer EL, Tate J, Punta M (2014). Pfam: the protein families database. *Nucl Acids Res,* 42:D222–230. doi: 10.1093/nar/gkt1223.

Fong SS, Joyce AR, Palsson BO (2005). Parallel adaptive evolution cultures of *Escherichia coli* lead to convergent growth phenotypes with different gene expression states. *Genome Res,* 15:1365–1372.

Fu W, Han B, Duan D, Liu W, Wang C (2008). Purification and characterization of agarases from a marine bacterium *Vibrio* sp. F-6. *J Ind Microbiol Biotechnol,* 35, 915–922.

Gacesa P (1988). Alginates.*Carbohydrate Polymers*, 8, 161-182

Goris J, Konstantinidis KT, Klappenbach JA, Coenye T, Vandamme P, Tiedje JM (2007). DNA-DNA hybridization values and their relationship to whole-genome sequence similarities. *Int. J. Syst. Evol. Microbiol,* 57, 81–91

González-Flecha B, Demple B (1999). Role for the *oxyS* gene in regulation of intracellular hydrogen peroxide in *Escherichia coli*. *J. Bacteriol,* 181,3833–3836.

Han F, Gong QH, Song K, Li JB, Yu WG (2004). Cloning, sequence analysis and expression of gene alyVI encoding alginate lyase from marine bacterium *Vibrio* sp. QY101. *DNA Seq*, 15, 344–350.

Herring CD, Raghunathan A, Honisch C, Patel T, Applebee MK, Joyce AR, Albert TJ, Blattner FR, van den Boom D, Cantor CR, Palsson BO (2006). Comparative genome sequencing of *Escherichia coli* allows observation of bacterial evolution on a laboratory timescale. *Nat. Genet*, 38,1406–1412.

Hu Q, Sommerfeld M, Jarvis E, Ghirardi M, Posewitz M, Seibert M, Darzins A (2008). Microalgal triacylglycerols as feedstocks for biofuel production: perspectives and advances. *Plant J,* 54,621–639.

Inoué T, Osatake H (1998). A new drying method of biological specimens for scanning electron microscopy: the t-butyl alcohol freeze-drying method. *Arch Histol Cytol* 51, 53-9.

Iwai M, Yokono M, Kono M, Noguchi K, Akimoto S, Nakano A (2015). Light-harvesting complex Lhcb9 confers a green-alga type photosystem I supercomplex in the moss *Physcomitrella patens*. *Nature Plants.* 1: 14008. doi: 10.1038/nplants.2014.8.

Iwamoto Y, Araki R, Iriyama K, Oda T, Fukuda H, Hayashida S, Muramatsu T (2001). Purification andcharacterization of bifunctional alginate lyase from *Alteromonas* sp. strain no. 272 and its action on saturated oligomeric substrates. *Biosci Biotechnol Biochem,* 65,133–142.

Jagtap SS, Hehemann JH, Polz MF, Lee JK, Zhao H (2014). Comparative biochemical characterization of three exolytic oligoalginate lyases from *Vibrio splendidus* reveals complementary substrate scope, temperature, and pH adaptations. *Appl Environ Microbial,* 80, 4207–4214.

John RP, Anisha GS, Nampoothiri KM, Pandey A (2011). Micro and macroalgal biomass: a renewable source for bioethanol. *Bioresour Technol,* 102,186–193.

Jenkins LS, Nunn WD (1987). Genetic and molecular characterization of the genes involved in short-chain fatty acid degradation in *Escherichia coli*: the *ato* system. *J. Bacteriol,* 169, 42–52.

Jukes TH, Cantor CR, (1969). Evolution of protein molecules. In *Mammalian Protein*

Metabolism. Munro HN edition, New York:Academic Press.

Kawai S, Ohashi K, Yoshida S, Fujii M, Mikami S, Sato N, Murata K (2014). Bacterial pyruvate production from alginate, a promising carbon source from marine brown macroalgae. *J Biosci Bioeng*, 117, 269–274.

Katashkina JI, Hara Y, Golubeva LI, Andreeva IG, Kuvaeva TM, Mashko SV (2009). Use of the λ Red-recombineering method for genetic engineering of *Pantoea ananatis*. *BMC Mol Biol*, 10:34. doi: 10.1186/1471-2199-10-34.

Katashkina JI, Skorokhodova AI, Zimenkov DV, Gulevich A, Minaeva NI, Doroshenko VG, Biriukova IV, Mashko SV (2005). Tuning the expression level of a gene located on a bacterial chromosome. *Mol Biol*, 39, 719–726.

Kikuchi Y, Kojima H, Tanaka T, Takatsuka Y, Kamio Y (1997). Characterization of second lysine decarboxylase isolated from *Escherichia coli*. *J. Bacteriol*, 179, 4486–4492.

Kim D, Baik KS, Hwang YS, Choi JS, Kwon J, Seong CN (2013). *Vibrio hemicentroti* sp. nov., an alginate lyase-producing bacterium, isolated from the gut microflora of sea urchin (*Hemicentrotus pulcherrimus*). *Int J Syst Evol Microbiol,* 63,3697–3703.

Kim M, Oh HS, Park SC, Chun J (2014). Towards a taxonomic coherence between average nucleotide identity and 16S rRNA gene sequence similarity for species demarcation of prokaryotes. *Int J Syst Bacteriol,* 64, 346-351.

Kim OS, Cho YJ, Lee K, Yoon SH, Kim M, Na H, Park SC, Jeon YS, Lee JH, Yi H, Won S, Chun J (2012). Introducing EzTaxon: a prokaryotic 16S rRNA Gene sequence database with phylotypes that represent uncultured species. *Int J Syst Evol Microbiol*, 62, 716–721

Kimura M (1980). A simple method for estimating evolutionary rates of base substitutions through comparative studies of nucleotide sequences. *J Mol Evol*, 16, 111–120.

Kita A, Miura T, Okamura Y, Aki T, Matsumura Y, Tajima T, Kato J, Nakashimada Y

(2015). *Dysgonomonas alginatilytica* sp. nov., an alginate-degrading bacterium isolated from a microbial consortium. *Int J Syst Evol Microbiol,* 65,3570–3575.

Kojima H, Ogawa Y, Kawamura K, Sano K (1994). Treaty patent WO95/16042. International Patent Cooperation.

Korshunov S, Imlay JA (2010). Two sources of endogenous hydrogen peroxide in *Escherichia coli. Mol Microbiol,* 75, 1389–1401.

Lee I, Kim YO, Park SC, Chun, J (2015). OrthoANI: An improved algorithm and software for calculating average nucleotide identity. *Int J Syst Evol Microbiol,* 66, 1100-1103.

Le Roux F, Zouine M, Chakroun N, Binesse J, Saulnier D, Bouchier C, Zidane N, Ma L,Rusniok C, Lajus A (2009). Genome sequence of *Vibrio splendidus*: an abundant marine species with a large genotypic diversity. *Environ Microbiol,* 11, 1959–1970.

Leuchtenberger W, Huthmacher K, Drauz K (2005). Biotechnological production of amino acids and derivatives: current status and prospects. *Appl Microbiol Biotechnol*, 69, 1–8.

Liao L, Xu XW, Jiang XW, Cao Y, Yi N, Huo YY, Wu YH, Zhu XF, Zhang X, Wu M. (2011). Cloning, Expression, and Characterization of a New β-Agarase from *Vibrio* sp. Strain CN41. *Appl Environ Microbiol*, 77, 7077–7079.

Magnuson K, Jackowski S, Rock CO, Cronan JE Jr (1993). Regulation of fatty acid biosynthesis in *Escherichia coli*. *Microbiol Rev*, 57, 522–542.

Maisonneuve E, Fraysse L, Lignon S, Capron L, Dukan S (2008). Carbonylated proteins are detectable only in a degradation-resistant aggregate state in *Escherichia coli*. *J Bacteriol*, 190, 6609–6614.

Mal M, Wong S (2011). A HILIC-Based UPLC / MS Method for the Separation of Lipid Classes from Plasma. *Waters Appl. Note* 1–5. http://www.waters.com/webassets/cms/library/docs/720004048en.pdf

Malik A, Sakamoto M, Hanazaki S, Osawa M, Suzuki T, Tochigi M, Kakii K (2003). Coaggregation among nonflocculating bacteria isolated from activated sludge. *Appl Environ Microbiol,* 69, 6056–6063.

Matsubara Y, Kawada R, Iwasaki K, Oda T, Muramatsu T (1998). Extracellular poly (alpha-L-guluronate) lyase from *Corynebacterium* sp.: purification, characteristics, and conformational properties. *J Protein Chem,* 17, 29–36.

Mazzella N, Molinet J, Syakti AD, Dodi A, Doumenq P, Artaud J, Bertland J C (2004). Bacterial phospholipid molecular species analysis by ion-pair reversed phase HPLC/ESI/MS. *J. Lipid. Res,* 45, 1355-1363.

Meier-Kolthoff JP, Auch AF, Klenk HP, Markus Goker M (2013). Genome sequence-based species delimitation with confidence intervals and improved distance functions. *BMC Bioinfomatics,* 14,60

Messner KR, Imlay JA (2002). Mechanism of superoxide and hydrogen peroxide

formation by fumarate reductase, succinate dehydrogenase, and aspartate oxidase. *J Biol Chem*, 277, 42563–42571.

Minnikin DE, Collins MD, Goodfellow M (1979). Fatty acid and polar lipid composition in the classification of *Cellulomonas, Oerskovia* and related taxa. *J. Appl. Bacteriol*, 47, 87-95.

Miller JH (1992). A short course in bacterial genetics. New York:Cold Spring Harbor.

Nachin L, Nannmark U, Nyström T (2005). Differential roles of the universal stress proteins of *Escherichia coli* in oxidative stress resistance, adhesion, and motility. *J Bacteriol*, 187, 6265–6272.

Nam YD, Chang HW, Park JR, Kwon HY, Quan ZX, Park YH, Kim BC, Bae JW (2007). *Vibrio litoralis* sp. nov., isolated from a Yellow Sea tidal flat in Korea. *Int J Syst Evol Microbiol*, 57, 562–565.

Nei M, Kumar S (2000). *Molecular Evolution and Phylogenetics.* New York:Oxford

University Press.

Nishio Y, Ogishima S, Ichikawa M, Yamada Y, Usuda Y, Masuda T, Tanaka H (2013). Analysis of L-glutamic acid fermentation by using a dynamic metabolic simulation model of *Escherichia coli*. *BMC Syst Biol* 7:92. doi: 10.1186/1752-0509-7-92.

Niu D, Tian K, Prior BA, Wang M, Wang Z, Lu F, Singh S (2014). Highly efficient L-lactate production using engineered *Escherichia coli* with dissimilar temperature optima for L-lactate formation and cell growth. *Microb Cell Fact,* 13:78. doi: 10.1186/1475-2859-13-78.

Perry LB (1973). Gliding motility in some non-spreading flexibacteria. *J Appl Bacteriol*, 36, 227–232.

Petersen TN, Brunak S, von Heijne G, Nielsen H (2011). *Nat Methods,* 8, 785–786.

Pradenas GA, Paillavil BA, Reyes-Cerpa S, Pérez-Donoso JM, Vásquez CC (2012). Reduction of the monounsaturated fatty acid content of *Escherichia coli* results in

increased resistance to oxidative damage. *Microbiology,* 158, 1279–1283.

Raba J, Mottola HA (1995). Glucose oxidase as an analytical reagent. *Crit Rev Anal Chem,* 25, 1–42.

Resnik E, Pan B, Ramani N, Freundlich M, LaPorte DC (1996). Integration host factor amplifies the induction of the aceBAK operon of *Escherichia coli* by relieving IclR repression. *J Bacteriol,* 178, 2715–2717.

Ronda T, Pedersen LE, Sommer MO, Nielsen AT (2016) .CRMAGE: CRISPR Optimized MAGE Recombineering. *Sci Rep*, 22:19452. doi: 10.1038/srep19452.

Rosenberg JN, Oyler GA, Wilkinson L, Betenbaugh MJ (2008). A green light for engineered algae: redirecting metabolism to fuel a biotechnology revolution. *Curr Opin Biotechnol,* 19, 430–436.

Saitou N, Nei M(1987). The neighbor-joining method: a new method for reconstructing phylogenetic trees. *Mol Biol Evol*, 4, 406-25.

Santos CN, Regitsky DD, Yoshikuni Y (2013). Implementation of stable and complex biological systems through recombinase-assisted genome engineering. *Nat Commun* 4: 2503. doi: 10.1038/ncomms3503.

Sato R, Sawabe T, Saeki H (2005). Characterization of fish myofibrillar protein by conjugation with alginate oligosaccharide prepared using genetic recombinant alginate lyase. *J Food Sci*, 70, 58–62.

Sawabe, T., Ogura Y, Matsumura Y, Feng G, Amin AR, Mino S, Nakagawa S, Sawabe T, Kumar R, Fukui Y, Satomi M, Matsushima R, Thompson FL, Gomez-Gil B, Christen R, Maruyama F, Kurokawa K, Hayashi T.(2013). Updating the *Vibrio* clades defined by multilocus sequence phylogeny: proposal of eight new clades, and the description of *Vibrio tritonius* sp. nov. *Front Microbiol*. 27;4:414

Sawabe, T., Setoguchi, N., Inoue, S., Tanaka, R., Ootsubo, M., Yoshimizu, M. & Ezura, Y. (2003). Acetic acid production of *Vibrio halioticoli* from alginate: a possible role for establishment of abalone-*V. halioticoli* association. *Aquaculture* 219, 671-679.

Sawabe, T., Sugimura, I., Ohtsuka, M., Nakano, K., Tajima, K., Ezura, Y. & Christen, R. (1998). *Vibrio halioticoli* sp. nov., a nonmotile alginolytic marine bacterium isolated from the gut of the abalone *Haliotis discus* hannai. *Int J Syst Bacteriol* 48, 573–580.

Service RF (2009) ExxonMobil fuels Venter's efforts to run vehicles on algae-based oil. *Science* 325:379.

Setsukinai K, Urano Y, Kakinuma K, Majima HJ, Nagano T (2003) Development of novel fluorescence probes that can reliably detect reactive oxygen species and distinguish specific species. *J Biol Chem* 278, 3170–3175.

Stackebrandt, E. & Goebel, B. M. (2006). Taxonomic parameters revisited: tarnished gold standards. *Microbiol Today* 33, 152-155.

Stephens E, de Nys R, Ross IL, Hankamer B (2013) Algae fuels as an alternative to petroleum. *J Pet Environ Biotechnol* 4:4.

Takeda H, Yoneyama F, Kawai S, Hashimoto W, Murata K (2011) Bioethanol production from marine biomass alginate by metabolically engineered bacteria. *Energy Environ Sci* 4, 2575–2581.

Tamaoka, J., Katayama-Fujimura, Y., & Kuraishi, H. (1983). Analysis of bacterial menaquinone mixtures by high performance liquid chromatography. *Journal of Applied Bacteriology*, 54, 31–36.

Tamura K., Peterson D., Peterson N., Stecher G., Nei M. & Kumar S. (2011). MEGA5: molecular evolutionary genetics analysis using maximum likelihood, evolutionary distance, and maximum parsimony methods. *Mol Biol Evol* 28, 2731-2739.

Tang JC, Taniguchi H, Chu H, Zhou Q, Nagata S. (2009) Isolation and characterization of alginate-degrading bacteria for disposal of seaweed wastes. *Lett Appl Microbiol* 48, 38–43.

Wang J, Cheng LK, Wang J, Liu Q, Shen T, Chen N (2013) Genetic engineering of *Escherichia coli* to enhance production of L-tryptophan. *Appl Microbiol Biotechnol*

97, 7587–7596.

Wang da M, Kim HT, Yun EJ, Kim do H, Park YC, Woo HC, Kim KH (2014) Optimal production of 4-deoxy-L-erythro-5-hexoseulose uronic acid from alginate for brown macro algae saccharification by combining endo- and exo-type alginate lyases. *Bioprocess Biosyst Eng* 37, 2105–2111.

Wargacki AJ, Leonard E, Win MN, Regitsky DD, Santos CN, Kim PB, Cooper SR, Raisner RM, Herman A, Sivitz AB, Lakshmanaswamy A, Kashiyama Y, Baker D, Yoshikuni Y (2012) An engineered microbial platform for direct biofuel production from brown macroalgae. *Science* 335, 308–313.

Yamamoto, S. & Harayama, S. (1998). Phylogenetic relationships of *Pseudomonas putida* strains deduced from the nucleotide sequences of *gyrB*, *rpoD* and 16S rRNA genes. *Int J Syst Bacteriol* 48, 813–819.

Yonemoto Y, Tanaka H, Yamashita T, Kitabatake N, Ishida Y, Kimura A, Murata K (1995) Promotion of germination and shoot elongation of some plants by alginate

oligomers prepared with bacterial alginate lyase. *J Ferment Bioeng* 75, 68–70.

Youngdeuk, L., Chulhong, O., Mahanama, D. Z., Hyowon, K., Niroshana, W. W. D., Ilson, W., Do-Hyung, K. & Jehee, Lee. (2013). Molecular cloning, overexpression, and enzymatic characterization of glycosyl hydrolase family 16 β-Agarase from marine bacterium *Saccharophagus* sp. AG21 in *Escherichia coli. J Microbiol Biotechnol* 23, 913-22.

Yumoto I., Iwata H., Sawabe T., Ueno K., Ichise N., Matsuyama H., Okuyama H. & Kawasaki K. (1999). Characterization of a facultatively psychrophilic bacterium, *Vibrio rumoiensis* sp. nov., that exhibits high catalase activity. *Appl Environ Microbiol* 65, 67-72.

Zhu LW, Li XH, Zhang L, Li HM, Liu JH, Yuan ZP, Chen T, Tang YJ (2013). Activation of glyoxylate pathway without the activation of its related gene in succinate-producing engineered *Escherichia coli*. *Metab Eng,* 20, 9–19.

Wargacki AJ, Leonard E, Win MN, Regitsky DD, Santos CN, Kim PB, Cooper SR,

Raisner RM, Herman A, Sivitz AB, Lakshmanaswamy A, Kashiyama Y, Baker D, Yoshikuni Y (2012). An engineered microbial platform for direct biofuel production from brown macroalgae. *Science,* 335, 308-313.

Wayne LG, Brenner DJ, Colwell RR, Grimont PAD, Kandler O, Krichevsky MI, Moore LH, Moore WEC, Murray RGE, Stackebrandt E, Starr MP, Truper HG (1987). Report of the Ad Hoc Committee on Reconciliation of Approaches to Bacterial Systematics. *Int J Syst Bacteriol,* 37, 463-464.

Wendisch VF, Bott M, Eikmanns BJ (2006). Metabolic engineering of *Escherichia coli* and *Corynebacterium glutamicum* for biotechnological production of organic acids and amino acids. *Curr Opin Microbiol.* 9, 268–274.

Xu Y, Heath RJ, Li Z, Rock CO, White SW (2001). The FadR.DNA complex. Transcriptional control of fatty acid metabolism in *Escherichia coli*. *J Biol Chem,* 276, 17373-17379.

Zheng M, Åslund F, Storz G (1998), Activation of the OxyR transcription factor by

reversible disulfide bond formation. *Science*, 179, 1718–17